ABSTRACT

Title of Thesis:	CABLE BACTERIA AND THEIR MICROBIAL ASSOCIATIONS IN LAB-INCUBATED SEDIMENT FROM CHESAPEAKE BAY
	Pinky Liau, Master of Science, 2021
Thesis Directed By:	Sairah Malkin, Assistant Professor Marine, Estuarine, and Environmental Science

Cable bacteria (*Ca.* Electrothrix) are long, filamentous, multicellular bacteria that grow in marine sediments and couple sulfur oxidation to oxygen reduction over centimeter-scale distances via an enigmatic long-distance electron transport mechanism. They can grow to tremendous densities and strongly modify the sediment environment in multiple ways, including efficient sulfide removal, stimulation of sulfate reduction, and alteration of porewater pH distribution. In this thesis, I asked if cable bacteria can influence the sympatric microbial community composition and activity, using a time-series manipulation experiment. As anticipated, based on their influence on sediment geochemistry, cable bacteria growth was associated with the stimulation of several genera of sulfate-reducing bacteria, and a sulfur-disproportionating genus (*Desulfocapsa*). I observed a positive relationship with the *OM27* clade of the predatory Bdellovibrionota. Finally, I detected evidence of interaction with two chemoautotrophic sulfur oxidizers (*Thiogranum*, *Sedimenticola*), which are good candidates for further examination of potential electrical connection with cable bacteria.

CABLE BACTERIA AND THEIR MICROBIAL ASSOCIATIONS IN LAB-INCUBATED SEDIMENT FROM CHESAPEAKE BAY

by

Pinky Liau

Thesis submitted to the Faculty of the Graduate School of the
University of Maryland, College Park, in partial fulfillment
of the requirements for the degree of
Master of Science
2021

Advisory Committee:
Assistant Professor Dr. Sairah Malkin, Chair
Professor Dr. Jeffrey Cornwell
Associate Professor Dr. Laura Lapham
Assistant Professor Dr. Clara Fuchsman
Assistant Professor Dr. Jacob Cram

Acknowledgements

I would first like to say a sincere thank you to my advisor, Dr. Sairah Malkin, for all the support and guidance she has provided me through my years at Horn Point Laboratory (HPL). While it was a very tough experience, Dr. Malkin was always encouraging and gave me words of advice whenever I needed it. Thank you. I have genuinely learned a lot during graduate school. I am grateful for the scientific knowledge and important skills I have gained that will continue to lead me forward in life.

I would also like to thank my committee: Dr. Jeffrey Cornwell, Dr. Clara Fuchsman, Dr. Jacob Cram, and Dr. Laura Lapham. I really appreciated each of you for being my mentors, meeting with me whenever I requested, and for providing insight towards my thesis work. I would also like to thank everyone who has helped me with my field and experimental work. Carol Kim for the constant support and helping me with troubleshooting methods. Andy McCarthy for helping with sediment collection in the field. Mike Owens for teaching me how to run gas chromatography and helping with sample runs. Dr. Greg Silsbe for collecting bay water from the field. Sabeena Nazar for sequencing my DNA samples. Jack Seabrease for helping me with the construction of experimental core tubes. Ralph Kimes and Gordy Dawson for assisting me with environmental chamber setup.

Thank you to UMCES and HPL for funding my graduate education. Thank you to NSF for funding my research efforts. Thank you UMD Graduate School, Center for Electromicrobiology, and HPL Education Committee for providing me with travel funding to a conference in Denmark. Also, a special thank you to the Saba family for funding to support my research.

I am incredibly grateful for everyone in the HPL community. Thank you to all my friends I have met here who supported me and laughed with me: Lexy McCarty, Sammy Gleich, Sophia Hyun, Wenfei Ni, Melanie Jackson, Megan Munkacsy, Hannah Morrissette, and Paulina Huanca. Finally, thank you to Steve Rudzinski and my family for the loving support.

Table of Contents

List of Tables

List of Figures

List of Abbreviations

BALOs	Bdellovibrio and like organisms
DIET	Direct Interspecies Electron Transfer
SRB	Sulfate-Reducing Bacteria
ANME	Anaerobic Methanotrophic Archaea
FISH	Fluorescence *in situ* Hybridization
ASV	Amplicon Sequence Variant
FDR	False Discovery Rate
FTAxC	Fractional Transcript Abundance * Bacterial Cell Counts
DOU	Diffusive Oxygen Uptake

Introduction and Literature Review

The overarching goal of my thesis is to identify whether there are specific microbial associations with marine cable bacteria (*Ca.* Electrothrix). To address this goal, I performed a manipulation experiment in which I enriched for cable bacteria growth in a set of slurried sediment cores and inhibited their growth in another set of otherwise identical sediment cores. I monitored the porewater geochemistry and microbial community composition over time. To uncover microbial associations with cable bacteria, I performed Spearman's Rank correlation on 16S rRNA transcript-based abundance normalized by microscopy counts data from samples with and without cable bacteria. In the thesis Introduction, I provide a literature review of cable bacteria, focusing on their physiology, phylogeny, biogeography, and their effects on sediment biogeochemistry. My overall goal is to identify potential ecological interactions with cable bacteria, therefore, I introduce different types of ecological and physiological microbial interactions, including trophic interactions, resource competition, cooperation such as syntrophy or electrical connections. I also introduce the concepts of ecosystem engineering and keystone species, and identify how these concepts apply to microbial communities. I end the Introduction with the thesis objectives.

Background on Cable Bacteria

Cable bacteria are long, filamentous, multicellular bacteria that perform long-distance electron transport by conducting electrons along their length, across distances of up to 3 centimeters (Nielsen et al., 2010; Pfeffer et al. 2012; Marzocchi et

al., 2014). Cable bacteria filaments connect oxygenated surface sediment, where they perform cathodic reduction of oxygen or nitrate, with deeper reducing sediment, where they perform anodic sulfide oxidation (Figure 1). The two redox half-reactions are spatially separated but are electrically linked by a novel and incompletely understood mechanism of long-distance electron transport (Nielsen et al., 2010; Pfeffer et al., 2012; Bjerg et al., 2018; Kjeldsen et al., 2019; Thiruvallur Eachambadi et al., 2020). Individual cells within a filament appear to be linked continuously with a ridge compartment containing periplasmic fiber sheath (Cornelissen et al., 2019) which aids in structural support as well as electrical conductivity (Thiruvallur Eachambadi et al.,2020). Recent metagenomic evidence suggests that marine and freshwater cable bacteria (*Candidatus* Electrothrix and *Candidatus* Electronema) conserve energy from the anodic sulfide oxidation, and not from the oxygen or nitrate cathodic reductions (Kjeldsen et al., 2019).

Two distinct, monophyletic clades represent freshwater (*Candidatus* Electronema) and marine (*Candidatus* Electrothrix) cable bacteria groups, affiliated to the family *Desulfobulbaceae* (Trojan et al., 2016). A groundwater clade of cable bacteria has also been reported (Einsiedl et al., 2015; Müller et al., 2016), although their phylogeny is still uncertain. The two candidate genera of cable bacteria are globally distributed (Malkin et al., 2014; Burdorf et al., 2017). The natural abundance of *Ca.* Electrothrix has been reported from marine habitats including the North Sea (Malkin et al., 2014; van de Velde et al., 2016), Grevelingen (Seitaj et al., 2015; Sulu-Gambari et al., 2016b), Baltic Sea (Marzocchi et al., 2018), Yaquina Bay (Li et al., 2020), mangroves (Burdorf et al. 2016), salt marshes (Larsen et al., 2015, Rao et al.,

2016b), bivalve reefs (Malkin et al., 2017), and Southern Mariana Trough (Kato and Yamagishi, 2016). Coastal sediments with oxygenated overlying water and high organic matter loads, in particular, appear to provide desirable conditions for the enrichment of cable bacteria. For example, following a major hydrodynamic inflow event in the Baltic Sea, reoxygenation of bottom water stimulated cable bacteria growth (Marzocchi et al., 2018). In Grevelingen, a seasonally hypoxic marine basin, cable bacteria were observed in high abundance each spring, while *Beggiatoa*, another cosmopolitan sulfur-oxidizing bacterium, thrived in the fall (Seitaj et al., 2015). Cable bacteria are also found in freshwater sediments (Risgaard-Petersen et al., 2015). Other habitats where cable bacteria may be present include worm burrows, specifically *Chaetopterus* tubes. Oxygen is supplied by the irrigation activities of worms, but the tubes are sufficiently stable to prevent rapid sediment overturning (Aller et al., 2019). Cable bacteria may also be in direct association with oxygen loss from root hairs in the rhizosphere of aquatic plants, including seagrasses *Halophila ovalis* and *Zostera muelleri*, as well as *Littorella uniflora, Oryza sativa*, *Lobelia cardinalis* and *Salicornia europaea* (Martin et al., 2019; Scholz et al., 2019).

Cable bacteria impart large and distinctive biogeochemical effects in surface sediments wherever they grow abundantly (Figure 1). The growth of cable bacteria leads to an expansion of a suboxic zone, defined as space devoid of sulfide and oxygen, through rapid kinetics of sulfide oxidation (Nielsen et al., 2010; Schauer et al., 2014; Meysman et al., 2015). Cable bacteria activity also alters the distribution of porewater acidity, generating a pH maximum in the oxic zone by cathodic activity, and a pH minimum in the suboxic zone by anodic activity (Nielsen et al., 2010;

Meysman et al., 2015). The decrease in pH with depth in sediment, associated with cable bacteria activity, causes dissolution of FeS and calcium/manganese- carbonates, leading to mobilization of sulfide, ferrous iron, calcium ions, and manganese ions (Risgaard-Petersen et al., 2012; Rao et al., 2016a; Sulu-Gambari et al., 2016b; Hermans et al., 2020). Dissolved ions including Fe^{2+}, Ca^{2+}, and Mn^{2+} diffuse upwards, where Fe and Mn precipitate as their respective oxides (Rao et al., 2016a; Sulu-Gambari et al., 2016b; Seitaj et al., 2015) and Ca^{2+} precipitates as carbonates at or near the sediment surface (Rao et al., 2016a). The precipitation of iron-oxides at the oxic-anoxic interface can affect the biogeochemical conditions for weeks after the cable bacteria population has declined, by sequestering free sulfides produced by ongoing sulfate reduction, which may delay the onset of euxinic bottom water conditions (Seitaj et al., 2015). Cable bacteria may also influence the nitrogen indirectly, by promoting DNRA via increased availability of Fe^{2+} due to the dissolution of FeS (Kessler et al., 2019). Cable bacteria can also influence the phosphorus cycle. Increased precipitation of iron oxides at the oxic-anoxic interface can retain more phosphorus in the sediment (Sulu-Gambari et al., 2016a). Finally, cable bacteria demonstrably stimulated sulfate reduction, by providing additional sulfate at depth in a sulfate-limited freshwater sediment (Sandfeld et al. 2020). As a consequence of enhanced sulfate reduction, cable bacteria may also decrease methanogenesis in the same sediments (Scholz et al. 2020).

Marine cable bacteria can grow to dominate in laboratory incubated sediments (Pfeffer et al., 2012; Schauer et al., 2014). They can grow rapidly in homogenized sediments with oxygenated overlying water (Schauer et al., 2014; Vasquez-Cardenas

et al., 2015) or without oxygen, but with amendments of nitrate or nitrite as electron acceptor (Marzocchi et al., 2014). Based on microscopy, cable bacteria have been reported to grow in association with poised anodes in benthic microbial fuel cells and bioelectrochemical reactor core tubes (Reimers et al., 2017; Li et al., 2020). Due to their vertical filamentous elongation, cable bacteria growth can be manipulated in incubation experiments by placement of barrier filter below the oxic region of sediment (Pfeffer et al., 2012; Schauer et al., 2014). I employed such a manipulative experiment to identify potential microbial associations with cable bacteria.

Figure 1. Schematic of major biogeochemical modifications as a result of electrogenic sulfide oxidation by cable bacteria.

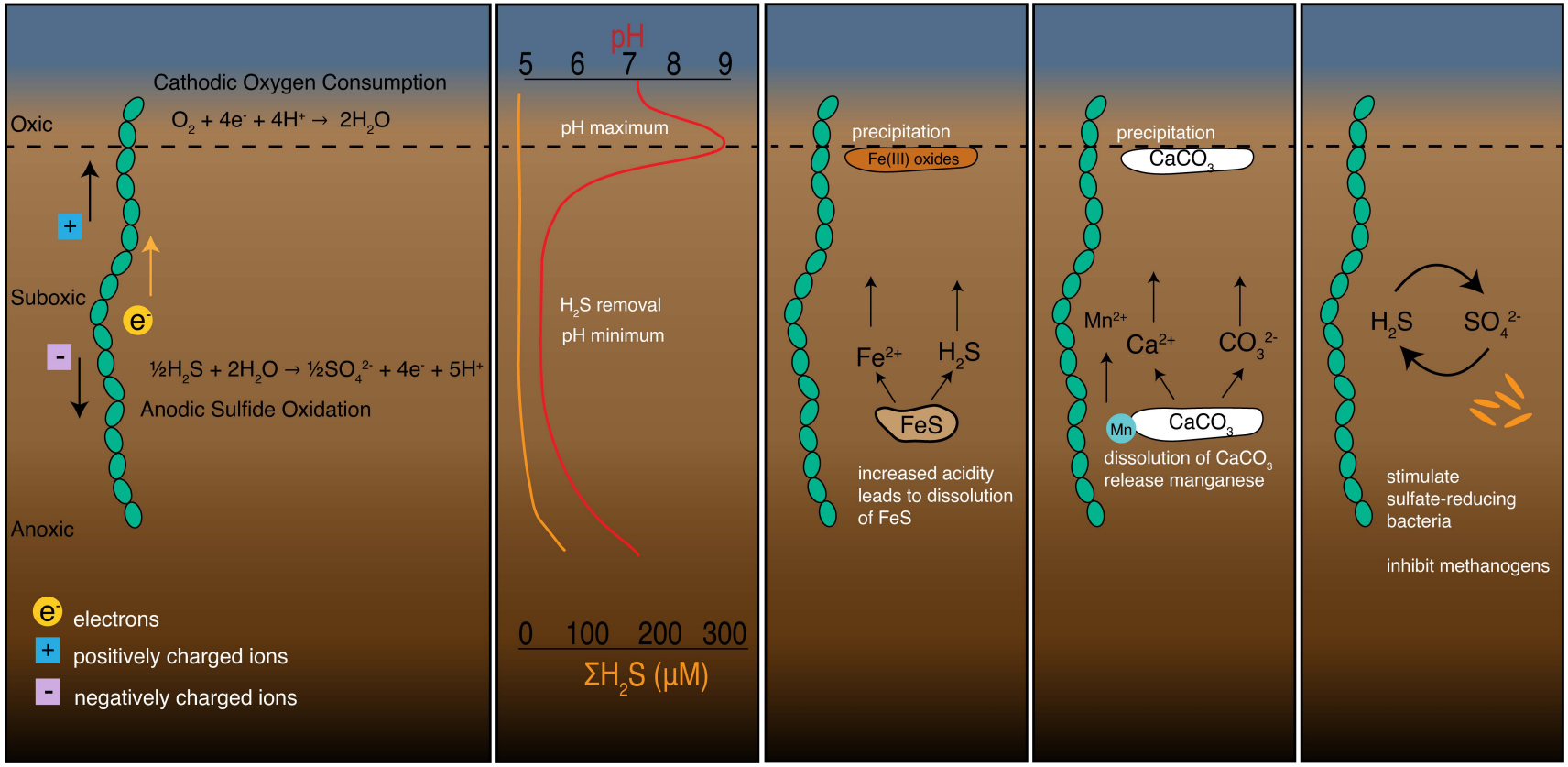

Microbial Community Interactions

In this thesis, I aim to identify microbial interactions with cable bacteria, using a correlation analysis approach (Weiss et al., 2016; Liu et al., 2019). In the next section of the Introduction, I review literature on potential microbial ecological interactions to inform the interpretation of my correlation results.

Predatory Bacteria (Sideways Control)

Predator-prey interactions play a major role in maintaining biodiversity of ecosystems, shaping community structure, and regulating nutrient cycles (Berryman, 1992; Jurkevitch, 2007; Chauhan et al., 2009). Microbial (or bacteriovorus) predators play key roles as top-down (also considered "sideways") control of microbial community structures (Jurkevitch, 2007; Pérez et al., 2016). Under oxic conditions with rich organic matter, predation by bacteria and microfauna can be the most important factor in controlling bacterial biomass and mortality (Jurkevitch, 2007; Perez et al., 2016; Tsai et al., 2013; Wang et al., 2020). In contrast, mortality attributed to viral lysis can be more prevalent in anoxic settings where aerobic predators are inhibited (Tsai et al., 2013). Bacterial predators employ different hunting strategies (Perez et al., 2016). Epibiotic predation involves a predator attaching to the outer surface of the prey cell then consumes the prey from the outside. Microbial predators can also attack prey by penetrating the periplasm and consuming from the inside. This endobiotic strategy is typical of most Bdellovibrio and like organisms (BALOs) (Jurkevitch, 2007; Sockett, 2009). Bdellovibrios are aerobic, obligate predators of Gram-negative bacteria such as Proteobacteria (Pérez et al., 2016). Wolfpack or group attack is typically used by Myxobacteria, which are facultative predators that secrete large quantities of hydrolytic enzymes to degrade

prey cells. Though they may grow without predation, close proximity to prey cells can trigger a swarming response where predation becomes the dominant tactic (Wrótniak-Drzewiecka et al., 2016; Muñoz-Dorado et al., 2016). While predators may control prey density, the diversity of prey can shape predator population structure (Chen et al., 2011). *Bacteriovorax* affiliated to BALOs appear to have a preference in what type of prey to consume, resulting in a prey-based community structure (Chen et al., 2011).

Competition

Microbial competition sustains community biodiversity through selective forces that determine evolutional trajectory of the competing players. Microorganisms compete and co-exist with one another through direct or indirect interactions. In the environment, microbes may compete for a variety of limiting resources, such as nutrients required for growth (Hibbings et al., 2010). Heterotrophs and mixotrophs may compete for organic carbon assimilated for growth (Ward et al., 2011). Phototrophs may compete for access to light, and/or compete with autotrophs for access to electron donors and acceptors. For instance, under anoxic, illuminated conditions, anoxygenic phototrophic bacteria, *Thiocapsa*, outcompeted an autotrophic sulfur bacteria, *Thiobacillus* (Visscher et al., 1992). Conversely, under oxygenated conditions, *Thiobacillus* can grow to much higher abundances relative to *Thiocapsa*.

In sediments, micro-organisms also compete for access to terminal electron acceptors for respiration. The overall rate of microbial respiration is ultimately controlled or limited by the organic carbon influx where community composition and spatial distribution are affected by kinetic and thermodynamic constraints (Jørgensen, 2006). Oxic respiration dominates with the highest energy yield, followed by

denitrification, manganese reduction, iron reduction, sulfate reduction, and methanogenesis (Canfield et al., 2005; Arndt et al., 2013). Microbes that use terminal electron acceptors with higher redox potential outcompete other microbes by keeping the products of fermentation low (e.g., H_2 and acetate) (Lovley et al., 1982; Schonheit et al., 1982; Lovley and Phillips, 1987; Lovley and Goodwin, 1988; Jørgensen, 2006).

Cooperation: Microbial Syntrophy and Direct Interspecies Electron Transfer

Sharing electrons (or reducing equivalents) is another potential mechanism by which microbes may interact, particularly in anaerobic sediments. Syntrophy, defined as "shared feeding", describes mutualistic metabolism between dependent partners (Morris et al., 2013). The first syntrophic interactions were discovered between fermentative bacteria and methanogenic communities (Bryant et al., 1967). This classic example of syntrophy involves cross-feeding of reducing equivalents, i.e., H_2 or formate, between fermenters, which produce H_2 from the fermentation of simple organic monomers, and methanogens, which utilize these products as electron donors (Stams and Plugge, 2009). In this example, methanogens take advantage of products of fermenters to reduce CO_2 to CH_4. By consuming the pool of H_2, methanogens shift the energy yield of the fermentative reaction towards thermodynamic favorability (Stams and Plugge, 2009; Morris et al., 2013). Therefore, the two microorganisms working cooperatively are able to thrive together in a low energy yield system. In the recent two decades, syntrophic interactions are found to be widespread in anoxic environments (Morris et al., 2013; Kouzuma et al., 2015). Other syntrophic relationships include the sharing of sulfur intermediates, or humic substances. For example, in a co-culture, sulfur-reducing bacteria co-existed with green sulfur

bacteria when both species sustained a desirable level of sulfide, which at high concentrations can inhibit sulfur reduction (reviewed in Morris et al., 2013).

In addition, syntrophic relationships can exist as electrical connections in the form of direct interspecies electron transfer (DIET) (Lovley, 2017b). The discovery of DIET was found in a co-culture with *Geobacter metallireducens* and *Geobacter sulfurreducens* (Summers et al., 2010). Together, *G. metallireducens* oxidizes ethanol and donates electrons to *G. sulfurreducens* to perform reduction of fumarate. During co-culture, *G. sulfurreducens* acquired a genetic mutation that promoted the expression of OmcS, a c-type cytochrome involved in electron transfer. Close aggregates of the two cells were packed with electrically conductive pili and cytochromes. Even before the discovery of DIET, extracellular electron transport was evident in anaerobic microbial cultures with amended electrodes (Bond et al., 2002; Gregory et al., 2004), through the mechanism of c-type cytochromes (Leang et al., 2003) as well as the use of pilin-associated nanowires by anaerobes as a conduit for electron transport (Reguera et al., 2005; Gorby et al., 2006). An increasing number of syntrophic electron-sharing communities have been uncovered (Shrestha and Rotaru, 2014; Lovley, 2017a).

Cooperative interactions can be stimulated with amendments of conductive materials such as magnetite or granular activated carbon (Kato et al., 2012a; Kato et al., 2012b; Liu et al., 2012; Liu et al., 2015). When *G. metallireducens* was co-cultured with *G. sulfurreducens*, they attached to granular activated carbon and metabolism was stimulated (Liu et al., 2012). A syntrophic relationship was also observed between *G. metallireducen*s and *M. barkeri* in the presence of granular

activated carbon (Liu et al., 2012). In addition, a recent study found aggregates of *G. metallireducens* and *M. barkeri* to share electrons, but when the partners were cultured with a mutant strain of *G. metallireducens* unable to produce pili, no syntrophic interaction was observed (Rotaru et al., 2014). DIET was stimulated again in the culture with the addition of granular activated carbon. The presence of conductive materials appears to be energetically beneficial for the electron-sharing community since it is much more energetically costly to produce pili or cytochromes. Likewise, magnetite stimulated growth in co-cultures of *G. metallireducens* and *G. sulfureducens* (Liu et al., 2015). Another study found a magnetite-induced syntrophic relationship between methanogens and *Thiobacillus denitrificans* which allowed the oxidation of acetate coupled to the reduction of nitrate (Kato et al., 2012b).

Another example of syntrophic aggregates is the relationship between sulfate-reducing bacteria (SRB) and anaerobic methanotrophic archaea (ANME) (Boetius et al., 2000) which have generally been attributed to the sharing of reducing equivalents such as H_2 or acetate (Hoehler et al., 1994; Nauhaus et al., 2002). It is thought that anaerobic oxidation of methane operates as methanogenesis in reverse, supplying H_2 to sulfate-reducing partners (Hoehler et al., 1994; Kevorkian et al., 2020). However, the true mechanism underlying this syntrophic relationship remains poorly understood. One proposition suggests that ANME are responsible for reducing sulfate to elemental sulfur or disulfide, then this sulfur intermediate becomes disproportionated by a Deltaproteobacteria partner (Milucka et al., 2012). Recent works identified that the ANME/SRB consortium may operate through DIET (McGlynn et al., 2015; Wegener et al., 2015). Despite proximity of the aggregated

cells, it is possible the microbial partners utilize multi-heme cytochromes for direct electron transfer (McGlynn et al., 2015). Within an ANME and SRB consortia, genomic results revealed highly expressed genes for extracellular cytochromes in both partners (Wegener et al., 2015). Furthermore, new evidence showed that ANME are capable of growing with added electron acceptors such as ferric iron or humic substances while their sulfate-reducing partners were inhibited (Scheller et al., 2016).

The mechanisms by which species share electrons is an active area of research. Proposed routes of interspecies electron transfer are by biological means or through conductive materials (Shrestha and Rotaru, 2014; Lovley, 2017b). Physically, conductive materials such as magnetite, biochar, granular activated carbon can facilitate the metabolism of syntrophic communities in co-cultures. Biologically, syntrophic partners may transfer electrons through the means of close cellular contact, the use of pili, or the use of c-type cytochromes (Leang et al., 2003; Reguera et al., 2005; Gorby et al., 2006; Shrestha and Rotaru, 2014). There are currently three model mechanisms of extracellular electron transport. One, *Geobacter sulfurreducens* produce conductive nanowires constructed by c-type cytochrome OmcS, which are important in transporting electrons to extracellular electron acceptors (Wang et al., 2019). Two, *Shewanella oneidensis* MR-1 transport electrons extracellularly with nanowires based on the MtrCAB porin-cytochrome system with cytochrome OmcA and flavins (Gorby et al., 2006; Xu et al., 2016). Three, Gram-positive *Listeria monocytogenes* affiliated to Firmicutes use a flavin-based electron transport system facilitated by the FmnB and PplA lipoproteins (Light et al., 2018). Overall, processes related to DIET remain elusive but new findings lead to exciting new research.

Ecosystem Engineering

Some microbes can also exert a strong influence on the microbial community structure and biogeochemical cycling through ecosystem engineering (Gokul et al., 2016; Roncoroni et al., 2019). Ecosystem engineers are defined as species that affect community composition through their influence on the environment and distribution of resources to other taxa. Ecosystem engineering results in the creation, maintenance, or modification of habitats (Jones et al., 1994). Ecosystem engineering can affect living spaces, control temperature, light, water, or nutrient availability, among other influences (Jones et al., 1994; Jones et al., 1997). Ecosystem engineers can alter the structure of the environment with their biomass, for instance, tree growth (Jones et al., 1997), coral reefs (Wild et al., 2011), and oyster reefs (Scyphers et al., 2011; Walles et al., 2015) leads to creation of habitats. Ecosystem engineers can also transform the environment from one state to another, such as the creation of dams by beavers (Wright et al., 2002), creek formation by burrowing crabs (Vu et al., 2017), burrow construction by fiddler crabs (Kristensen et al., 2008), and bioturbation by worms (Thayer, 1979). Through the modification of habitats, ecosystem engineers inevitably destroy some niches but at the same time also create new ones (Jones et al., 1997).

Studies on ecosystem engineers traditionally focused on classical ecology of macro-organisms like burrowing worms as physical ecosystem engineers (Passarelli et al., 2014). Apart from macro-organisms, many microorganisms can also be classified as ecosystem engineers, serving as drivers of nutrient dynamics and biogeochemical cycling. Ecosystem engineers that alter the physical environment are also prevalent in the microbial realm. For example, bacterial assemblages that form

biofilm with extracellular polymeric substances can aid in sediment stabilization and, therefore, prevent sediment erosion (Gerbersdorf et al., 2009). Ciliates affect the spatial heterogeneity of bacterial biofilms by crawling and grazing across the structure (Weerman et al., 2011). Ecosystem engineering microorganisms can also change the availability of resources for others or by modifying abiotic environmental conditions (i.e., pH, redox potential), thereby, affect biogeochemical cycling mediated by other microbial species. Filamentous cyanobacteria found on glacial ice caps are crucial in the formation of cryoconite aggregates, which harbors a diverse network of heterotrophs that participate in carbon and nitrogen cycling in Arctic conditions (Gokul et al., 2016). Notably, ecosystem engineering is distinguished from trophic interactions or competition. The concept of ecosystem engineers focuses on the alteration of resource availability and/or habitat modification to other organisms which can have positive or negative consequences to other species (Jones et al., 1997).

Keystone Species

Although the keystone species concept was first introduced in the 1960s (Paine 1969), since its inception, the usage of the term in ecology literature has been fraught with vague or shifting, sometimes contradictory, definitions (reviewed in Cottee-Jones and Whittaker 2012). Keystone species are most commonly described as species which exert disproportionately large impact on the community, relative to their abundance (Power et al., 1996; Krebs, 2009). A microbial keystone species or taxon impacts the structure and functioning of the community, which can include effects from abundant or rare keystone taxa (Banerjee et al. 2018). Specifically, microbes belonging to the rare biosphere driving biogeochemical cycling can be

responsible for ecosystem processes (Jousset et al., 2017). For example, methanotrophs representing <0.5% of total microbial community provided disproportionately large effects in regulating methane oxidation from flooded sediments (Bodelier et al., 2013). In contrast to the definition of an ecosystem engineer, a species may be defined as keystone if its major impact occurs through trophic interactions, such as a top predator (Wright and Jones 2006). Here, I will use the following definition to evaluate if a microorganism is a keystone species (or taxon): a species that exerts large effects on the community function or structure relative to its biomass.

Thesis Objectives

In this thesis, I aimed to test if the growth of marine cable bacteria (*Ca.* Electrothrix) influences the associated microbial community composition. Cable bacteria impose a strong influence on the local biogeochemistry raising the possibility that they may influence the microbial community as ecosystem engineers. Additionally, as long-distance electron conductors, I hypothesized cable bacteria may act as electron sinks for chemoautotrophic bacteria co-located at anaerobic depths. This hypothesis arises from the results of a manipulation experiment, in which chemolithoautotrophic activity linked to Epsilon-and Gammaproteobacteria sulfur oxidation was found to be stimulated in the presence of cable bacteria (Vasquez-Cardenas et al., 2015). When cable bacteria activity was arrested, the authors found that chemoautotrophic activity was also interrupted, suggesting a potential direct interaction. To identify microbes that are correlated with cable bacteria, I conducted a time series incubation experiment using slurried sediment cores. Cable bacteria growth was inhibited in a set of sediment cores with a barrier filter to prevent growth

below 0.5 cm, and cable bacteria were allowed to grow freely in another set of cores without filters. I hypothesized that growth of members of the sulfur-oxidizing community is coupled to the growth of cable bacteria. Due to ecosystem engineering effects of cable bacteria, I also hypothesized that sulfate-reducing bacteria will be positively correlated with cable bacteria as sulfate generated through sulfide oxidation will benefit the growth of sulfate-reducing bacteria. As sulfate-reducers are likely to outcompete methanogens for electron donors, I hypothesized that cable bacteria and methanogens will be negatively correlated, leading to an indirect association between the two.

Experimental Procedures

Methods Overview

To investigate potential microbial community interactions with marine cable bacteria, I performed an incubation experiment in which I allowed cable bacteria to grow freely in one set of sediment cores and, in another set of sediment cores, I embedded a 0.2 μm filter at 0.5 cm depth as a barrier to prevent downward growth of cable bacteria. Employing a destructive sampling design, I tracked cable bacteria growth over time and through depth using microscopy. This was combined with microsensor profiling, and porewater sampling to track the changes in the sediment associated with cable bacteria growth. Amplicon sequencing of DNA and RNA, across time and through depth was used to examine the changes in community composition that occurred concomitantly with cable bacteria growth. In the sediment cores where cable bacteria were allowed to grow freely, they grew prolifically. I was able to capture the growth time course of cable bacteria starting with a lag phase of 6

days, an exponential growth phase between Days 10-20, and followed by senescence (detected on Day 46). I used Spearman's Rank correlation based on normalized transcript data of all microbial taxa to assess which microbes are potentially associated with the marine cable bacteria.

Sediment Collection and Experimental Setup

Sediment used in the experiment was collected in August 2018 from the main channel of the Chesapeake Bay at a mesohaline site that experiences severe seasonal hypoxia (CB4.3C; 38° 33' 18.18" N, 76° 25' 40.584" W). Samples were collected using a Uwitec gravity core sampler (nylon core liners: 60 cm length; 9 cm inner diameter). The upper 10 cm of sediment was sub-sectioned and stored in a sealed glass container in a fridge (dark, 4°C) until the experiment was performed in December 2018. The *in situ* conditions of this site are described elsewhere (Malkin et al., in preparation). Sediments are sulfide rich and are nearly devoid of burrowing macrofauna. *Beggiatoa*-like filaments were present *in situ*, but at low density, and were not observed by microscopy later during the experiment. Cable bacteria (*Candidatus* Electrothrix) were not detected by amplicon sequencing at the time of sampling but were observed at high relative abundance in the winter and spring (up to 2.0% of 16S rDNA reads; Malkin et al. in prep). Pilot experiments further revealed that cable bacteria would readily grow in these sediments, given aerobic overlying water conditions.

To set up the experiment, the collected sediment was homogenized with a spatula in a glass tank and packed into polycarbonate core liners (8 cm height; 2.5 cm diameter). During homogenization, oxygenation of the sediment was limited by directly circulating the headspace of mixing tank with nitrogen gas. The core tubes

were sealed with neoprene rubber stopper at the bottom, and open at the top. A total of 70 sediment core tubes were prepared. A subset of sediment cores (n=35) was set up to block downward cable bacteria growth following a design adapted from Pfeffer et al. (2012). To accomplish this, a 2.5 cm diameter polycarbonate filter, with 0.2 μm porosity (Millipore, St. Louis, MO, USA) was embedded at 0.5 cm depth, which was below the oxygen penetration depth. Filters were secured in place with a specially constructed filter-holder with a rubber O-ring to ensure a water-tight seal.

All cores were incubated in two identical aerated aquaria filled with artificial seawater (Red Sea Salt, Red Sea, Houston, Texas) adjusted to *in situ* bottom salinity of 15.5 ppt in a climate-regulated environmental chamber at 16°C under dark conditions. Both tanks were kept oxygenated by continuous bubbling of the overlying water with needle attached to tubing at 3 spots across the aquarium. All sediment cores including those with the embedded filter barriers were randomly distributed between the two tanks. The aquaria were covered with plastic food wrap and monitored for water evaporation daily and replenished with freshwater if needed.

At each of seven time points (Days 1, 3, 6, 10, 14, 20, 46), three sediment cores were randomly selected for sampling. Microsensor profiling was first performed on the cores, followed by sectioning for geochemistry, microscopy, and nucleic acid analyses. Sediment cores with barrier filters were similarly sampled on Days 3, 20, 46 for microscopy and nucleic acid analyses. Sediment samples were sectioned at 0.5 cm increments from the surface to 2 cm for nucleic acids and microscopy and at 0.5 cm increments to 3 cm for porewater geochemistry analyses.

Cores sectioned for porewater geochemistry were sectioned in an anaerobic glove bag (Glas-Col LLC) under a nitrogen atmosphere.

Cell Enumeration

Samples for microbial enumeration were preserved in 96% ethanol (1:1 v/v), gently mixed with sterile autoclaved toothpicks, and stored at -20°C. For analysis, sediment-associated microbial cells were carefully separated from sediment grains, collected on filters, stained with either targeted oligoprobes or general DNA stain (SYBR Green), and mounted on slides for examination.

Cells were separated from sediment particles using procedures modified from Kallmeyer et al., (2008) and Lunau et al., (2005). Samples were initially diluted 1:5 in NaCl solution (20 ppt). Carbonates were dissolved with a mild acid (acetate buffer: 20 mL/L glacial acetic acid and 35 g/L sodium acetate in NaCl, adjusted to pH 4.6) for 2 hours, which were subsequently separated by centrifugation (3000 g for 5 minutes). Pellets were washed twice with a NaCl solution (20 ppt) by gentle mixing with autoclaved toothpicks, followed by centrifugation (3000 g for 5 minutes). Supernatants were collected from all rounds of washing. Following carbonate removal, cells were detached from sediment particles using a detergent mixture (37.2 g/L disodium EDTA dihydrate, 44.6 g/L sodium pyrophosphate decahydrate, 1% Tween 80 [v/v], 50 µL of methanol, and 400 µL of NaCl added to 50 µL of sediment). The sediment pellet was resuspended into the slurry by gentle stirring with an autoclaved toothpick. Sample slurries were incubated with rotisserie mixing at room temperature for at least 30 minutes. Cells were recovered from slurries via density centrifugation. To accomplish this, Nycodenz® (50% w/v) was added to below the slurries with a 12-gauge needle (due to high viscosity of the solution) and

subsequently centrifuged at 3000 g for 10 minutes. The aqueous phase was carefully collected and combined with supernatant collected earlier. Density centrifugation was repeated twice. Finally, cells from the supernatant were collected on a filter (0.2 μm black polycarbonate Whatman Nuclepore) and allowed to air-dry. Separate filters were prepared for cable bacteria and total cell enumeration, to obtain appropriately diluted filters. A dilution of 1:5 was prepared for filters for cable bacteria enumeration. A dilution of 1:50 – 1:100 was used for filters for total cell enumeration.

Filters were kept frozen until staining (-20ºC), at which time, filters were divided into sections for either cable bacteria cell counts, or total cell counts. Cable bacteria filaments were quantified via fluorescence *in* situ hybridization (FISH), following SILVA protocol (Fuchs et al., 2007). The oligonucleotide probe DSB706, which is specific to most *Desulfobulbaceae* and *Thermodesulforhabdus*, was used with a 40% formamide solution (Manz et al., 1992). Total cell counts were performed following staining with 1:200 diluted SYBR Green I in 1X TAE (adjusted to pH 7.5) (Molecule Probes). Cells were stained in the dark for 30 minutes and air-dried completely. Stained filters were mounted with ProLong™ Gold Antifade Mountant (Molecular Probes) and stored at -20°C. Cable bacteria were enumerated in 100-200 fields (depending on the density of filaments) at 630X magnification following up-down transects conducted across the filter. Total cell counts were enumerated at 1000X magnification to capture at least 400 cells in 10-20 randomly selected fields, using a Zeiss Axiophot Fluorescent Microscope equipped with a digital Zeiss AxioCam MR camera. Cable bacteria filament lengths were measured in Zeiss Zen Pro Software (2012).

At each depth, cumulative cable bacteria filament densities (m cm^{-3}) were calculated to determine total cable bacteria length (m) per volume of sediment (cm^3) examined, thereby allowing comparison with earlier published observations. Depth-integrated cable bacteria cell density was also determined by multiplying density (m cm^{-3}) with depths (cm). Then, cable bacteria cell abundance (cells cm^{-3}) were determined by assuming an average length of 3 µm per cable bacteria cell. Cable bacteria growth rate and doubling time during exponential growth were calculated using FISH counts.

Microsensor Profiling

High-resolution microsensor profiling of O_2, pH, and H_2S was performed on sediment cores with commercial microsensors operated with a motorized micromanipulator (Unisense A.S., Denmark). Three sediment cores were examined by microsensor profiling per sampling time point. Oxygen microsensors had 50 µm tip diameter, and oxygen was profiled at 100 µm resolution to below the oxygen penetration depth, while overlying water was aerated gently. The pH microsensors had 200 µm tip diameter and H_2S had a 50 µm tip diameter. Both pH and H_2S profiles were measured at 200 µm resolution until 2 mm, then at 400 µm until 4 cm. H_2S measurements were performed in darkness, maintained with black-out curtains around the room. The initial height of the microsensors were adjusted to the sediment surface, using a stereo microscope (10X) mounted sideways to observe the sediment water interface.

The pH microelectrode was calibrated with NBS standards (pH 4, 7, 10). The H_2S microsensor was calibrated with a range of Na_2S standards at 5 concentrations within the range of 0 to 300 µM. The measurements for the sum of H_2S were

corrected with corresponding pH, as previously described (Malkin et al. 2014). The O_2 microelectrode was calibrated with a 2-point calibration using 100% air saturation of bubbled seawater and the anoxic region of sediment. Total diffusive oxygen uptake (DOU) was calculated from O_2 microsensor profiles using Fick's First Law, as previously described (Malkin et al. 2014), using an estimated porosity of 0.9.

In sediment cores with barrier filters, microsensor profiling was performed on days 3, 10, 20, 46 and in two sections, above filter and below filter. The top 0.5 cm portion of sediment were microsensor profiled until ~0.4 cm. To perform microsensor profiling below embedded filter, the filter was first removed, and overlying water was bubbled with nitrogen gas to create anoxic condition before profiling. Microsensor profiling below the filter was measured starting from ~ 0.6 cm.

Porewater Analyses

Sediments used for porewater analyses were sectioned under anaerobic conditions in a glove bag and collected in 15 mL polyethylene centrifuge tubes (Falcon). Porewater was extracted by centrifugation (3500 rpm for 10 minutes). Subsequently, sealed centrifuge tubes were returned to the glove bag, where porewater was filtered (0.2 µm Target2™ Nylon Syringe Filters) into acid-cleaned 7mL polyethylene tubes, and then aliquoted. For nutrient and anion analyses, filtered porewater was pipetted into 2 mL cryotubes and frozen (-20ºC) until analysis. For ferrous iron analysis, porewater was preserved in 2 mL cryotubes with trace-metal grade nitric acid (final pH<2) and stored at room temperature until analysis. NH_4^+ concentrations were measured colorimetrically following the ammonium indophenol blue colorimetric method (Solorzano, 1969). Dissolved Fe^{2+} concentration was quantified with the Ferrozine assay (Stookey, 1970). NH_4^+ and Fe^{2+} colorimetric

assays were measured with Thermo-Scientific GENESYS UV/Vis spectrophotometer at wavelengths of 640 nm and 562 nm, respectively.

16S rRNA gene (DNA) and transcript (mRNA) Amplicon Sequencing

Samples collected for nucleic acid sequencing were frozen immediately after sampling in a liquid nitrogen dry-shipper and stored frozen (-80°C). DNA and RNA were extracted separately from 0.2 mL slurried sediments, according to methods adapted from Lever et al. (2015). All reagents were sterilized by autoclave or filtration (0.2 μm). During RNA extraction, all working surfaces and equipment were decontaminated with RNase AWAY™.

For both DNA and RNA, the extraction proceeded as follows: 0.2 mL aliquots of sediment samples were first combined with 0.1 M sodium pyrophosphate solution to prevent nucleic acid adsorption to mineral particles. Carbonates were dissolved from sediments with a mild acetic acid mixture, as described in Kallmeyer et al., (2008), adjusted to pH 4.7, incubated for 2 hours under gentle mixing with rotisserie assembly, and then washed in TE buffer with gentle mixing for 1 hour (Lever et al., 2015). Cells were pelleted by centrifugation (10,000 g for 20 minutes; Eppendorf 5424R) and the supernatant containing soluble (i.e., extracellular) DNA was discarded. Cell lysis was subsequently accomplished using a lysis solution of 0.5% Triton X-100 and guanidium hydrochloride dissolved in a Tris-HCL and EDTA solution adjusted to pH 10, combined with bead beating (0.1 mm zirconium silicate beads coated with PBS; 10 seconds high-speed vortex), followed by a heat-freeze-thaw cycle (50 ºC for 60 minutes, -80 ºC for at least 20 minutes, 4 ºC until thawed). The heat-freeze-thaw procedure was repeated 3 times. Following centrifugation (10,000 g for 20 minutes at 4ºC), the supernatant containing the intracellular nucleic

acid was carefully pipetted. Extracted DNA or RNA was purified with chloroform-isoamyl alcohol (CI) (1:1 v/v). Following CI addition, samples were emulsified by vortex (Vortex Genie II, maximum speed for 10 seconds), then separated by centrifugation (10,000 g for 10 minutes at 4ºC). The top aqueous phase containing the nucleic acid was carefully pipetted to a new sterile tube. A second round of CI emulsification was performed with the newly pipetted aqueous phase to ensure purification. Following centrifugation, the top aqueous phase was pipetted to a new tube. CI was kept ice-cold for RNA extraction.

The procedures for DNA and RNA precipitation differed slightly. DNA was precipitated with linear polyacrylamide (LPA, 20 µL mL^{-1}) together with PEG-8000 NaCl, and incubated overnight at 4 ºC, then centrifuged (14,000 g for 30 minutes at room temperature). The supernatant was discarded, and the remaining pellet was washed with 70% ethanol and centrifuged at 14,000 g for 10 minutes, repeated twice. Extracted samples were air-dried within an hour. Pellets were then dissolved in 100 µL of autoclaved DI and used for downstream analysis. The nucleic acids were quantitated by fluorometry (Qubit 2.0), using Qubit dsDNA Broad Range assay. For DNA, further purification was found to be unnecessary. RNA was precipitated with LPA along with ice-cold isopropanol and 3M NaOAc. Samples were incubated in the dark overnight at -20 ºC, then centrifuged at 14,000 g for 30 minutes at 4 ºC. Supernatant was discarded and ice-cold 70% ethanol was added to wash pellets only once (centrifuge for 10 mins at 14,000 g). The pellet was air-dried then dissolved in 100 µL of nuclease-free PCR grade water. RNA quantity was measured fluorometrically using Qubit RNA Broad Range assay kit.

For RNA, further purification, and cDNA synthesis was necessary. Extracted RNA was further purified with Norgen CleanAll DNA/RNA Clean-Up and Concentration Kit (Norgen Biotek Corp., Canada), following manufacturer's Protocol C. Residual DNA in RNA extracts was digested with two rounds of DNAse treatment as recommended by Lever et al., 2015. DNase mixture included 2 µL TURBO DNase in 10 µl of TURBO DNase buffer (Invitrogen). Following DNase addition, samples were incubated and shaken gently (600 rpm for 30 minutes at 37 ºC; Thermomixer Comfort R). Genomic DNA and RNA were quantitated with Qubit dsDNA and RNA Broad Range assay kits using Qubit 2.0 fluorometer to confirm successful DNA removal. DNase-digested RNA samples were purified again with Norgen CleanAll DNA/RNA Clean-Up and Concentration Kit (Norgen Biotek Corp.).

Following clean-up and concentration of DNA-free RNA extracts, synthesis of cDNA was performed with reverse transcription-polymerase chain reaction following manufacturer protocol of SuperScript III First-Strand Synthesis System for RT-PCR (Invitrogen). The first reaction mixture (total volume of 10 µL) was composed of 1µL of 10 mM dNTPs, 1 µL of random hexamers (50 ng/µL), 6µL of DEPC water, and 2 µL of DNase-digested RNA. RNA-primer mixture was incubated in an S1000 thermocycler (Bio-Rad Laboratories, Hercules, California, USA) with the following sequence: 65 ˚C for 5min, 2 ˚C for 3min, 4 ˚C hold. Subsequently, cDNA synthesis mixture which consisted of 1µL of RNaseOUT (40 U/µL), 1 µL of SuperScript III RT (200 U/µL), 4 µL of 25 mM $MgCl_2$, 2 µL of 0.1M DTT, and 2 µL of 10X RT Buffer was added to each RNA-primer mixture (final volume of 20 µL). Samples were incubated in the thermocycler with the following sequence: 25˚C for

10min, 50˚C for 50min, 85˚C for 5min, 4˚C hold. Negative controls for each RNA sample were prepared with 18 µL of nuclease-free water and 2 µL of respective RNA samples as well as a no-template control. Finally, RNase H (Invitrogen) was added to each sample as well as negative controls to digest any remaining RNA template and incubated (37°C for 20 minutes; Bio-Rad) to improve downstream PCR amplification. RNA and cDNA quantities were again measured with Qubit Broad Range assays (Invitrogen, Life Technologies, Thermo Fisher Scientific, Waltham, MA, USA) to ensure quantity and quality.

For amplicon sequencing, the V4-V5 region was amplified using the modified primer pair of the Earth Microbiome Project (515F-Y/926R; GTG YCA GCM GCC GCG GTA A) / (CCG YCA ATT YMT TTR AGT TT; Parada et al., 2015). DNA amplicons were amplified, barcoded, and sequenced at Bioanalytical Services Laboratory at Institute of Marine and Environmental Technology (Baltimore, MD, USA). Two-steps of amplification was conducted, first for gene amplification and second for adding indices. Clean up was accomplished with AMPure XP beads (Beckman Coulter). DNA sequencing was performed on an Illumina Miseq platform (2 x 300 bp).

For RNA amplicon sequencing, cDNA products were amplified in-house. Samples were prepped in triplicates in an AirClean 600 PCR workstation following Platinum™ Green Hot Start PCR Master Mix protocol (Invitrogen, Life Technologies). The PCR reaction mixture (total volume 25 µL) consisted of 7.5 µL of nuclease-free water, 12.5 µL of 2X Platinum Hot Start Master Mix, 1 µL of 10 µM forward primer, 1 µL of 10 µM reverse primer, and 3 µL of cDNA template. Negative

controls were prepared with 3 µL of nuclease-free water instead of DNA template. The following thermocycler setting was used: 94˚C for 2 minutes, 25 cycles of 94˚C for 30 seconds, 55˚C for 40 seconds, 72˚C for 90 seconds, then 72˚C for 5 minutes, and ended with 4˚C hold. Triplicate PCR products were pooled together. Purity and assessment of amplification were verified with gel electrophoresis using a 1.5 % agarose gel ran on 120 V for 25 minutes. Loaded gel was carefully stained with EtBr solution for 15 minutes and visualized under UV light. Amplicon clean-up was carried out using Zymo Research DNA Clean and Concentrator-5 (Irvine, California, USA) following the manufacturer's instructions. cDNA amplicons were sequenced on an Illumina Miseq platform with v2 kit reagents (2 x 250 bp) by Genewiz Amplicon E-Z (South Plainfield, NJ, USA).

Bioinformatic Analysis

Raw sequence reads were processed using the DADA2 pipeline (Callahan et al., 2016) in *R* (v 3.6.3, R Core Team), separately for DNA and RNA datasets. Primer reads were trimmed from sequences using the filterAndTrim function. DNA sequences were truncated, based on inspection of sequence quality plots, at position 280 and 220 for forward and reverse reads, respectively. cDNA sequences were truncated at position 240 for forward reads and 220 for reverse reads. The maximum expected error rate parameter (maxEE) was set to a stringent level (2 for both forward and reverse reads). After paired reads were merged, chimeras were screened and removed. Long-tailed reads (>382 nt for DNA; >381 for cDNA; representing < 0.01% reads) were considered to be likely erroneous and removed. Amplicon sequence variants (ASVs) were taxonomically assigned using SILVA ribosomal SSU database (v 138, Pruesse et al., 2007; Glöckner et al., 2017). Phylogenetic trees were

constructed with Maximum Likelihood Inference using RAxML (v 8.0; Stamatakis, 2014) after sequence alignment with DECIPHER (Wright, 2015).

The package *phyloseq* (McMurdie and Holmes, 2013) in *R* was used to further prune data and to perform downstream analyses. Only ASVs belonging to the Domains of Bacteria and Archaea were kept. ASVs without Kingdom assignment and ASVs without Phylum assignment within Bacteria were considered errors and removed. Sequences identified as mitochondria (0.09% in DNA, 0% in RNA datasets), chloroplast (0.22% in DNA, 0.05% in RNA datasets), and ASV singletons (8.7% in DNA, 1.7% in RNA datasets) were removed. Differences in the communities with cable bacteria and without cable bacteria were assessed via principal coordinates analysis (PCoA) and PERMANOVA (permutations = 999) using the Bray-Curtis dissimilarity distance.

Correlation Analysis

Microbial associations between cable bacteria and their sympatric microbial community were explored using Spearman's Rank correlation based on fractional 16S rRNA transcript abundance data normalized with microscopy counts. Raw microscopy counts exhibited stochastic variability between depths over time, which likely reflected methodological variance, rather than changing population sizes. To eliminate the effect of this methodological variability on the correlation analyses, I fit the raw counts to two models based on their spatial and temporal distribution. First, total subsurface bacterial cell abundance was averaged for all depths through time. Among surface samples, a decline in cell numbers was observed during the first 10 days of the experiment. The raw counts were fit to a natural log decline between Days 3 and 10.

The fractional transcript abundance was multiplied by the bacterial cell abundance numbers (FTAxC) to obtain an estimate of the change of transcripts with depth and time. A similar procedure, though for DNA amplicons, was applied to quantify changes in abundance of Archaea with sediment depth (Kevorkian et al. 2021) Other estimates of absolute abundances of different microbial taxa have been based on 16S rRNA gene data (Props et al., 2017; Tkacz et al., 2018; Barlow et al., 2020). Here, I chose to examine the fractional transcript abundance and FTAxC to explore ecological interactions among the most active microbial populations.

I performed correlation analysis on the FTAxC of *Ca.* Electrothrix (marine cable bacteria) against the FTAxC of all other microbes on the ASV and genus level. Genera FTAxCs were calculated by agglomerating all ASVs from the same genus using the *tax_glom* function in *phyloseq*. Each set of correlations were performed independently among surface samples (0 - 0.5 cm) and samples from subsurface depths (0.5 - 2.0 cm). Spearman's Rank correlations and *p*-values were calculated using package *psych* (v2.0.9; Revelle, 2020) in R. False discovery rate (FDR) for multiple testing was calculated according to the Benjamini-Hochberg method (Benjamini and Hochberg, 1995).

Spearman's Rank correlation could yield spurious correlation driven by taxa responding to changes in the sediment unrelated to cable bacteria. Moreover, Spearman's Rank correlation assumes independence of the samples which was not the case in my time-series incubation study. To clearly identify microbes associated with cable bacteria, the FTAxC time course of the cable bacteria population was also used as a reference point. The FTAxC of correlated taxa with p-value < 0.05 were

scrutinized against the FTAxC of cable bacteria. For example, ASVs or genera were considered potentially associated with cable bacteria only if they were correlated ($p < 0.05$) and if their FTAxC followed the FTAxC of cable bacteria, including a change on the last time point after cable bacteria population plummets. In addition, abundance patterns of ASVs and genera estimated from subsurface samples were cross-checked with respective depths in the sediment cores where cable bacteria growth was inhibited. Specifically, an ASV or genus was not considered a potential associate if its FTAxC trend in sediment cores without cable bacteria behaved similarly to that of the sediment cores dominated by cable bacteria.

Furthermore, after adjusting the *p*-values with false discovery rate, the correlation dataset resulted in high FDR values throughout which suggested likelihood of numerous false positives. The nature of my experiment was underpowered and led to numerous correlations, but with weak strength. Correlated microbes that followed the FTAxC temporal trend of cable bacteria and were measured with FDR values < 0.6 were considered worthy of further scrutiny and discussion.

Results

Microscopy Counts

Cable bacteria filaments were not detected by FISH (using oligoprobe DSB-706; herein "DSB Cells"), on Days 3 or 6 (Figure 2, Table 1). Cable bacteria were first observed at the sediment surface on Day 10 (length density: 267.0 m cm^{-3}) and their abundance increased and progressed downward, reaching a maximum density of 1063.7 m cm^{-3} at 0.5 – 1.0 cm on Day 20, accounting for 35% of total microbial cells.

Depth-integrated cable bacteria filament density, estimated to 2 cm, was 133.5 m cm^{-2} and 1154.8 m cm^{-2} for Days 10 and 20. During exponential growth at the surface between Days 6 to 10, cable bacteria multiplied with a doubling time of <42 hours (growth rate, r=0.40 d^{-1}) (Figure 3, Table 2). In the subsurface samples, exponential growth took place between Days 10 to 20 in which the fastest rate of growth (r=2.38 d^{-1}) and doubling time (<7 hours) of cable bacteria was observed at 1.0-1.5 cm depth. By Day 46, cable bacteria density plummeted to 8.5 m cm^{-3} at the sediment surface, which represented <1% of all cells, and was not detected in subsurface sediment. In the cores with barrier filter, no cable bacteria filaments were encountered below the filter during the entirety of the experiment, indicating successful inhibition of cable bacteria below the filter (Figure 2g-i).

Figure 2. Direct microscopy counts of total bacterial abundance using SYBR Green staining and direct FISH counts of cable bacteria ("DSB cells") hybridized with DSB706 oligonucleotide probe. Panels a-f show cell abundances of sediment cores where cable bacteria grew down to 2 cm. Panels g-i depict cell abundance in cores with barrier where cable bacteria growth was prevented below 0.5 cm.

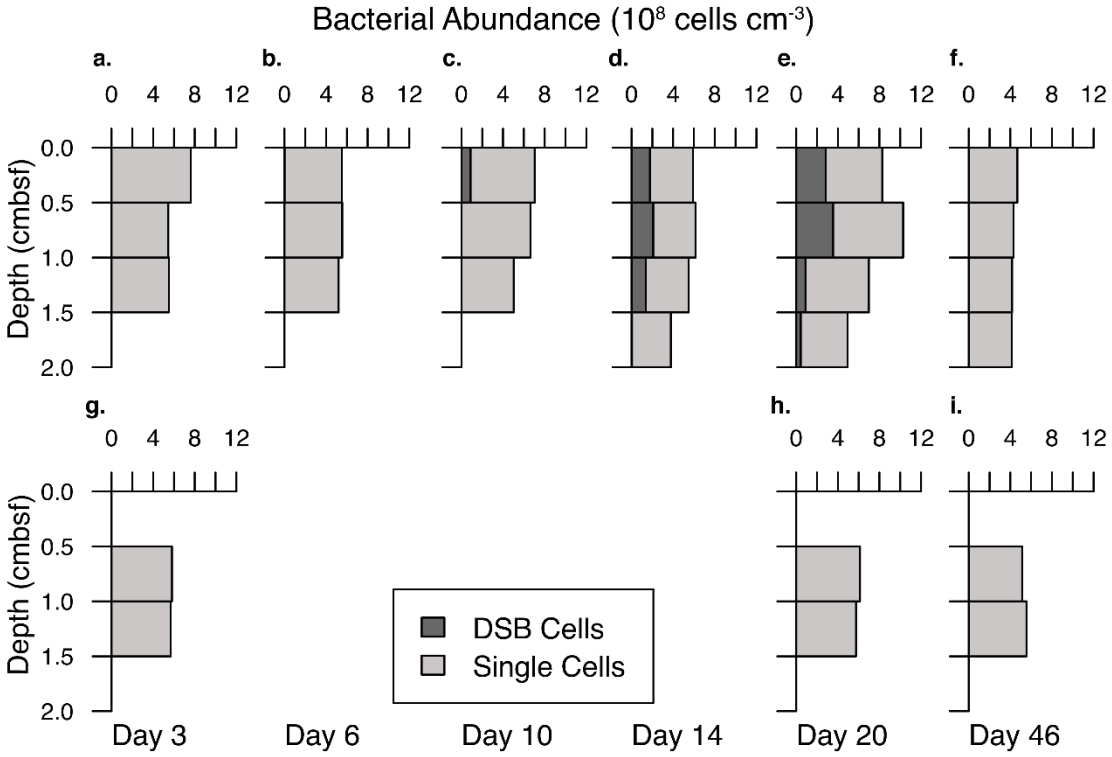

Time (day)	*Depth (cm)*	*DSB Density (m cm^{-3})*	*Depth-intergrated DSB Density (m cm^{-2})*
Day 3	0 - 0.5	1.0	0.5
	0.5 - 1.0	*n.d.*	
	1.0 -1.5	*n.d.*	
Day 6	0 - 0.5	3.1	1.6
	0.5 - 1.0	*n.d.*	
	1.0 -1.5	*n.d.*	
Day 10	0 - 0.5	267.0	133.5
	0.5 - 1.0	*n.d.*	
	1.0 -1.5	*n.d.*	
Day 14	0 - 0.5	526.4	788.0
	0.5 - 1.0	627.5	
	1.0 -1.5	407.4	
	1.5 - 2.0	14.6	
Day 20	0 - 0.5	848.2	1154.8
	0.5 - 1.0	1063.7	
	1.0 -1.5	265.8	
	1.5 - 2.0	131.8	
Day 46	0 - 0.5	8.5	4.3
	0.5 - 1.0	*n.d.*	
	1.0 -1.5	*n.d.*	
	1.5 - 2.0	*n.d.*	

Table 1. Cable bacteria "DSB cells" filament density (m cm^{-3}) distribution through time and depth and depth-integrated cable bacteria density (m cm^{-2}). Cable bacteria cells were hybridized with DSB706 oligonucleotide probe and measured with fluorescent in-situ hybridization (FISH) microscopy.

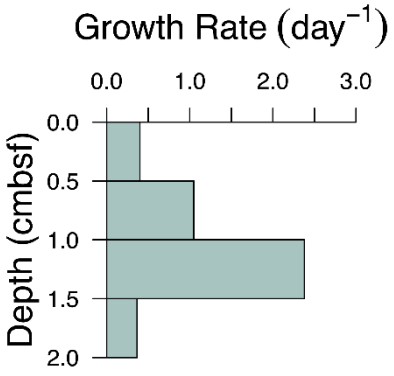

Figure 3. Cable bacteria growth rate (r) during exponential phase at each depth.

Table 2. Cable bacteria growth rate and doubling time during exponential growth phase at each respective depth.

Cable Bacteria Exponential Growth Rate at Each Depth			
Depth (cm)	***Growth rate (day^{-1})***	***doubling time (day)***	***doubling time (hour)***
0 - 0.5	0.40	1.73	41.5
0.5 - 1.0	1.05	0.66	15.9
1.0 -1.5	2.38	0.29	6.99
1.5 - 2.0	0.37	1.89	45.4

Geochemical Characterization

The combined microsensor profile data (O_2, pH, and H_2S) were indicative of the development and termination of cable bacteria activity in the sediment cores across the incubation period (Figure 4a-f). Cable bacteria activity may be identified by a pH maximum in the oxic zone, indicative of cathodic oxygen reduction or nitrate reduction, combined with an absence of sulfide, and a corresponding pH minimum indicative of anodic sulfide oxidation (Nielsen et al. 2010, Meysman et al. 2015). Sulfide was initially present to the sediment surface on Day 3. The sulfide horizon progressed downwards, creating a suboxic zone, defined as a space where oxygen and sulfide are not detectable. The suboxic zone was, on average, 6.8 mm thick on Day 10 and 23.3 mm thick on Day 20. Concomitantly, the pH profile developed a minimum near the sulfide horizon, initially pH 6.8 at 5.9 mm on Day 10, which progressed downwards and to lower pH values, reaching pH 5.5 at 15.0 mm by Day 20. A pH maximum in the oxic zone developed in one of three replicate cores on Day 14 and two out of three cores on Day 20, reaching pH up to 8.7. After 46 days of incubation, pH extreme values receded towards neutrality with an average pH 7.6 in the oxic zone and pH 6.1 in the suboxic zone.

In contrast, below the embedded filters, the cores with barriers did not indicate electrogenic sulfide oxidation by cable bacteria (Figure 4g-j). A suboxic zone was not observed in the profiles below the filter on any days. On Day 10, H_2S was detectable right below the filter at a concentration of 30 µM at 5.8 mm reaching up to 621 µM by 40 mm. H_2S was also detectable near the filter on both Days 20 and 46 between 5 to 6 mm and H_2S remained detectable through depth, reaching a mean of 358 µM on

Figure 4. Microsensor profiles of O2 (red), pH (black), and H2S (blue) on 6 sampling timepoints (Day 3, 6, 10, 14, 20, 46). Sediment cores showing geochemical fingerprint of increasing cable bacteria activity between Days 10 and 20 are depicted in panels a-f. Cores with barrier filter where cable bacteria growth was inhibited are depicted in panels g-j. Shaded regions indicate sections of sediment core sampled for DNA and RNA sequencing.

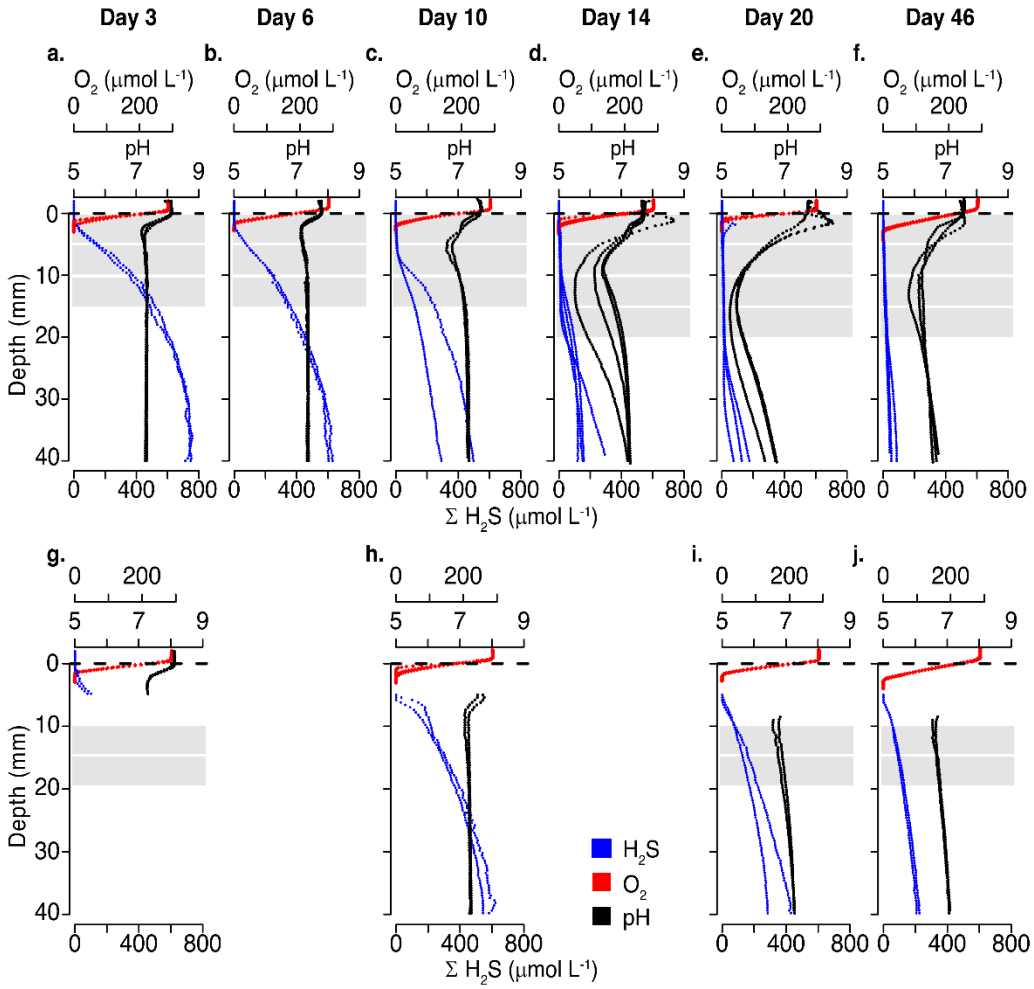

Day 20 and 216 μM on Day 46 by 40 mm. Also, a pH minimum was absent below the filter. In the surface sediment above the barrier filter, there was evidence of cable bacteria activity. For example, a low H_2S concentration at a mean of 23 μM was detected in the top 5 mm. Thus, the barrier was effective in preventing cable bacteria growth below. The microbial communities of the surface samples (0 -0.5 cm) from cores with barrier filters were not further examined because cable bacteria were allowed to grow above the filter and the communities are assumed to be the same as the cores without barrier filters.

Rates of diffusive oxygen uptake (DOU) extracted from the oxygen microsensor profiles exhibited different patterns between the two sets of sediment cores. In sediment cores where cable bacteria were allowed to grow, DOU rates increased between Days 6 and 20 from 17.0 ± 1.7 to 27.8 ± 4.0 mmol m^{-2} d^{-1} and then declined (Figure 5; Table 3). In the cores with barrier filters, DOU rates did not change from Days 3 to 20. On Day 20, DOU was 27.8 ± 4.0 mmol m^{-2} d^{-1} in the sediment cores with cable bacteria and 20.6 ± 2.1 mmol m^{-2} d^{-1} in the cores with barrier. A one-sided Student's t-test identified the values on Day 20 as being close to significantly different (t-test, df=4, t-value=2.614, $p < 0.08$). By Day 46, DOU in both

sets of cores declined, reaching similar rates (sediment cores with no barrier: 12.5 ± 1.2; sediment cores with barrier filter: 12.5 ± 1.6 mmol m^{-2} d^{-1}).

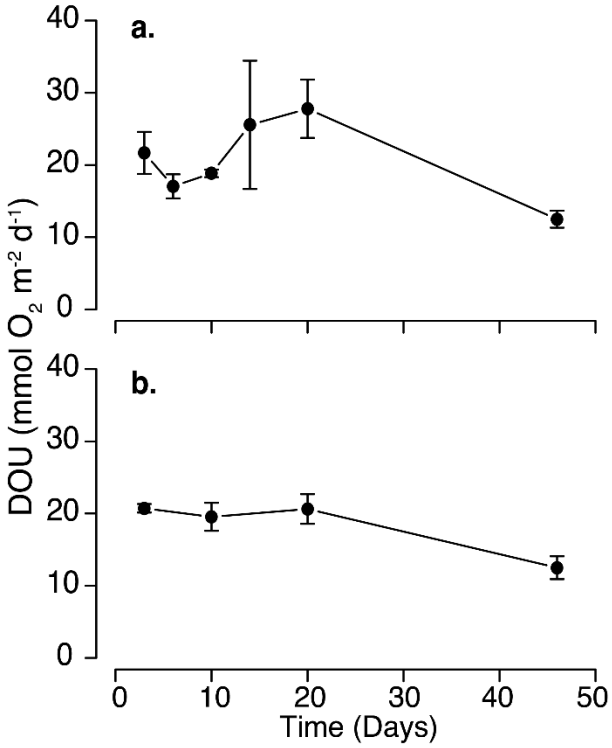

Figure 5. Diffusive oxygen uptake rates through 46 days of incubation. Fluxes were calculated from microsensor profiles using Fick's First Law. DOU increased from Day 10 to 20 and decreased by Day 46 in (**a**) sediment cores where cable bacteria were allowed to grow. In the cores with filter barrier (**b**) where cable bacteria growth was inhibited, DOU remained unchanging until a decrease on Day 46.

Table 3. Diffusive oxygen uptake rates calculated from microsensor profiles.

Sample Type	*Day*	*DOU (mmol O_2 m^{-2} d^{-1})*
Sediment Cores	3	21.7 ± 2.9
	6	17.0 ± 1.7
	10	18.8 ± 0.5
	14	25.6 ± 8.9
	20	27.8 ± 4.0
	46	12.5 ± 1.2
Sediment Cores with Barrier	3	20.7 ± 0.6
	10	19.5 ± 1.9
	20	20.6 ± 2.1
	46	12.5 ± 1.6

During the course of the experiment, porewater ammonium concentrations exhibited decreasing concentration through time in both cores with and cores without barrier filters (Figure 6a & b). On Day 1, ammonium concentration was 0.5 mM at the sediment surface, increasing to 1.9 mM by 3 cm depth. By Day 46, ammonium concentration had declined to 0.1 mM at the surface and 0.5 mM at 3 cm. The cores with barrier filters exhibited a similar pattern, but at a slightly lower concentration, with a maximum detected ammonium of 1.5 mM on Day 1 at 3 cm, and 0.5 mM on Day 46.

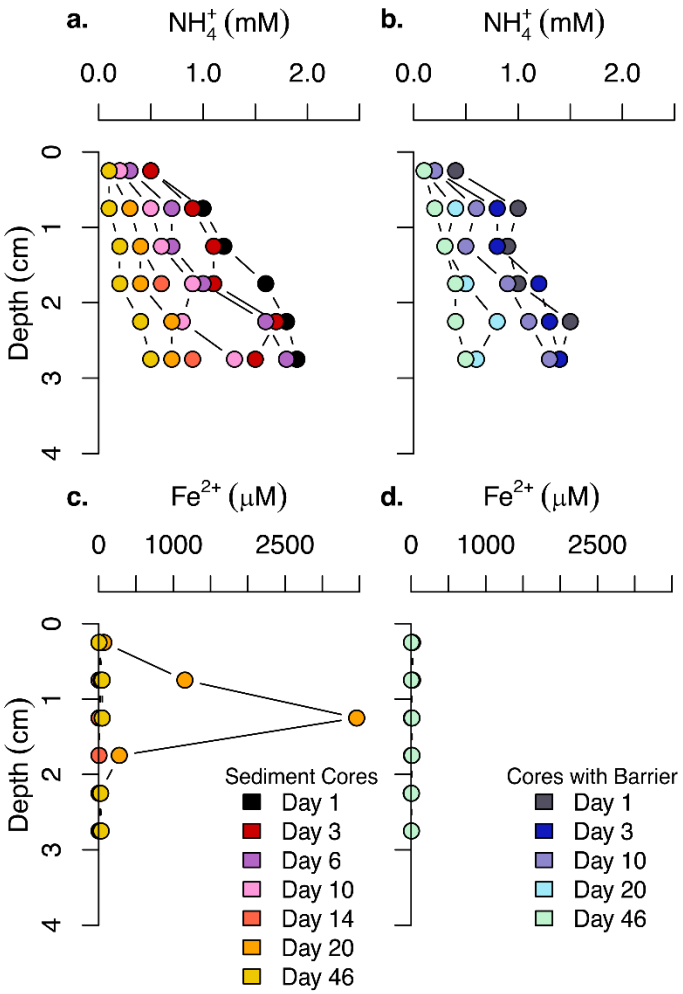

Figure 6. Porewater analyses of ammonium and dissolved iron. Ammonium concentration decreased over time in (**a**) sediment cores with cable bacteria and (**b**) cores with barrier filters at 0.5 cm depth. (**c**) A highly concentrated peak of dissolved iron was detected on Day 20 between 0.5 – 2.0 cm. (**d**) No dissolved iron was detected at any depth or sampling timepoints in the cores with barrier.

Porewater ferrous iron exhibited a major difference between the two sets of cores. On all dates in the cores with barrier filters, ferrous iron was not detected through depth. By contrast, in the sediment cores with cable bacteria at depth, ferrous iron was not detected through depth on all dates, except on Day 20, when the Fe^{2+} concentration profiles exhibited a maximum concentration of 3462 μM at 1.5 cm depth (Figure 6c). The ferrous iron maximum at 1.5 cm decreased to 48 μM by Day 46.

Microbial Community Composition (16S rRNA amplicons from DNA)

The dominant microbial taxa identified by amplicon sequencing were affiliated to groups belonging to the phyla Acidobacteriota, Bacteroidota, Calditrichota, Chloroflexi, Desulfobacterota, Proteobacteria, Latescibacterota, Planctomycetota, and Thermoplasmotota (Figure 7). Archaea were observed in all samples, with a mean of 5.7% of reads. The most abundant bacterial phyla were Bacteroidota (mean 18.2% of reads); Proteobacteria (14.3%); Chloroflexi (15.5%); Desulfobacterota, excluding *Ca.* Electrothrix (12.8%); Planctomycetota (7.3%); and Acidobacteriota (5.0%).

ASVs affiliated with *Ca.* Electrothrix were not detected on Days 3 and 6 at any depth in the sediment cores (Figure 7 & 9). Reads affiliated to this genus were first observed at the sediment surface on Day 10 (2.1% of reads) and increased in relative abundance then progressed downward over time, reaching a maximum 4.4% at the 1.0-1.5 cm depth interval on Day 20. *Ca.* Electrothrix reads were detectable down to the maximum depth examined (2.0 cm) by Day 20. By Day 46, *Ca.* Electrothrix reads were detected at <0.2% of reads at all depths. *Ca.* Electrothrix was

represented by three ASVs, of which one dominant ASV represented 99.9% of *Ca.* Electrothrix reads on average. Dominance did not change during the experiment. Nucleotide Basic Local Alignment Search Tool (BLASTn; National Center for Biotechnology Information) revealed 100% sequence similarity between the dominant ASV and both *Ca.* Electrothrix communis and *Ca.* Electrothrix aarhusiensis. Conversely, in the sediment cores with barrier filters (sequenced at depths below the filter barrier on Days 3, 20, and 46), ASVs affiliated with *Ca.* Electrothrix were not detected in any samples.

Figure 7. Microbial community composition based of 16S rRNA gene amplicon sequencing data (DNA). Cores were sectioned at 0.5 cm increments down to 2.0 cm and sequenced at 6 sampling timepoints. Cable bacteria presence was detected in intact sediment cores but not in cores with barrier below the depth of 0.5 cm. Cable bacteria growth began at the surface. Filaments grew deeper into the cores by Day 14 and Day 20, then the population declined by Day 46.

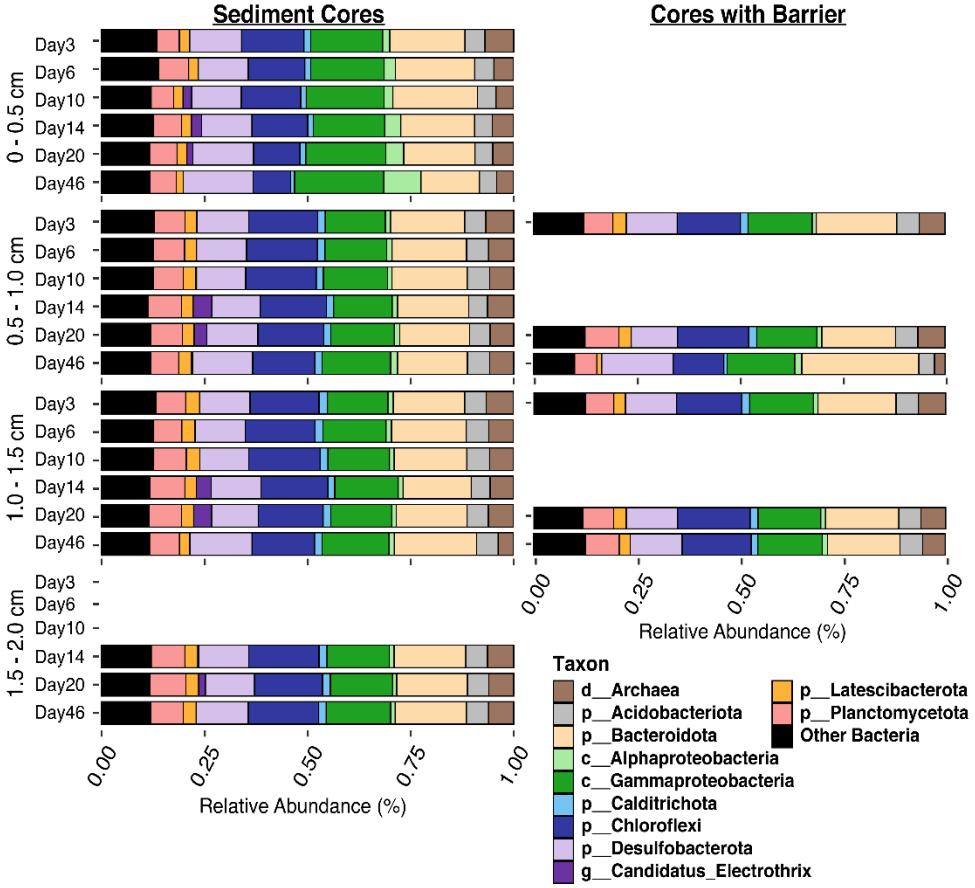

Microbial Community Composition (16S rRNA transcripts from RNA)

Ca. Electrothrix dominated the transcript amplicons on Days 10 to 20. Other major phyla were represented by Desulfobacterota excluding *Ca.* Electrothrix (18.6%), Proteobacteria (14.7%), Bacteroidota (10.9%), Chloroflexi (6.9%), and Latescibacterota (5.0%). Other taxa detected at >2% of the reads in at least one sample were affiliated with the phyla Acidobacteriota, Bdellovibrionota, Calditrichota, Campilobacterota, Nitrospinota, Nitrospirota, Planctomycetota, Spirochaetota, Asgardarchaeota, Crenarchaeota, Halobacterota, and Thermoplasmatota (Figure 8).

16S rRNA transcripts affiliated to *Ca.* Electrothrix largely followed the same temporal and spatial patterns as the DNA amplicons, but at relative abundance approximately an order of magnitude greater (Figure 8 & 9). RNA transcripts affiliated with *Ca.* Electrothrix were not detected on Days 3 and 6 in the sediment cores. Transcript reads affiliated to this genus were first observed at the sediment surface on Day 10 (18.4% reads), and increased in relative abundance, and progressed downward over time, reaching a maximum of 65.3% of the transcript reads at the 1.0-1.5 cm depth interval on Day 20. *Ca.* Electrothrix reads were detectable down to the maximum depth examined (2.0 cm) by Day 20. By Day 46, *Ca.* Electrothrix reads were greatly diminished, detected at a maximum of 2.4%. In the transcript dataset, forty-five ASVs were affiliated with *Ca.* Electrothrix. Similar to the DNA dataset, one ASV affiliated to *Ca.* Electrothrix was dominant representing 96.2% of *Ca.* Electrothrix on average. The same *Ca.* Electrothrix sequence was dominant in both DNA and RNA datasets. In the cores with barrier, reads affiliated with *Ca.*

Electrothrix were observed at <0.35% below the filter on Days 3 and 20 but were absent on Day 46.

Figure 8. Microbial community composition based of 16S rRNA transcript sequencing data (RNA). Cores were sectioned at 0.5 cm increments down to 2.0 cm and sequenced at 6 sampling timepoints. Initial cable bacteria activity was detected on Day 10. Cable bacteria activity dominated through depth and time where they accounted for 60% of the community by Day 20 at a depth of 1.0 – 1.5 cm. Relative abundance of cable bacteria decreased by Day 46.

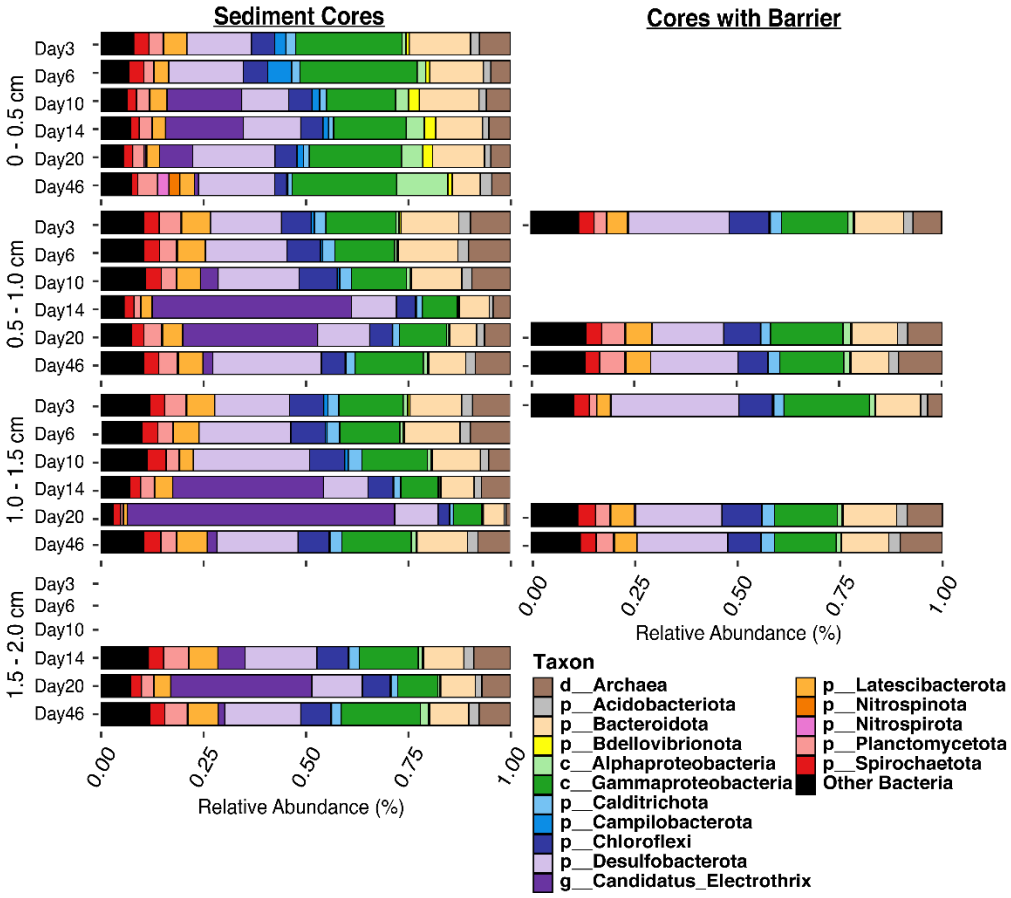

When comparing the RNA to DNA ratio of *Ca.* Electrothrix on Days 10, 14, and 20, there were higher proportions of cable bacteria RNA at the deepest depth during growth compared to the DNA proportions (Figure 10).

Figure 9. 16S DNA and RNA relative abundance of *Candidatus* Electrothrix (cable bacteria). The relative abundance of cable bacteria in the RNA dataset were an order of magnitude higher than the DNA relative abundance. Cable bacteria growth progression can be seen in both sets of data where initial growth began at the surface on Day 10, followed by an increase in abundance deeper into the sediment for the next 10 days. Finally, the cable bacteria population encountered a senescence phase by Day 46. Relative abundance of cable bacteria is plotted in light grey for the DNA dataset and dark grey for the RNA dataset.

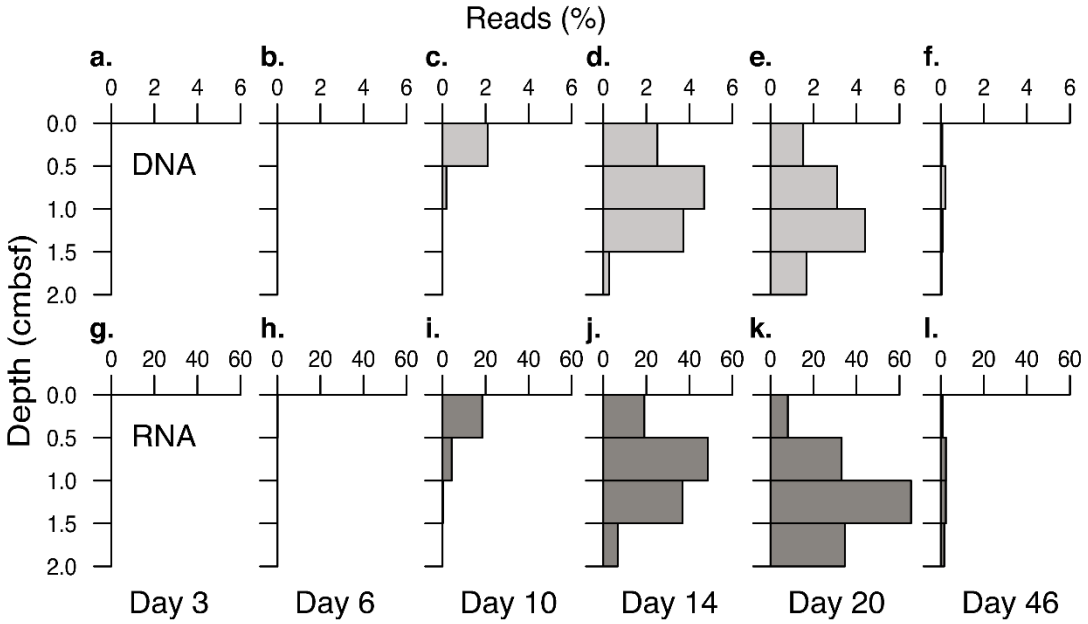

Figure 10. RNA to DNA ratio of *Candidatus* Electrothrix (cable bacteria) on Days 10, 14 and 20 when cable bacteria dominated the microbial population. The ratio between cable bacteria RNA to DNA increased with depth as cells penetrated deeper into the sediment to access sulfidic pools.

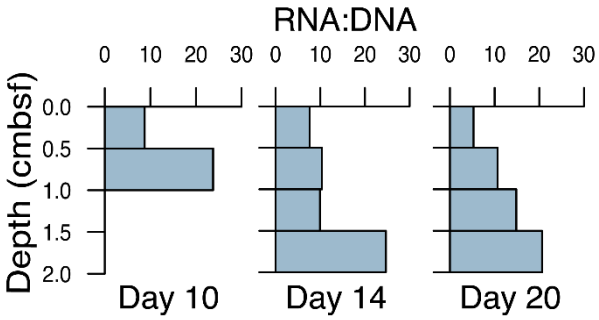

Principal coordinates analysis (PCoA) of the FTAxC dataset with Bray-Curtis dissimilarity distance exhibited three distinct clusters, representing surface samples, subsurface samples with abundant cable bacteria, and subsurface samples where cable bacteria were not detected (Figure 11). Among the subsurface samples, clustering patterns were mainly driven by the presence versus absence of cable bacteria. Comparing the FTAxC dataset in paired sediment cores with and without filter barriers revealed the communities were not quite detectably different (depths 0.5-1.5 cm, Days 3, 20, and 46; PERMANOVA; $p = 0.12$; Contrast 1, Table 4). By contrast, comparing paired sediment cores with cable bacteria against those without cable bacteria, the communities were significantly different (depths 0.5-1.5 cm; Days 3, 20, and 46; $p = 0.013$; Contrast 2, Table 4). This suggest that the presence of cable bacteria is driving the differences seen between the samples. To test for a residual influence of *Ca.* Electrothrix on the remaining community composition, the same samples were contrasted, but with *Ca.* Electrothrix reads excluded from the analysis. In this case, there were no significant differences in the community composition between samples with and without cable bacteria (depths 0.5-1.5 cm; Days 3, 20, and 46; $p = 0.065$; Contrast 3, Table 4).

The surface sediment microbial communities exhibited a different trajectory over time (Figure 11). Alphaproteobacteria abundance increased over the course of the experiment at the surface (Figure 8). Bdellovibrionota were abundant (> 2.6% transcript reads) on Days 10, 14, and 20. Day 46 was unique, with Nitrospinota and Nitrospirota appearing at > 2% of transcript reads.

Figure 11. Principal coordinates analysis (PCoA) of FTAxC data using Bray-Curtis dissimilarity distance. Samples are characterized by core types either with the presence of filter barrier where cable bacteria were inhibited below 0.5 cm (circles), or sediment cores without barrier where cable bacteria were absent (triangle) and where cable bacteria were present (squares). Surface samples with cable bacteria, below surface samples with cable bacteria, and below surface samples without cable bacteria formed distinct clusters.

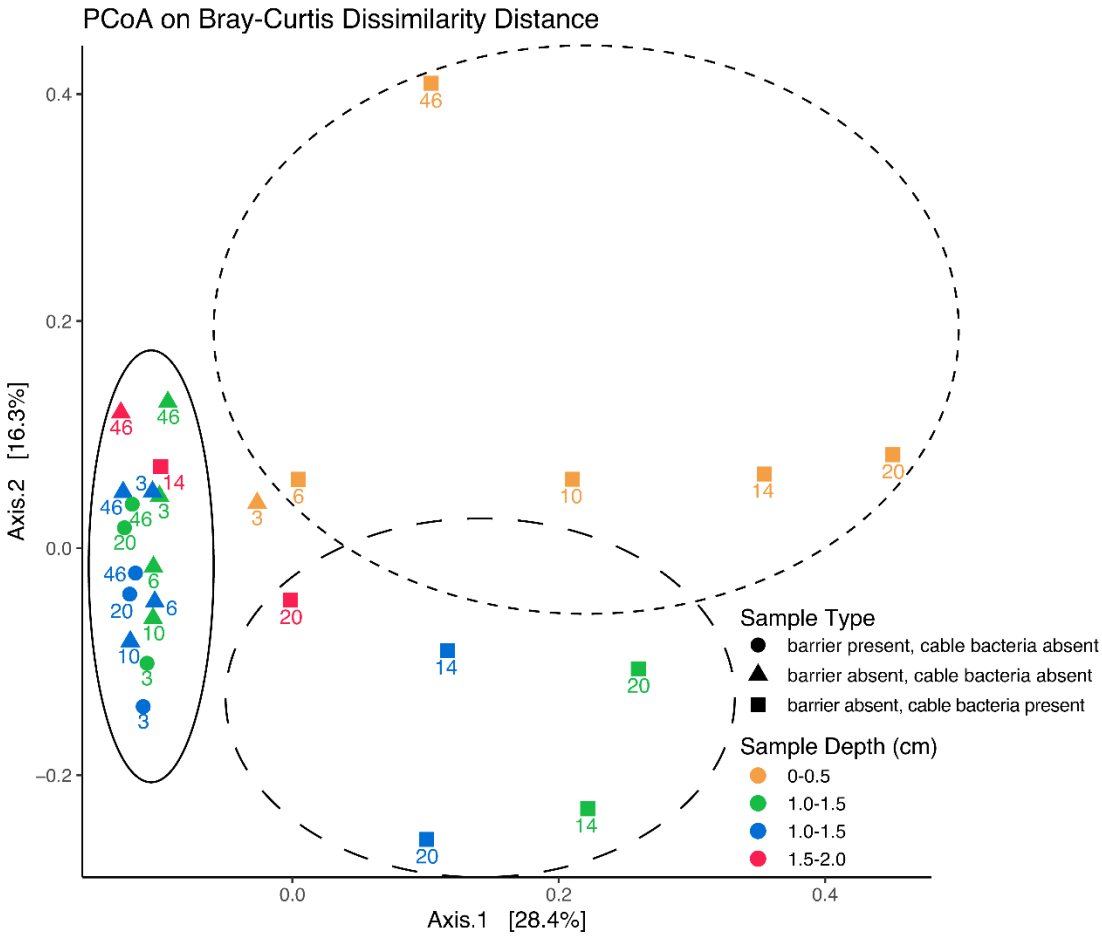

Table 4. Contrasts between microbial communities in paired sediment cores with and without a filter barrier as well as cores with and without cable bacteria using PERMANOVA. Communities contrasted include samples from 0.5-1.0 cm and 1.0-1.5 cm depths on Days 3, 20, and 46 of both sets of sediment cores (filter vs no filter embedded).

		PERMANOVA			
Community Contrast	***Parameter***	***Df***	***F.Model***	***Pr(>F)***	***Homogeneity of Dispersion Test, Pr(>F)***
Contrast 1	filter absence vs presence	1,10	1.3956	0.12	0.245
Contrast 2	cable bacteria absence vs presence	1,10	3.6731	0.013*	0.325
Contrast 3†	cable bacteria absence vs presence	1,10	1.6151	0.065	0.922

† Cable bacteria removed from dataset

Correlation Analysis between FTAxC of *Ca.* Electrothrix and Other Microbes

Microbes Positively Correlated with *Ca.* Electrothrix at the Sediment Surface

Among the surface samples, 43 ASVs were positively correlated (Spearman; $p < 0.05$; Appendix Table A1) with *Ca.* Electrothrix, of which 9 ASVs (FDR < 0.6) met the time course criteria for being likely associated with the growth of *Ca.* Electrothrix (i.e., increased in FTAxC during growth of *Ca.* Electrothrix and decreased in FTAxC during senescence of *Ca.* Electrothrix; Figure 12 & 13).

Figure 12. *Ca.* Electrothrix FTAxC time course through depth which was used as a reference point to examine for potential associated ASVs or genera with cable bacteria (see Methods).

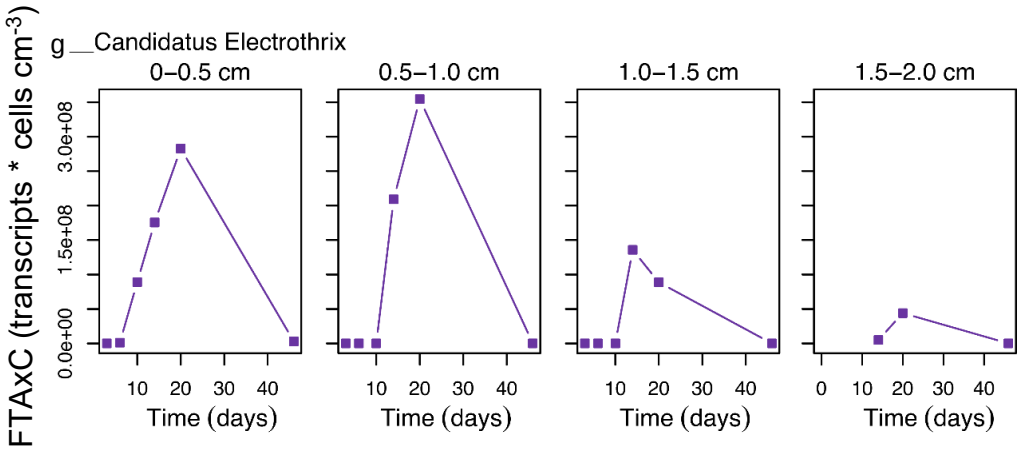

These ASVs were affiliated to the following phyla: Bdellovibrionota, Desulfobacterota, Myxococcota, and Proteobacteria. In further detail, a strongly significant and positive correlation was observed between two ASVs affiliated to the genus *Magnetovibrio* and *Ca.* Electrothrix (FDR < 0.005). ASV_0687, affiliated to the genus *Thioalkalispira-Sulfurivermis* had a significant and positive correlation with *Ca.* Electrothrix (rho: 0.986; p-value: 3.09E-04; FDR: 0.102). ASV_1463,

Figure 13. Time course of **ASVs** identified with robust positive correlations with cable bacteria (FDR < 0.6) at the sediment surface (0 - 0.5 cm). Taxon identity are included for each ASV at the finest known phylogenetic resolution.

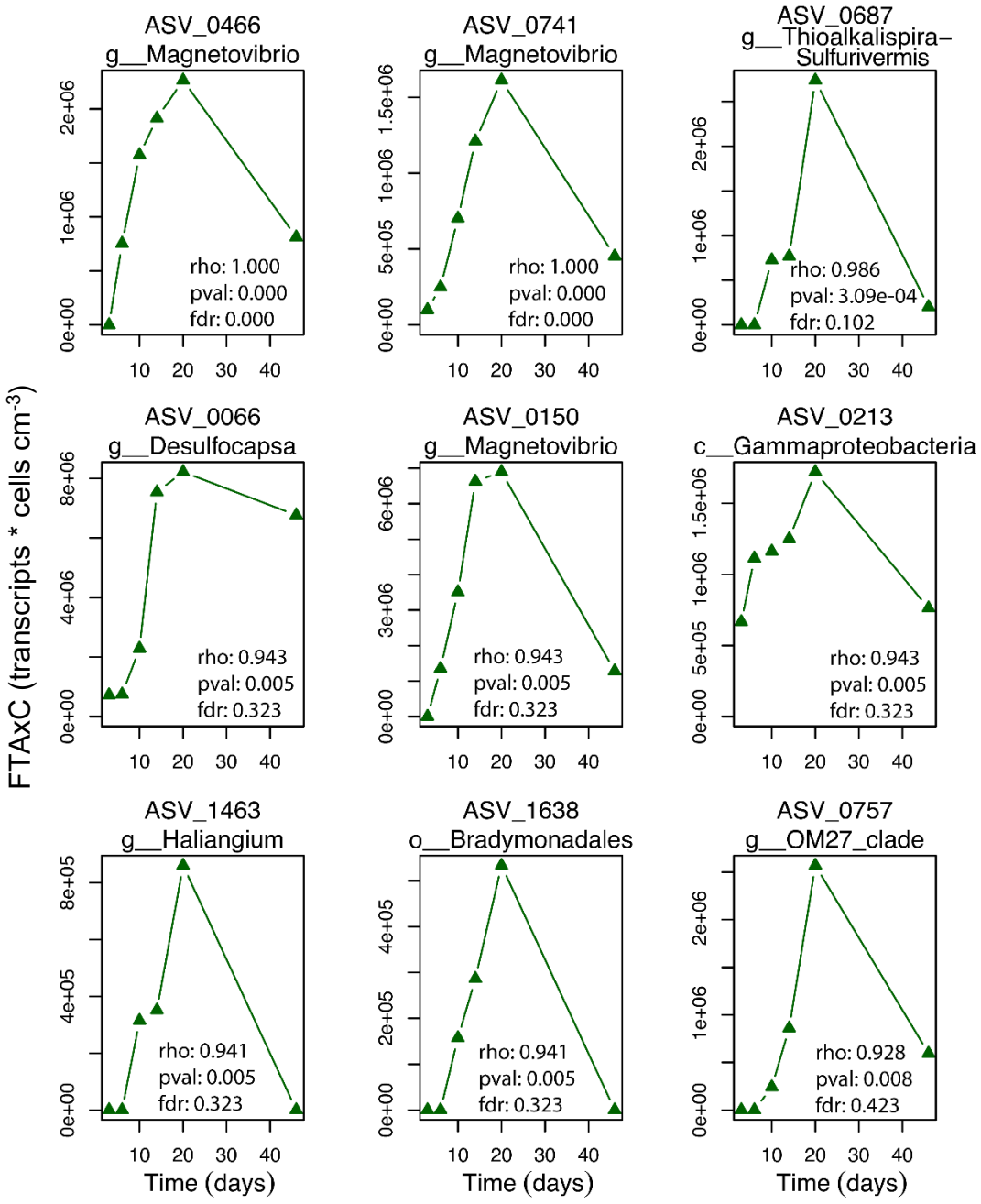

affiliated to the genus *Haliangium*, was weakly correlated with *Ca.* Electrothrix (rho: 0.943, p-value: 0.005, FDR: 0.323). ASV_0066, affiliated to the genus *Desulfocapsa*

also exhibited a weak and positive correlation with *Ca.* Electrothrix (rho: 0.943; p-value: 0.005; FDR: 0.323). Positive but not significant correlation was detected between ASV_0757, belonging to the genus *OM27* clade (Bdellovibrionota), and *Ca.* Electrothrix (rho: 0.928; p-value: 0.008; FDR: 0.423).

Agglomerated at the genus level, 8 genera were positively correlated ($p < 0.05$) with *Ca.* Electrothrix among surface sediment samples (Appendix Table A2), of which all genera (FDR < 0.6) met the time course criteria for being likely associated with *Ca.* Electrothrix (Figure 14). These microbes affiliated to the genera *Aureispira, Portibacter,* and *Crocinitomix* in Phyla Bacteroidota*, OM27* clade (Bdellovibrionota)*, Truepera* (Deinococcota)*, Haliangium* (Myxococcota)*, Magnetovibrio* (Proteobacteria)*, and Diplosphaera* (Verrucomicrobiota). Of these, the most closely correlated genera with *Ca.* Electrothrix were *Magnetovibrio* (rho: 0.943; p-value: 0.005; FDR: 0.223) and *Haliangium* (rho: 0.943; p-value: 0.005; FDR: 0.223). Additionally, the genus-level *OM27* clade was positively associated with *Ca.* Electrothrix with weak strength (rho: 0.829; p= 0.042; FDR: 0.502).

Figure 14. Time course of **genera** identified with robust positive correlations with cable bacteria (FDR < 0.6) at the sediment surface (0 - 0.5 cm).

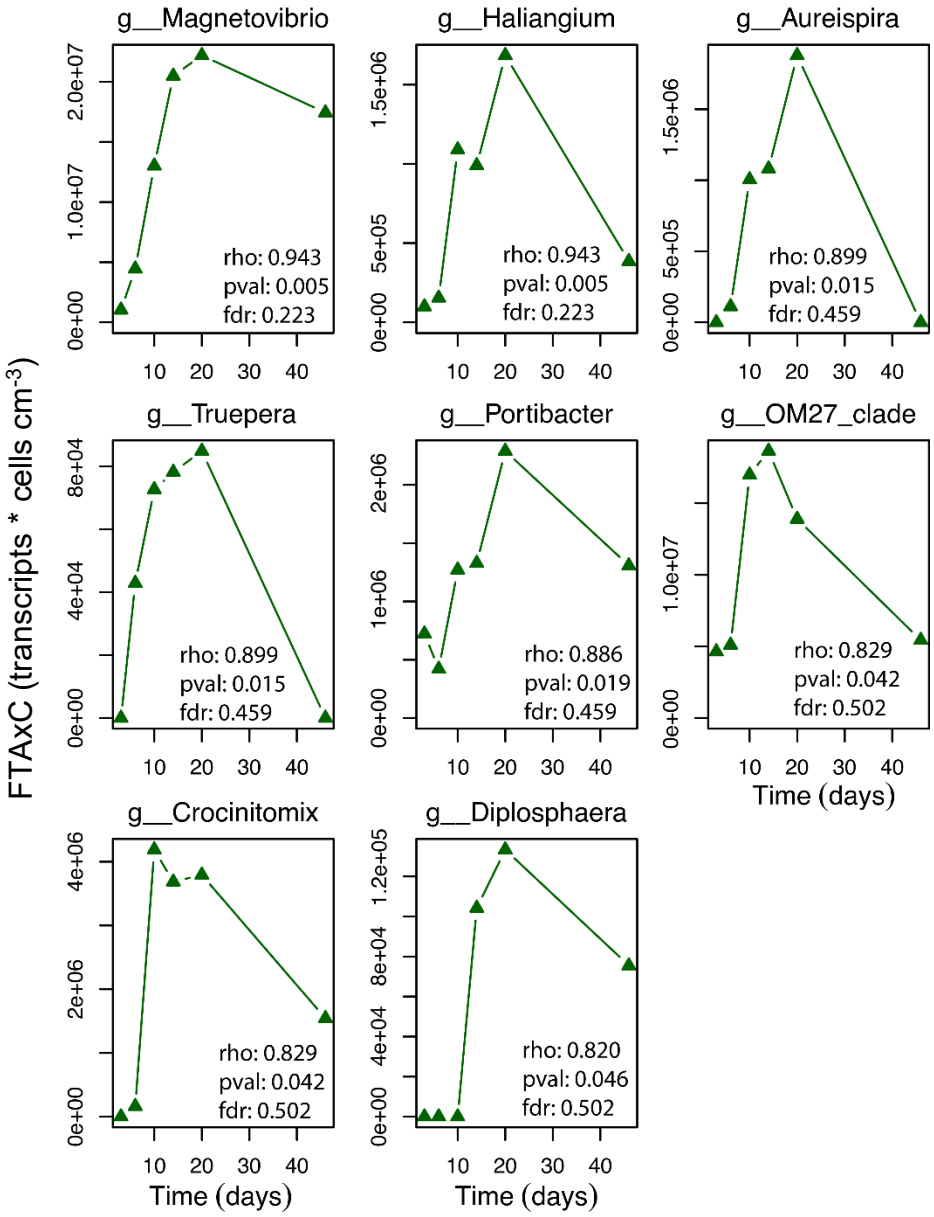

Microbes Negatively Correlated with *Ca.* Electrothrix at the Sediment Surface

Among samples from the sediment surface, 149 ASVs were significantly negatively ($p < 0.05$) correlated with the dominant *Ca.* Electrothrix (Appendix Table

A1), of which 34 ASVs (FDR < 0.6) fulfilled the time course criteria for being likely negatively associated with the growth of *Ca.* Electrothrix (i.e., decreased in FTAxC during growth of *Ca.* Electrothrix and increased in FTAxC during senescence of *Ca.* Electrothrix; Figure 15). These negatively correlated ASVs affiliated to phyla Asgardarchaeota, Thermoplasmatota, Acidobacteriota, Bacteroidota, Desulfobacterota, Fermentibacterota, Latescibacterota, Planctomycetota, and Proteobacteria. Within Desulfobacterota, 10 ASVs were negatively correlated (FDR < 0.423) with *Ca.* Electrothrix and met the criteria of likely cable bacteria association. In detail, these included ASVs affiliated to the genera *Desulfatiglans*, *SEEP-SRB1*, *Sva0081_sediment_group*, *Desulfuromusa*, and an unidentified genus affiliated to the family *Desulfosarcinaceae*. Among Gammaproteobacteria, ASV_0127, affiliated to the genus *Sedimenticola,* and ASV_0173, belonging to the class B2M28, both exhibited highly significant and negative correlations with *Ca.* Electrothrix (rho: -1.000; p-value < 0.005; FDR: 0). ASV_0345, affiliated to the genus *Thiogranum*, was weakly negatively correlated with *Ca.* Electrothrix (rho: -0.941; p-value: 0.005; FDR: 0.323).

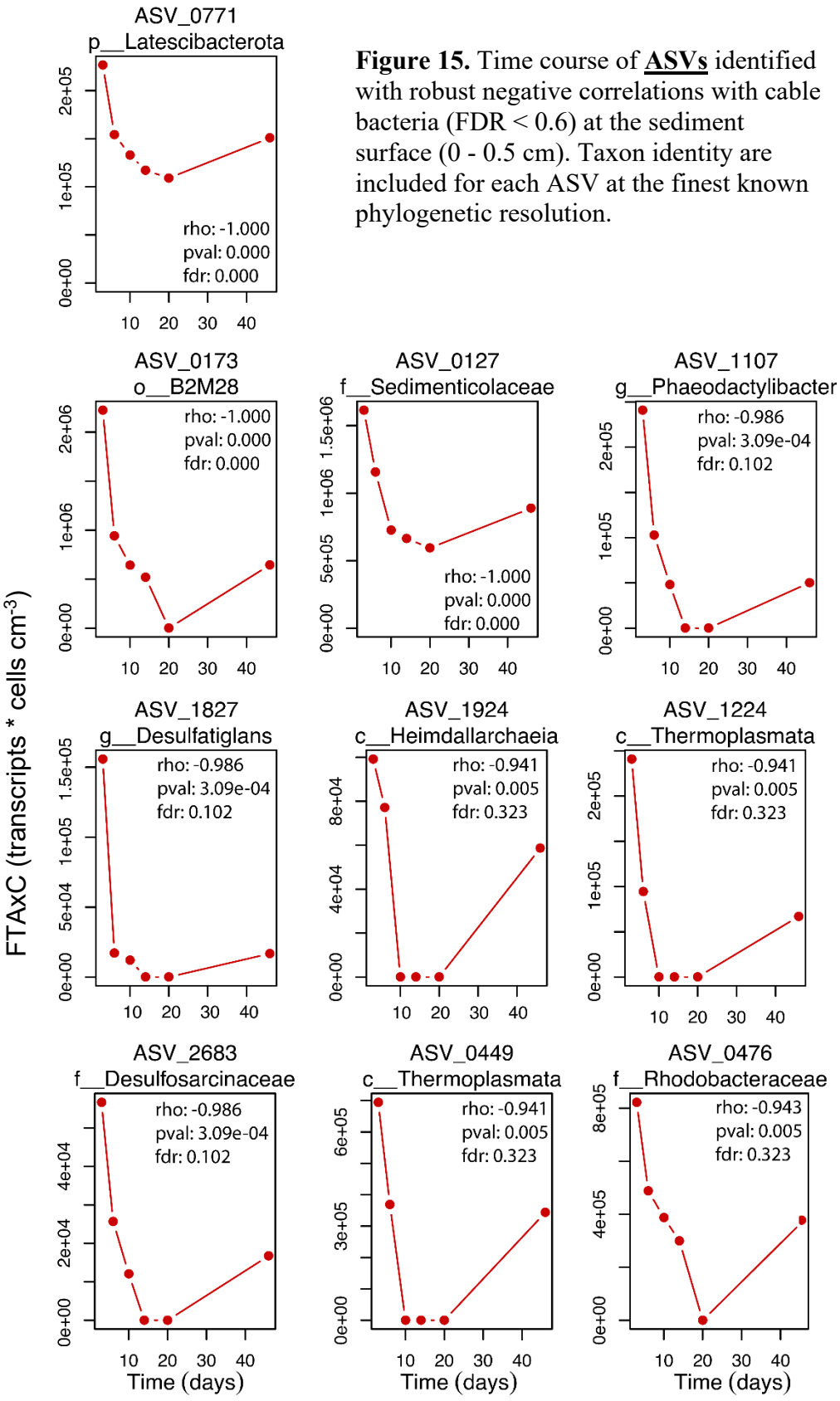

Figure 15. Time course of **ASVs** identified with robust negative correlations with cable bacteria (FDR < 0.6) at the sediment surface (0 - 0.5 cm). Taxon identity are included for each ASV at the finest known phylogenetic resolution.

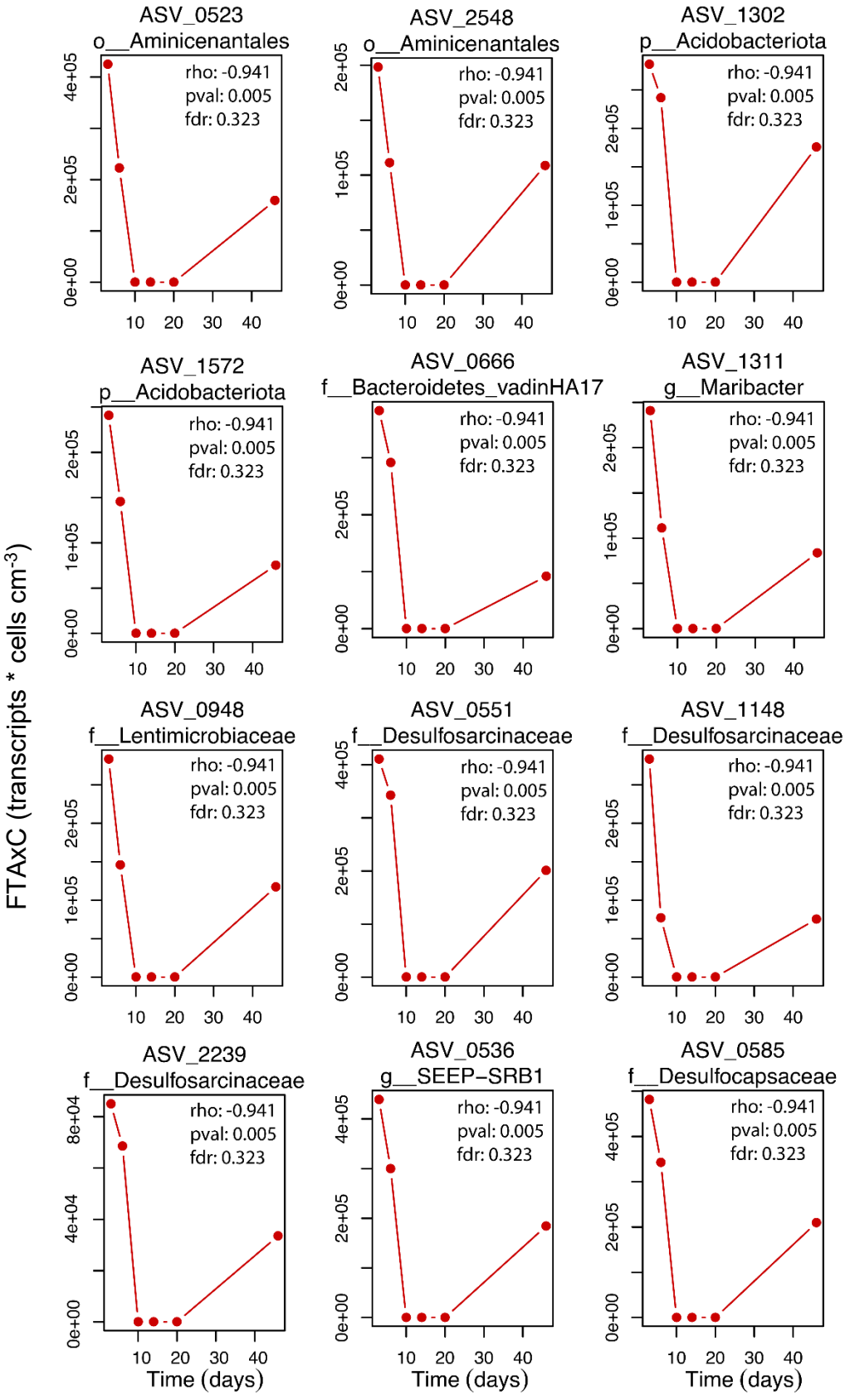
ASV_0523
o__Aminicenantales
ASV_2548
o__Aminicenantales
ASV_1302
p__Acidobacteriota
ASV_1572
p__Acidobacteriota
ASV_0666
f__Bacteroidetes_vadinHA17
ASV_1311
g__Maribacter
ASV_0948
f__Lentimicrobiaceae
ASV_0551
f__Desulfosarcinaceae
ASV_1148
f__Desulfosarcinaceae
ASV_2239
f__Desulfosarcinaceae
ASV_0536
g__SEEP-SRB1
ASV_0585
f__Desulfocapsaceae
rho: -0.941
pval: 0.005
fdr: 0.323
FTAxC (transcripts * cells cm-3)
Time (days)

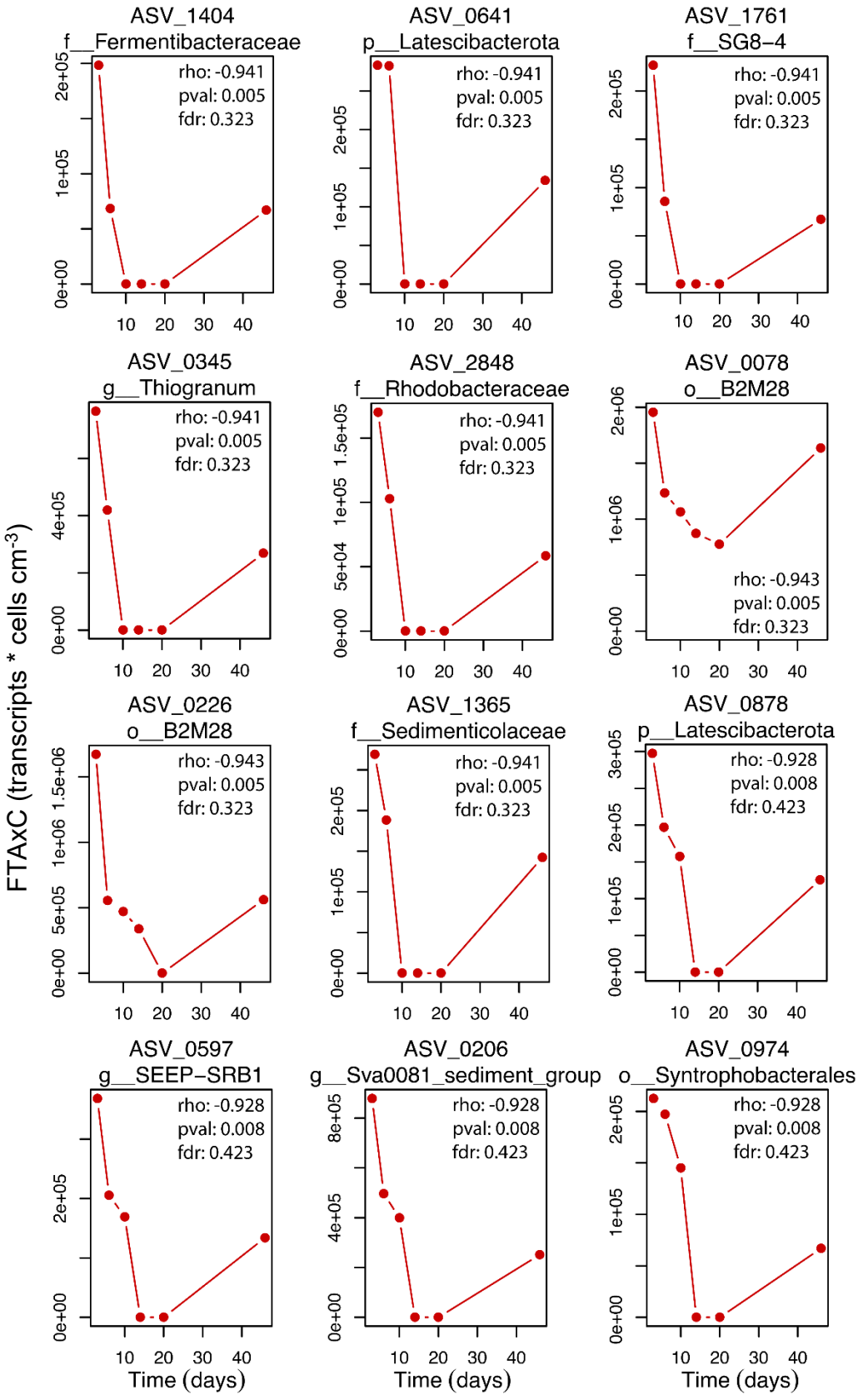
ASV_1404
f__Fermentibacteraceae
rho: -0.941
pval: 0.005
fdr: 0.323
ASV_0641
p__Latescibacterota
rho: -0.941
pval: 0.005
fdr: 0.323
ASV_1761
f__SG8−4
rho: -0.941
pval: 0.005
fdr: 0.323
ASV_0345
g__Thiogranum
rho: -0.941
pval: 0.005
fdr: 0.323
ASV_2848
f__Rhodobacteraceae
rho: -0.941
pval: 0.005
fdr: 0.323
ASV_0078
o__B2M28
rho: -0.943
pval: 0.005
fdr: 0.323
ASV_0226
o__B2M28
rho: -0.943
pval: 0.005
fdr: 0.323
ASV_1365
f__Sedimenticolaceae
rho: -0.941
pval: 0.005
fdr: 0.323
ASV_0878
p__Latescibacterota
rho: -0.928
pval: 0.008
fdr: 0.423
ASV_0597
g__SEEP−SRB1
rho: -0.928
pval: 0.008
fdr: 0.423
ASV_0206
g__Sva0081_sediment_group
rho: -0.928
pval: 0.008
fdr: 0.423
ASV_0974
o__Syntrophobacterales
rho: -0.928
pval: 0.008
fdr: 0.423
FTAxC (transcripts * cells cm-3)
Time (days)

Among surface sediment samples, when individual ASV abundances were agglomerated at the genus level, 13 genera were found to be negatively correlated ($p < 0.05$) with *Ca.* Electrothrix (Appendix Table A2), of which 9 genera (FDR < 0.52) met the time course criteria for being likely negatively associated with cable bacteria (Figure 16). The nine genera were: *Maribacter, JdFR-76, Desulfatiglans, SEEP-SRB1, Sva0081_sediment_group, Desulfuromusa, Halioglobus, Sedimenticola, and Thiogranum*. Similar to correlations found on the ASV level, several genera affiliated to the phylum Desulfobacterota exhibited negative but not significant correlation with *Ca.* Electrothrix, including the genus of *Desulfatiglans* (rho: -0.829; p-value: 0.042; FDR: 0.502), *SEEP-SRB1* (rho: -0.886; p-value: 0.019; FDR: 0.459), *Sva0081_sediment_group* (rho: -0.943; p-value: 0.005; FDR: 0.223), and *Desulfuromusa* (rho: -0.812; p-value: 0.050; FDR: 0.520). Furthermore, negative correlations were observed in the surface samples between *Ca.* Electrothrix and *Thiogranum* (rho: -0.829; p-value: 0.042, FDR: 0.502) as well as *Sedimenticola* (rho: -0.943; p-value: 0.005, FDR: 0.223).

Figure 16. Time course of **genera** identified with robust negative correlations with cable bacteria (FDR < 0.6) at the sediment surface (0 - 0.5 cm).

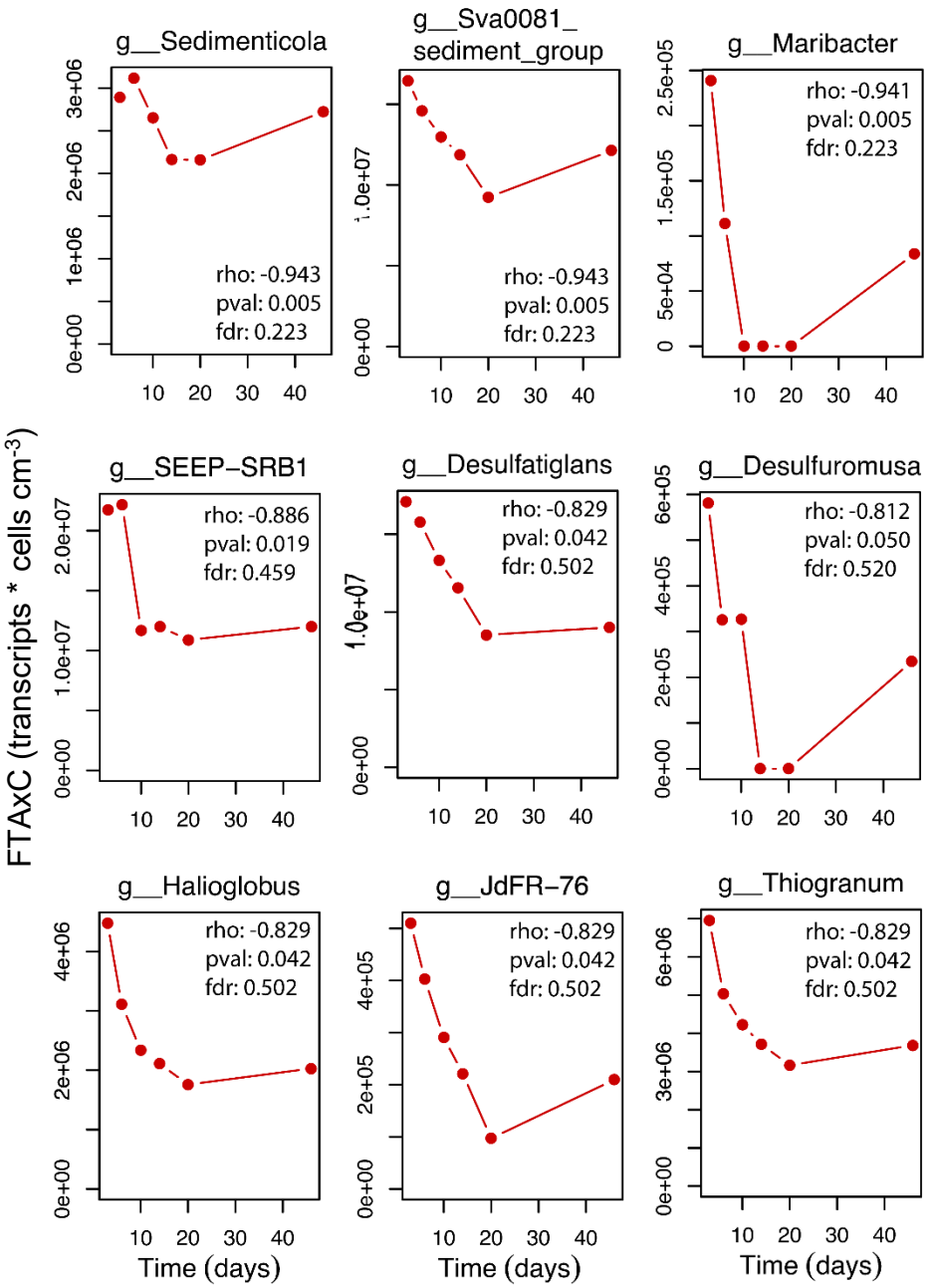

Microbes Positively Correlated with *Ca.* Electrothrix at Subsurface Sediment Depths (0.5 -2.0 cm)

Among subsurface sediment samples, 144 ASVs were positively correlated ($p < 0.05$) with *Ca.* Electrothrix (Appendix Table A1), of which 15 ASVs (FDR < 0.6) met the time course criteria for being likely associated with *Ca.* Electrothrix (Figure 17). These ASVs were affiliated to the following phyla: Thermoplasmatota, Bacteroidota, Calditrichota, Desulfobacterota, Myxococcota, Nitrospinota, Planctomycetota, and Proteobacteria. Correlation analysis among these samples revealed positive correlations between *Ca.* Electrothrix and members of Desulfobacterota belonging to the genus *Desulfatiglans*, and the families *Desulfosarcinaceae* and *Desulfobulbaceae*. The positive correlation detected with *Ca.* Electrothrix and ASV_0441 (family *Desulfobulbaceae*) was strongly significant (rho: 0.0891; p-value: 6.09E-08; FDR: 2.71E-04). A significant and positive correlation was detected between ASV_3457 (order *Desulfobacterales*) and *Ca.* Electrothrix (rho: 0.792, p-value: 1.90E-05, FDR: 0.042). ASV_0453, affiliated with the genus *Desulfatiglans* exhibited a weak significant positive correlation with *Ca.* Electrothrix (rho: 0.707; p-value: 3.43E-04; FDR: 0.218). Moreover, there was a significant and positive correlation between *Ca.* Electrothrix and ASV_1392 (rho: 0.755, p-value: 7.73E-05, FDR: 0.086), which is affiliated to the class *Polyangia* (Myxococcota). One ASV affiliated to the genus *Nitrospina* (rho: 0.684, p-value: 0.001, FDR: 0.276) was positively correlated with *Ca.* Electrothrix. ASVs affiliated to the genera *Sedimenticola* and *Thiogranum* also exhibited a positive correlation with *Ca.* Electrothrix. In particular, a positive correlation with *Ca.* Electrothrix was seen with

ASV_0509 (genus *Sedimenticola*, rho: 0.585; p-value: 0.005; FDR: 0.497) and

ASV_0080 (genus *Thiogranum*, rho: 0.643; p-value: 0.002; FDR: 0.299).

Figure 17. Time course of **ASVs** identified with robust positive correlations with cable bacteria (FDR < 0.6) at the subsurface sediments (0.5 – 2.0 cm). Surface samples (grey) were included for additional information and contrast. Taxon identity are included for each ASV at the finest known phylogenetic resolution.

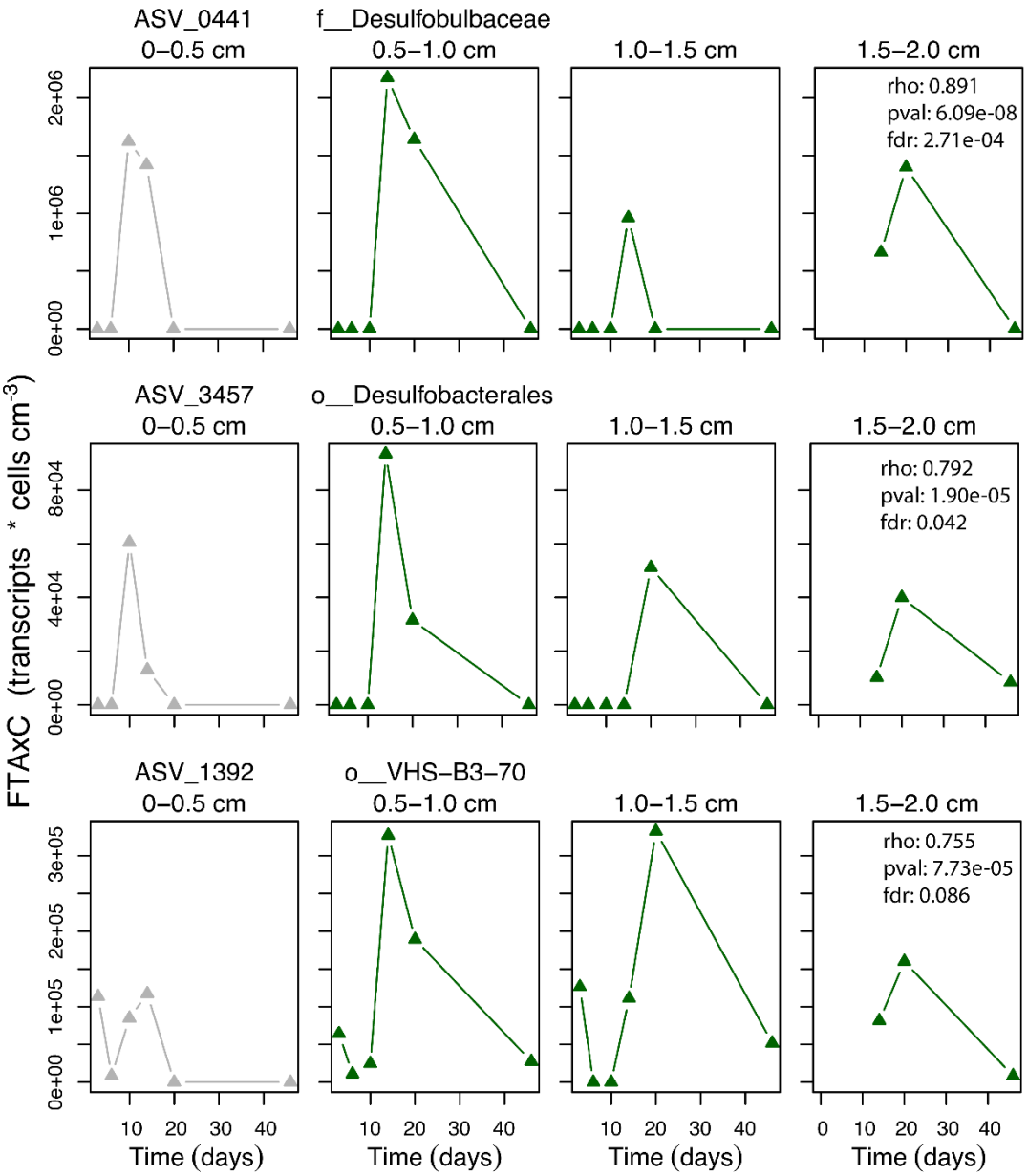

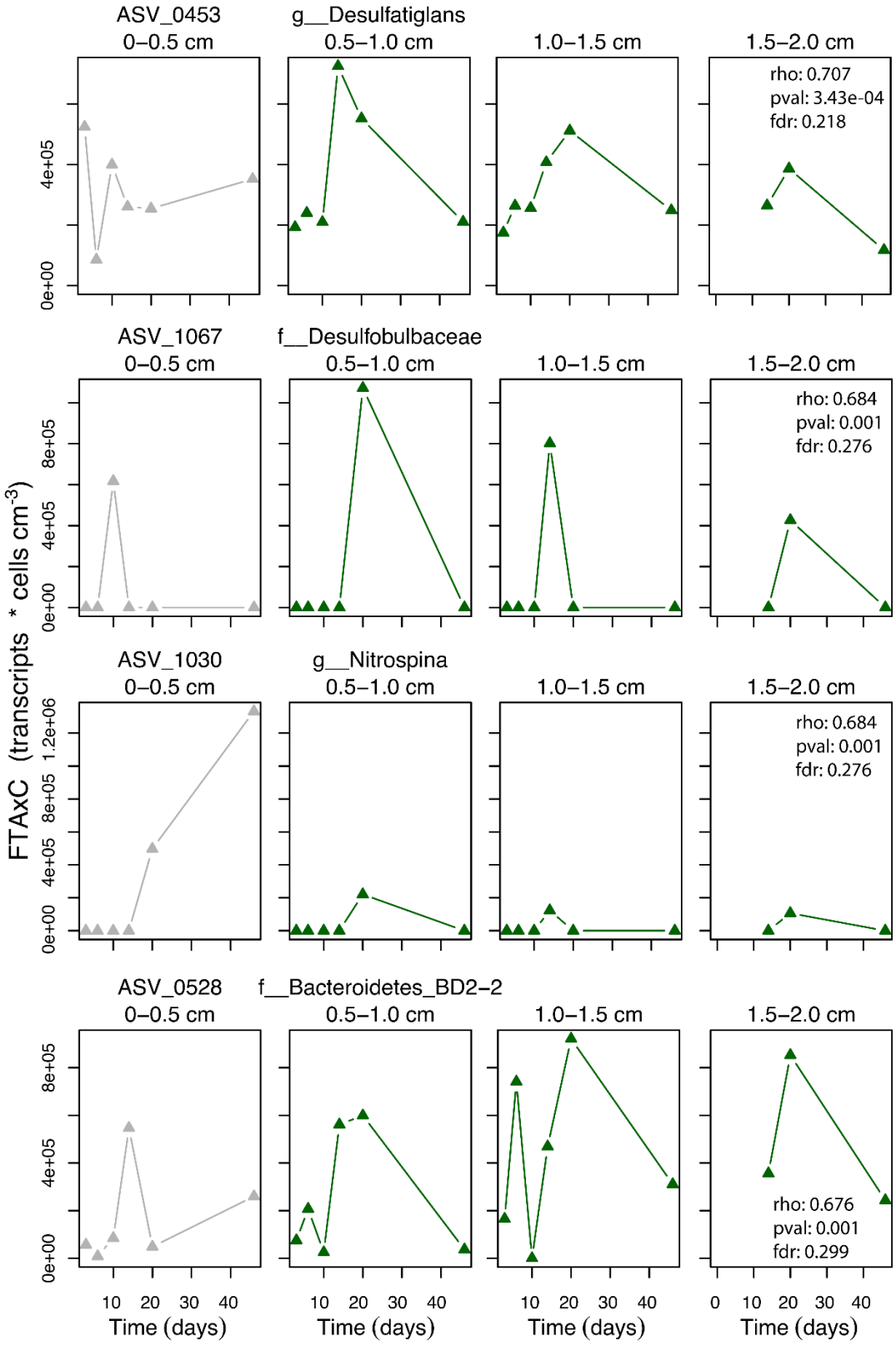
ASV_0453
0–0.5 cm
g__Desulfatiglans
0.5–1.0 cm
1.0–1.5 cm
1.5–2.0 cm
rho: 0.707
pval: 3.43e-04
fdr: 0.218
ASV_1067
0–0.5 cm
f__Desulfobulbaceae
0.5–1.0 cm
1.0–1.5 cm
1.5–2.0 cm
rho: 0.684
pval: 0.001
fdr: 0.276
ASV_1030
0–0.5 cm
g__Nitrospina
0.5–1.0 cm
1.0–1.5 cm
1.5–2.0 cm
rho: 0.684
pval: 0.001
fdr: 0.276
ASV_0528
0–0.5 cm
f__Bacteroidetes_BD2-2
0.5–1.0 cm
1.0–1.5 cm
1.5–2.0 cm
rho: 0.676
pval: 0.001
fdr: 0.299
FTAxC (transcripts * cells cm-3)
0e+00
4e+05
8e+05
1.2e+06
10 20 30 40
0 10 20 30 40
Time (days)

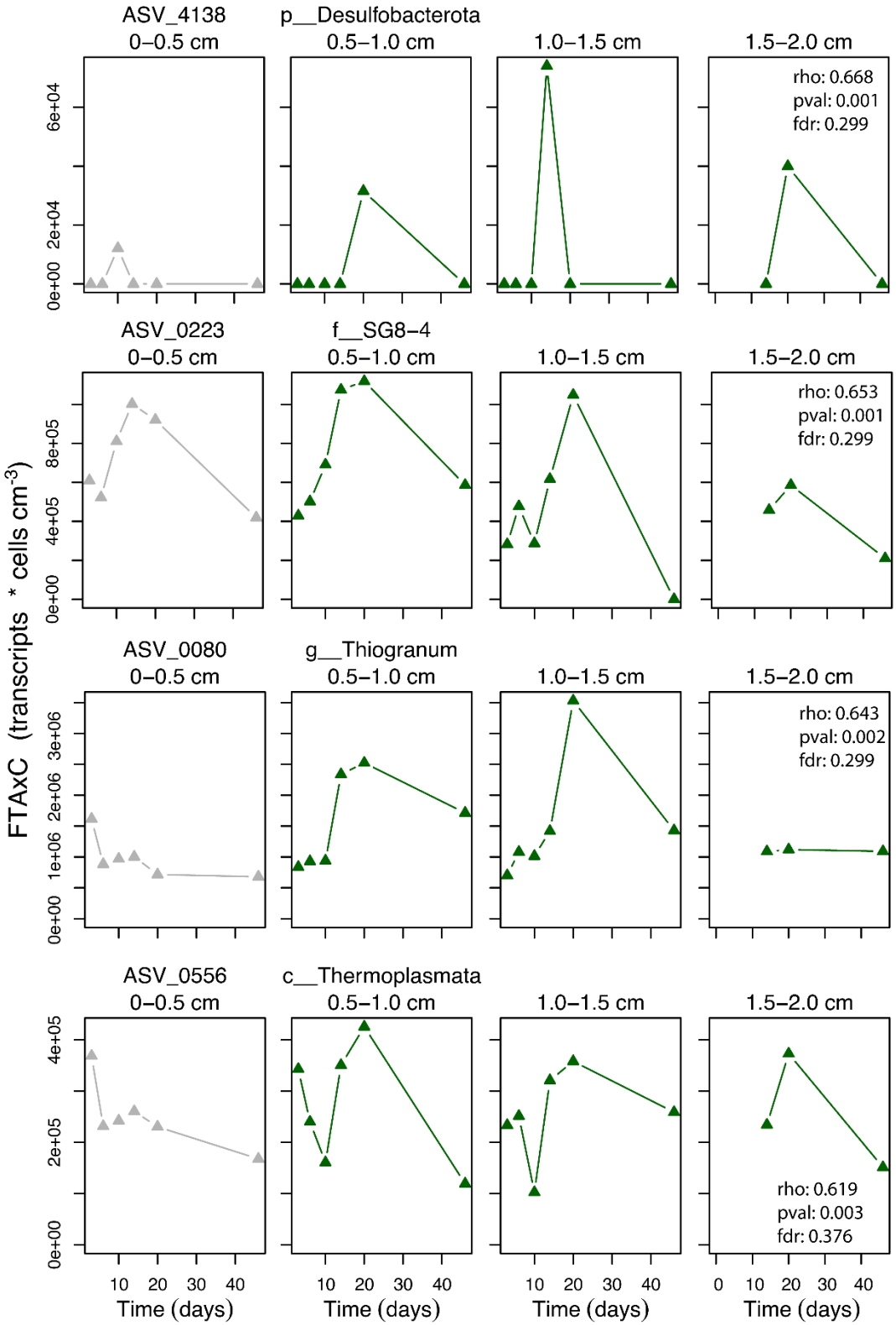
ASV_4138
p__Desulfobacterota
0–0.5 cm
0.5–1.0 cm
1.0–1.5 cm
1.5–2.0 cm
rho: 0.668
pval: 0.001
fdr: 0.299
ASV_0223
f__SG8–4
rho: 0.653
pval: 0.001
fdr: 0.299
ASV_0080
g__Thiogranum
rho: 0.643
pval: 0.002
fdr: 0.299
ASV_0556
c__Thermoplasmata
rho: 0.619
pval: 0.003
fdr: 0.376
FTAxC (transcripts * cells cm-3)
0e+00
2e+04
6e+04
4e+05
8e+05
1e+06
2e+06
3e+06
2e+05
4e+05
10 20 30 40
0 10 20 30 40
Time (days)

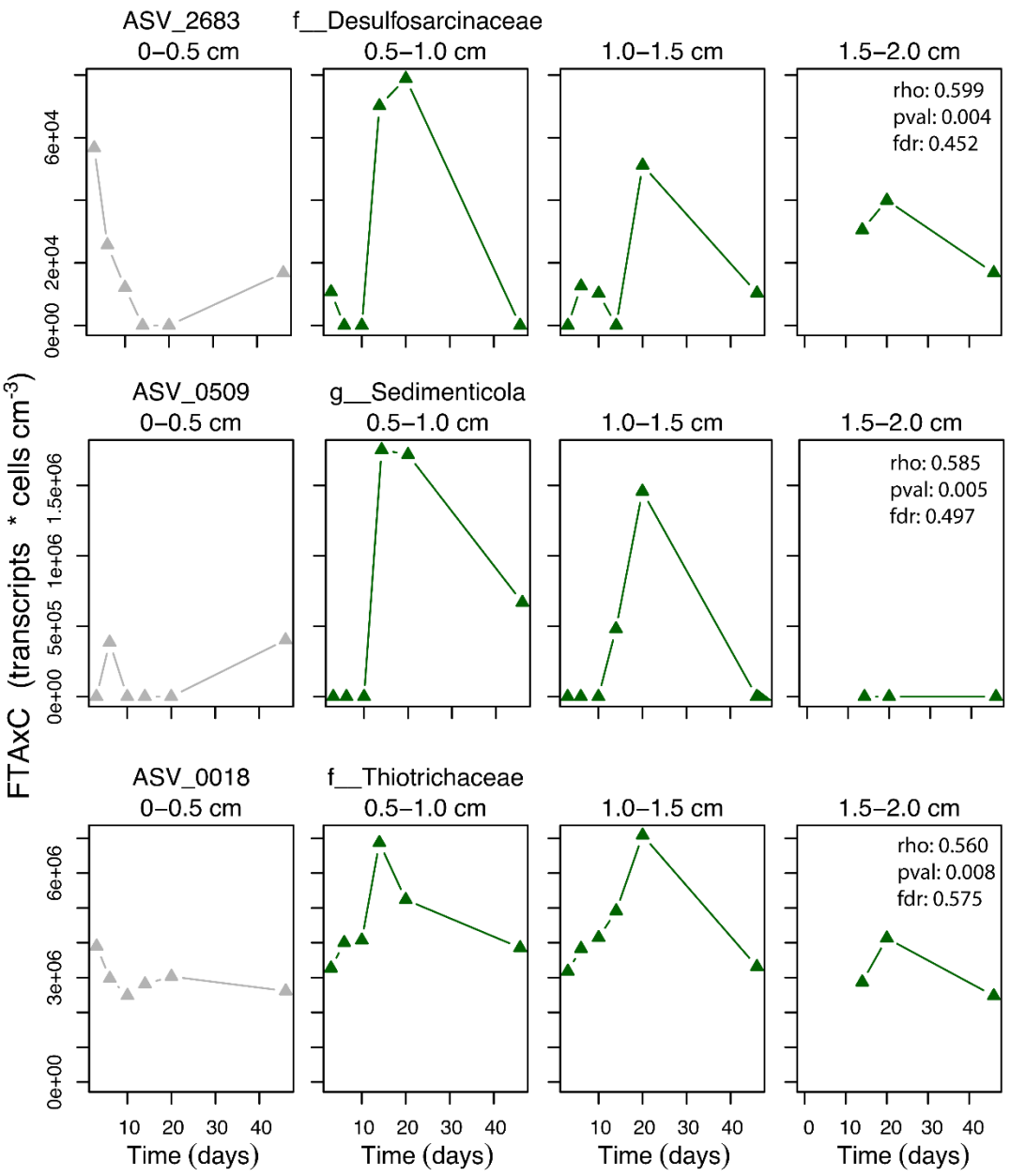

Among subsurface sediment samples, when ASVs were agglomerated to the genus level, 5 genera were positively correlated ($p < 0.05$) with *Ca.* Electrothrix (Appendix Table A2). Of these, *Thiogranum* was weakly correlated but met the time

course criteria for being likely associated with cable bacteria (rho: 0.477; p-value: 0.029; FDR: 0.557; Figure 18).

Figure 18. Time course of **genera** identified as robustly correlated with cable bacteria (FDR < 0.6) at the subsurface sediments (0.5 – 2.0 cm). Surface samples were included for additional information and contrast. Grey plot = surface samples; green triangles = positively correlated genera; red circles = negatively correlated genera.

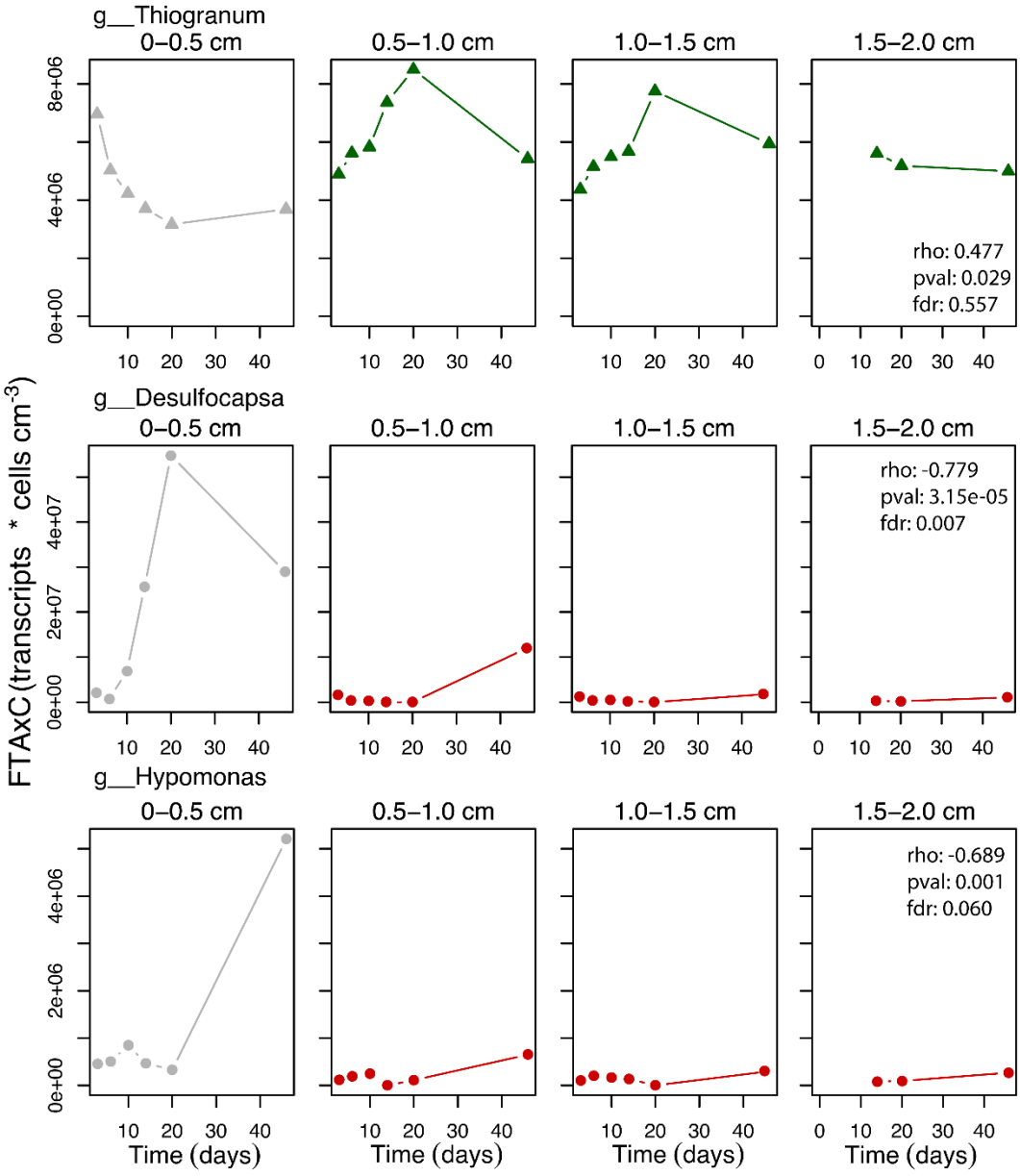

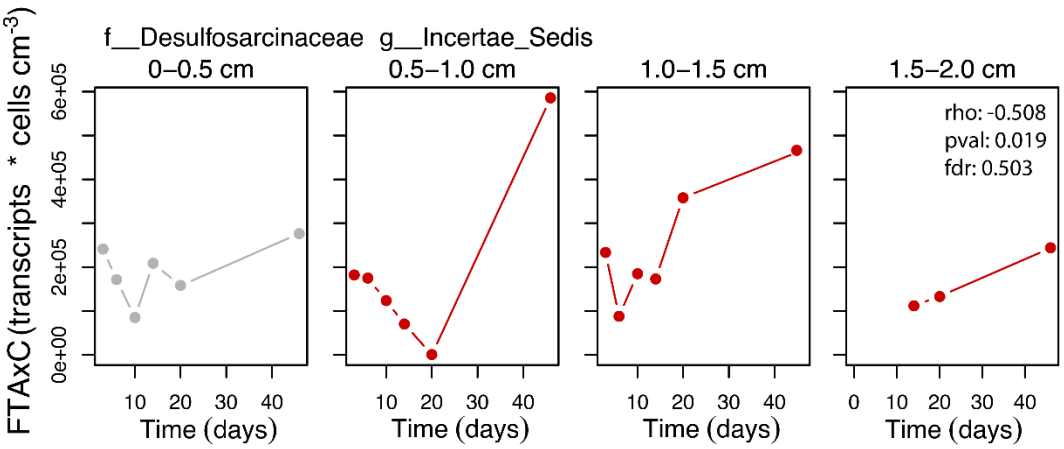

Microbes Negatively Correlated with *Ca.* Electrothrix at Subsurface Sediment Depths (0.5 -2.0 cm)

Among subsurface sediment samples, 102 ASVs were negatively correlated ($p < 0.05$) with *Ca.* Electrothrix (Appendix Table A1), of which 6 ASVs (FDR < 0.6) met the time course criteria for being likely negatively associated with the growth of *Ca.* Electrothrix (Figure 19). These ASVs were affiliated with the following phyla: Bacteroidota, Chloroflexi, Desulfobacterota, and Proteobacteria. Within the genus of *Desulfocapsa,* there was a strongly significant negative correlation between ASV_0066 and *Ca.* Electrothrix (rho: -0.779; p-value: 3.15E-05; FDR: 0.047). ASV_0275, affiliated to Gammaproteobacteria, exhibited a strong negative correlation with *Ca.* Electrothrix (rho: -0.726; p-value: 1.94E-04; FDR: 0.173). A negative correlation was also detected between *Ca.* Electrothrix and ASV_0294, which was affiliated to the order *Ardenticatenales* (rho: -0.699; p-value: 4.22E-04; FDR: 0.234). In addition, ASV_0754 (family *Marinilabiliaceae,* FDR < 0.374), ASV_0424 (class *Anaerolineae,* FDR < 0.452), and ASV_0475 (genus *Thiogranum,*

FDR < 0.519) were all observed as weak negative correlations with *Ca.* Electrothrix at depth.

Figure 19. Time course of **ASVs** identified with robust negative correlations with cable bacteria (FDR < 0.6) at the subsurface sediments (0.5 – 2.0 cm). Surface samples (grey) were included for additional information and contrast. Taxon identity are included for each ASV at the finest known phylogenetic resolution.

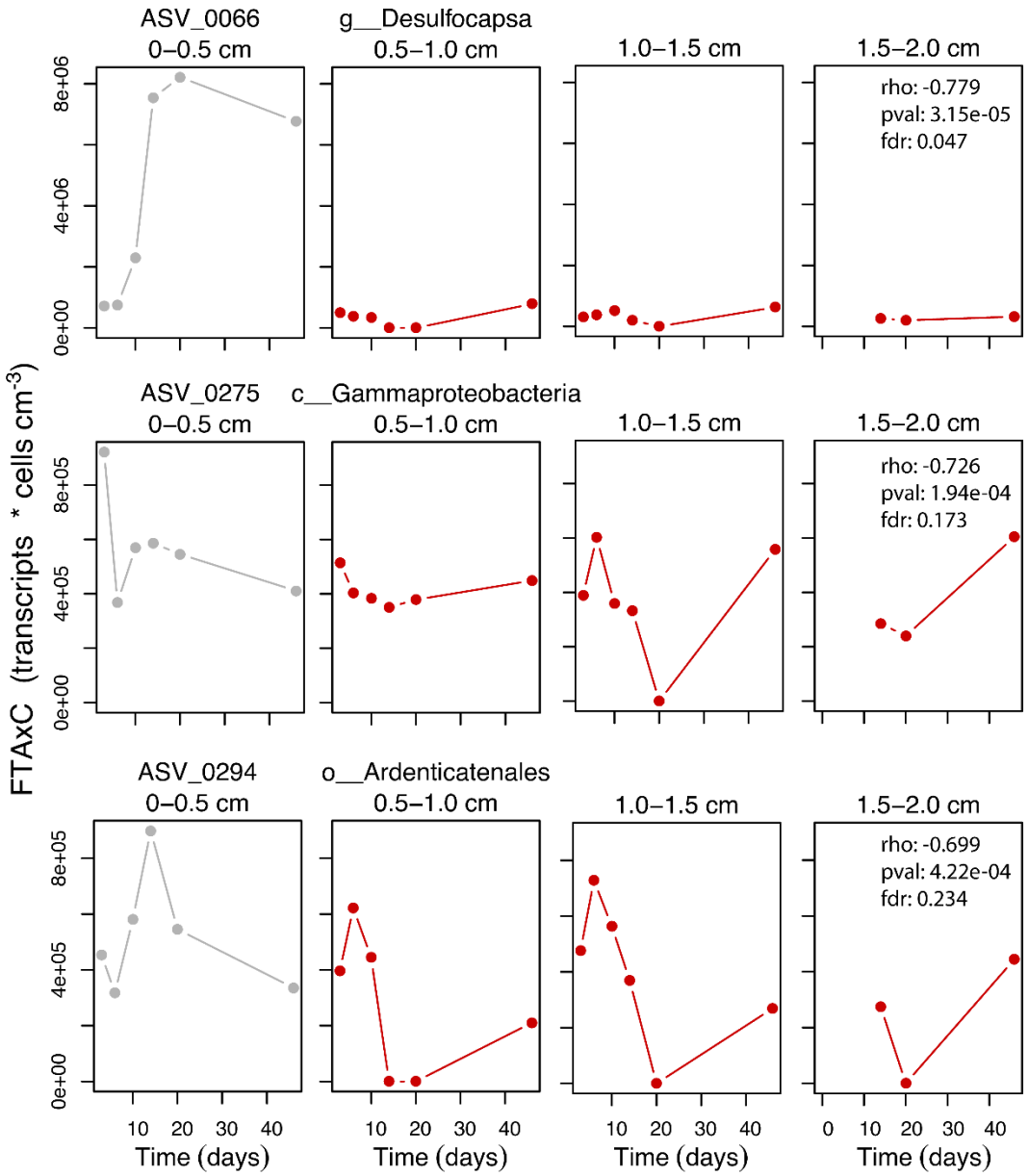

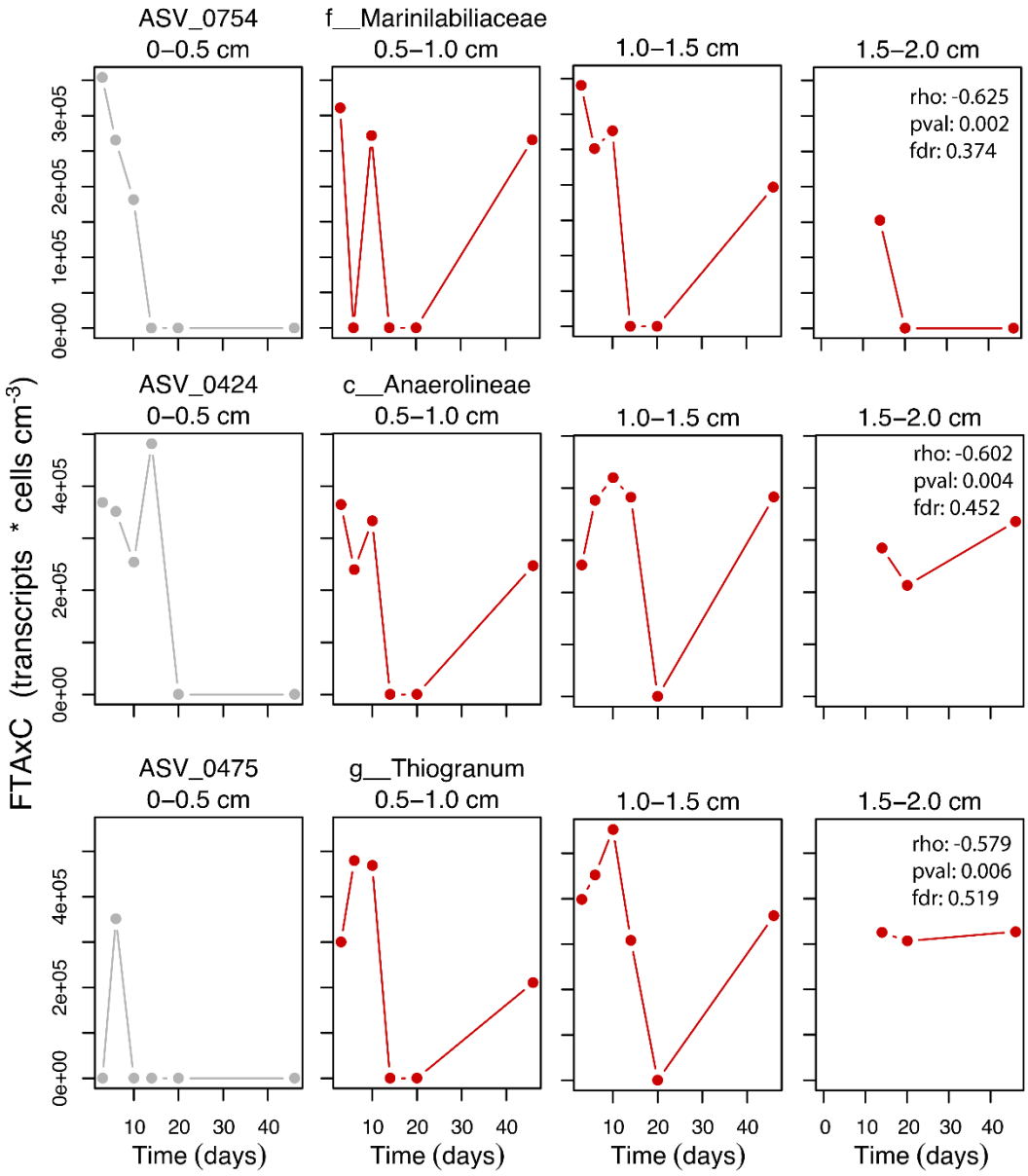

Among subsurface sediment samples, when ASVs were agglomerated to the genus level, 10 genera were negatively correlated with cable bacteria (Appendix Table A2). Of these, 3 genera (FDR < 0.503) met the time course criteria for being likely negatively associated with *Ca.* Electrothrix (Figure 18). These genera included: *Desulfocapsa*, *Hyphomonas,* and *Incertae-Sedis* in the family *Desulfosarcinaceae*. At

depth, *Ca.* Electrothrix exhibited strongly significant and negative correlations with the genus *Desulfocapsa* (rho: -0.779; p-value: 3.15E-05; FDR: 0.007) as well as *Hyphomonas* (rho: -0.689; p-value: 0.001; FDR: 0.060).

Discussion

The central objective of this study was to identify potential associations between cable bacteria and their sympatric microbes using correlation-based analyses. Sediment cores were constructed from homogenized sediment obtained from a Mid-Bay station of Chesapeake Bay. In one set of sediment cores, marine cable bacteria (*Ca.* Electrothrix) were allowed to grow unimpeded, and grew to dominate microbial abundance, while in another set of sediment cores, the downward growth of cable bacteria was blocked at 0.5 cm depth by embedded barriers made of polycarbonate filters. The filters allowed for diffusion of porewater constituents, but successfully blocked the downward growth of filamentous cable bacteria. Using Spearman's Rank correlation analysis on FTAxC data at the ASV and genus level, combined with considerations of temporal trends of microbial FTAxC, I discuss 10 taxa that were most likely associated, positively or negatively, with the growth of marine cable bacteria. Based on the ecology of these taxa, I infer their potential interactions with cable bacteria include predation, competition, and syntrophic relationships. Potential indirect interactions are also possible, based on biogeochemical impacts imposed by cable bacteria acting as an ecosystem engineer in the sediments.

Cable Bacteria Growth Progression in Incubation Cores

Over the course of the experiment, cable bacteria growth began with a lag phase, observed for 6 days, followed by an exponential growth phase, which began at the sediment surface and progressed downward observed between Days 10-20, and

finally terminated with a senescence phase observed by Day 46. On this final date, there were few filaments observed, and they were only observed at the sediment surface. Previous laboratory studies have reported a similar time course for cable bacteria in homogenized sulfidogenic sediments, with cable bacteria abundance reaching a maximum within 2-4 weeks of incubation in oxygenated water, followed by a population crash (Schauer et al., 2014; Rao et al., 2016a). Based on microscopy, cable bacteria accounted for up to 35% of the total microbial cell counts on Day 20, which is similar to a previous report in which cable bacteria represented up to an estimated 25% of microbial cells during their peak biomass (Schauer et al. 2014). On the same date, based on 16S amplicon sequencing data, marine cable bacteria (*Ca.* Electrothrix) represented the dominant DNA (up to 5% reads) and RNA pools (up to 64% reads).

The porewater geochemistry revealed by microsensor profiling was consistent with patterns expected based on the growth and senescence of cable bacteria (Schauer et al., 2014; Rao et al., 2016a). The microsensor profile data revealed an expansion of a suboxic zone and increasing acidity at depth during the exponential phase of cable bacteria growth, indicative of electrogenic sulfide oxidation by cable bacteria. In tandem with the growth of cable bacteria (Days 6-20), there was also an increase in dissolved oxygen uptake (DOU), which was followed by a decrease in DOU when cable bacteria experienced senescence (Day 46). This observed change in DOU is in line with previous reports which observed increases in DOU during cable bacteria growth (Schauer et al., 2014; Malkin et al., 2014; Vasquez-Cardenas et al., 2015; Rao et al., 2016a; Hermans et al., 2020). Moreover, the lack of increase in DOU from

cores with barrier filters supports that electrogenic sulfide oxidation by cable bacteria is responsible for increased DOU between Days 10-20 in cores where they are abundant. While heterotrophic activity maintains a baseline oxygen consumption rate with the organic matter present, the observed increase in DOU is likely due to the utilization of another electron donor since no additional organic matter were supplemented to the cores. The increase in DOU in sediment cores with growing cable bacteria can be attributed to their ability to exploit FeS pools, which is made available by acidification of the porewaters through their anodic activity (Risgaard-Petersen et al., 2012; Larsen et al., 2015, Rao et al., 2016a). The cause of the senescence of cable bacteria after 46 days of incubation is uncertain but has also been reported in other studies (Schauer et al., 2014; Vasquez-Cardenas et al., 2015). Cable bacteria population collapses have been previously explained by the depletion of the FeS pools (Schauer et al., 2014; Seitaj et al., 2015; Larsen et al., 2015). Based on genomic studies of cable bacteria, other hypotheses have also been put forward to explain the senescence of cable bacteria. Specifically, cable bacteria cathodic activity causes an increase in pH at the sediment surface, which has been hypothesized to cause protein denaturation of the cells (Kjeldsen et al. 2019). Additionally, viral lysis has been put forward as a potential controlling mechanism (Kjeldsen et al., 2019). With this study, I add the hypothesis that cable bacteria populations may be controlled by bacterial predation (more below).

During exponential growth, cable bacteria cell abundance increased more rapidly at suboxic depth than at the sediment surface. During exponential growth, cable bacteria doubling time was under 7 hours at 1.0-1.5 cm depth, and 41.5 hours at

the sediment surface. Integrated over all depths, cable bacteria experienced a doubling time of ~28 hours during exponential growth, which is comparable to a previously study, reporting a net doubling time of ~20 hours (Schauer et al., 2014). The faster growth rate detected at suboxic depths is consistent with the depth distribution of cable bacteria 16S rRNA transcript production (Figure 9). Interestingly, during cable bacteria exponential growth, the RNA to DNA ratio of *Ca.* Electrothrix was highest at its deepest depth (Figure 10), indicating higher cable bacteria transcriptional activity in the suboxic region. The greater RNA to DNA ratio at depth indicates higher biosynthesis activity, consistent with the faster growth rate of cells observed at suboxic depths. This observation is consistent with energy conservation associated with anodic, rather than cathodic activity of cable bacteria filaments, as recently proposed based on their genome (Kjeldsen et al. 2019). Specifically, cable bacteria appear to generally lack terminal oxidases, essential for oxygen reduction to proton translocation, implying the filaments conserve energy from anaerobic metabolism only (Kjeldsen et al., 2019). Additionally, a study using NanoSIMS revealed cable bacteria filaments exhibited high assimilation rates of carbon and nitrogen in the suboxic zone but participate in little biosynthesis in the oxic zone (Geerlings et al., 2020). My observations further identify cable bacteria exhibit elevated transcriptional activity and cell growth in the suboxic zone, where their anodic activity takes place. The reduction of oxygen (or nitrate) by cable bacteria appears to be primarily a mechanism for electron discharge, rather than a mechanism for the cells to obtain and conserve energy (Kjeldsen et al., 2019; Geerlings et al., 2020).

The development of a pH minimum in the suboxic layer aids in the dissolution of FeS, in which, a high concentration of Fe^{2+} was generated on Day 20 detected at 1.5 cm in the sediment cores with active cable bacteria. In contrast, the cores with barriers did not exhibit any peak in Fe^{2+} concentration. The released ferrous iron diffuses upwards and can result in the formation of iron oxide in the oxic zone (Risgaard-Petersen et al., 2012; Rao et al., 2016a, Hermans et al., 2020), retention of phosphorus in the sediment (Sulu-Gambari et al., 2016b), stimulation of dissimilatory nitrate reduction to ammonium (DNRA) (Robertson et al., 2016; Kessler et al., 2019), and possibly facilitation of a cryptic iron cycle (Otte et al., 2018). The "engineering" capacity of cable bacteria extends beyond the iron, sulfur, phosphorus, and nitrogen cycles. Additionally, elevated acidity in the sediment also influences the manganese (Sulu-Gambari et al., 2016a) and carbonate (Risgaard-Petersen et al., 2012) cycles.

Direct Microbial Association with Cable Bacteria

Based on correlation analysis, I detected possible direct and indirect microbial associations with cable bacteria.

Interaction with Sulfur-Oxidizers: Syntrophy vs Competition

Sedimenticola and *Thiogranum* (Class Gammaproteobacteria) were negatively correlated with *Ca.* Electrothrix in the surface sediment. These genera are described as sulfur-oxidizing chemoautotrophs which grow by oxidation of sulfide, thiosulfate, tetrathionate, and elemental sulfur coupled with oxygen or nitrate reduction (Flood et al., 2015b; Mori et al., 2015). Their negative association at the sediment surface suggest a potentially competitive relationship with *Ca.* Electrothrix for substrate such

as sulfide in which *Ca.* Electrothrix may outcompete other sulfide-oxidizers (Figure 20a).

By contrast, at suboxic depths*, Thiogranum* was positively correlated with *Ca.* Electrothrix. The genus *Thiogranum* and the type species, *Thiogranum longum,* are described as obligate aerobes (Mori et al., 2015), which makes their growth at sediment depths that are fully anoxic intriguing. It has been frequently observed that extant microbes in sediments exhibit metabolic capacities that extend beyond the observed capacities of those in culture (Lenk et al., 2012; Mußmann et al., 2016; Dyksma et al., 2016). Therefore, it is possible that the growth of *Thiogranum* at suboxic depths reflects more diverse metabolic abilities, including the capacity for anaerobic respiration or fermentation, than previously reported. An intriguing alternative hypothesis is that *Thiogranum* may couple their chemoautotrophic sulfide oxidization with electron donation directly or indirectly to anodic cells of *Ca.* Electrothrix (i.e., utilize *Ca.* Electrothrix as an electron sink at suboxic depths). A syntrophic relationship (which is canonically defined as "shared feeding") may be plausible between *Thiogranum* with *Ca.* Electrothrix if *Ca.* Electrothrix conversely provides reduced sulfur intermediates to *Thiogranum* (Figure 20b). In a ^{13}C-labeling study, the presence of cable bacteria stimulated chemoautotrophic sulfur oxidation by Epsilon- and Gammaproteobacteria (Vasquez-Cardenas et al., 2015). When cable bacteria activity was halted by manipulation, chemoautotrophic sulfur oxidation also halted. Vasquez-Cardenas et al. hypothesized that the chemolithoautotrophs may be linked to cable bacteria via electron transport such as using cable bacteria as an electron sink. Based on my observations, I hypothesize that the increased abundance

of *Thiogranum* at suboxic depths alongside *Ca.* Electrothrix is due to syntrophy, potentially by electrical connections with *Ca.* Electrothrix acting as an electron acceptor. Alternatively, *Ca.* Electrothrix may solely act as an electron acceptor for other microbes without gaining any benefits, suggesting a commensal relationship.

At suboxic depths*, Sedimenticola* was also positively correlated with *Ca.* Electrothrix. Unlike *Thiogranum*, *Sedimenticola* is known to be capable of oxidizing sulfur aerobically or anaerobically using electron acceptors such as nitrate or selenate (Flood et al., 2015a; Narasingarao, P. and Häggblom, 2006). Nevertheless, the positive correlation between *Sedimenticola* and *Ca.* Electrothrix at suboxic depths is curious and may similarly indicate a syntrophic or commensal relationship. In sediments with graphite electrodes embedded, *Sedimenticola* cells colonized as biofilm on the anode surface likely mediating sulfur oxidation with electron transfer to the electrode (Matturo et al., 2017). If *Sedimenticola* can transport electrons extracellularly, one proposition is that cable bacteria and *Sedimenticola* cells may be syntrophic partners involved in interspecies electron transfer and/or the sharing of sulfur intermediates. However, the mechanism by which *Sedimenticola* can transfer electron extracellularly in currently unknown. This potential relationship between *Ca.* Electrothrix and chemoautotrophic sulfur oxidizers (*Thiogranum* and *Sedimenticola*) at suboxic depths opens an exciting route to further research on direct interspecies electron transfer (Lovley, 2017a) in sediment systems.

Figure 20. Conceptual diagrams of potential microbial interactions with cable bacteria. (**a.**) competition, (**b.**) syntrophy, (**c.**) predation, (**d.**) indirect association attributed to ecosystem engineering effects of cable bacteria. Green filamentous multicellular bacteria represent cable bacteria.

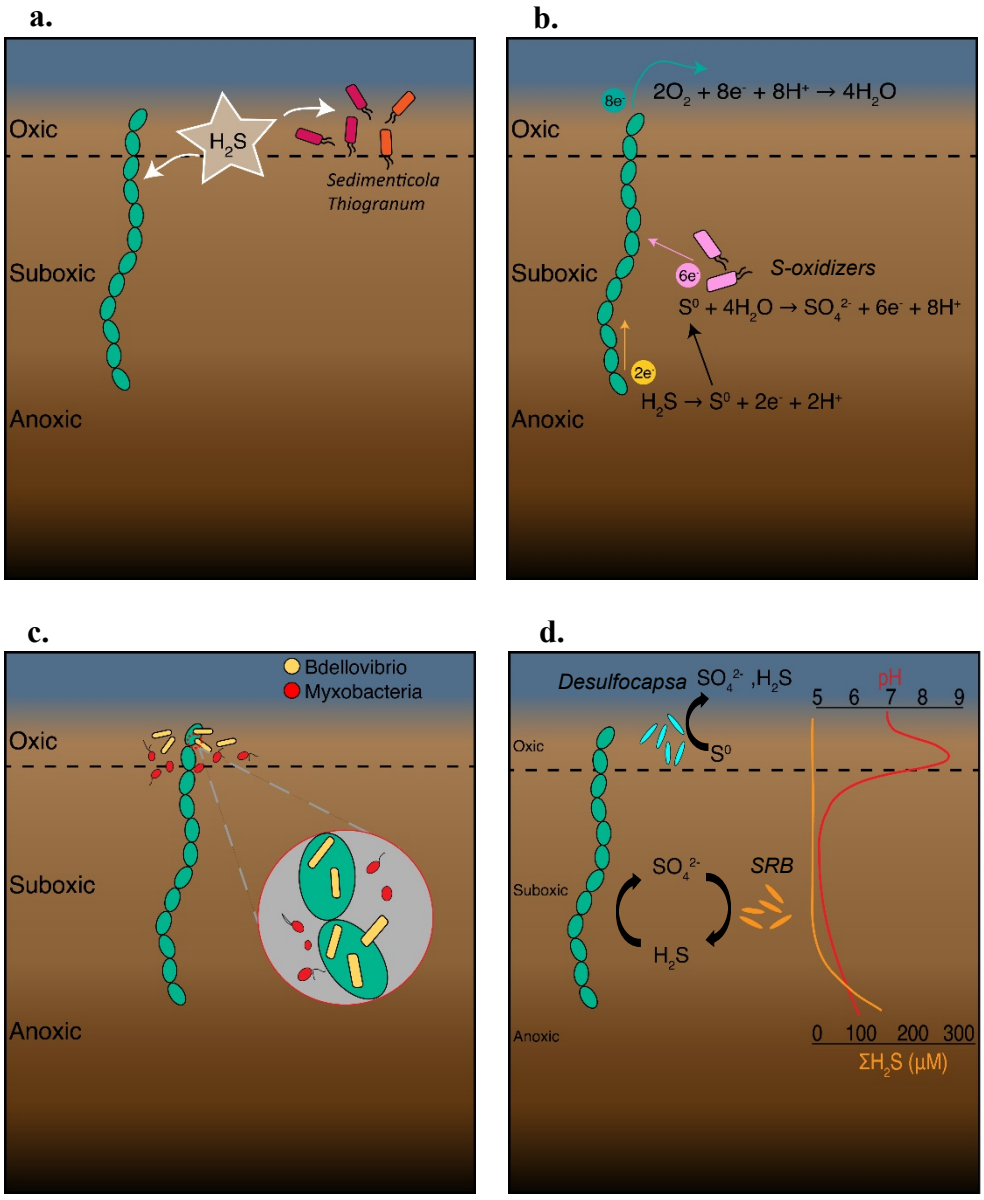

Predator-Prey Interactions

I detected positive correlations between *Ca.* Electrothrix and predatory microbes belonging to the phylum Bdellovibrionota in the surface sediment and the phylum Myxobacteria in both the surface and suboxic sediment depths. Specifically, *Ca.* Electrothrix was positively correlated with the genus-level *OM27* clade (Phylum Bdellovibrionota). Bdellovibrio and like organisms (BALOs) are aerobic, obligate predators of Gram-negative bacteria. Previously studied BALOs replicate by penetrating the periplasmic space of Gram-negative bacteria, where they grow and divide, and subsequently lyse their prey/host (Jurkevitch, 2007; Sockett et al., 2009; Pérez et al., 2016). The growth course of BALOs in our surface samples very closely followed the trend of cable bacteria abundance, suggesting that bacteria affiliated to the genus-level *OM27* clade may be predators of cable bacteria at the oxic sediment (Figure 20c). In the suboxic zone, viral attack may be more prevalent for bacterial mortality (Tsai et al., 2013). Other Gram-negative bacteria belonging to Proteobacteria are also susceptible to attack by BALOs (Pérez et al., 2016). In the oxic sediment, an increase in Alphaproteobacteria was detected (Figure 7) which may be vulnerable to predation by BALOs. Cable bacteria, however, are far likelier the prey/hosts for the *OM27* clade because their abundance dropped off the last date, coinciding with a senescence of cable bacteria, but continued mounting abundance of Alphaproteobacteria.

Similarly, *Haliangium* (Phylum Myxococcales) was positively correlated with *Ca.* Electrothrix in the sediment surface. *Haliangium* are described as predatory swarmers (Fudou et al., 2002). Generally, myxobacteria are facultative predators, capable of degrading live or dead cells, and specialize in wolfpack group attack with

secretion of hydrolytic enzymes (Muñoz-Dorado et al., 2016; Pérez et al., 2016). Unlike BALOs, myxobacteria have a broader host range including Gram-positive and Gram-negative bacteria (Livingstone et al., 2017) as well as yeast, fungi, protozoa, and nematode (Pérez et al., 2016). The mode of predation by myxobacteria is induced by close cell-to-cell proximity (Muñoz-Dorado et al., 2016). The rapid bloom of cable bacteria makes them a likely prey in which myxobacteria swarms as proximity increases. At suboxic depths, there was a significantly positive correlation between *Ca.* Electrothrix and one ASV of myxobacteria affiliated to the Class *Polyangia* (Figure 17). This suggests a possible association or predation by myxobacteria even in microoxic to anoxic regions. Myxobacteria possess Type IV pili for swarm communication, motility, and attachment to prey cells (Wrótniak-Drzewiecka et al., 2016). This is noteworthy because *Geobacter sulfurreducens* can transport electrons extracellularly via Type IV pili (Reguera et al., 2005). Moreover, certain strains of myxobacteria affiliated the genus *Anaeromyxobacter* are facultative anaerobic (Sanford et al., 2002) and are able to utilize a broad range of electron acceptors from oxygen to halophenols to uranium (Wu et al., 2006). Although electrical interaction between Myxobacteria and other conductive surfaces has not been previously reported, the relationship between Myxobacteria and *Ca.* Electrothrix at suboxic depths was noteworthy and warrants further investigation.

The observation that cable bacteria abundance declines after a period of prolific growth has been reported in several previous lab studies (Schauer et al., 2014; Rao et al., 2016a) and one year-round field study in a seasonally hypoxic marine basin (Seitaj et al., 2015). The senescence (or decline) of cable bacteria has been

attributed to diminishing stocks of FeS (Schauer et al., 2014; Seitaj et al., 2015). Alternatively, susceptibility to viral attack, protein denaturation in alkaline conditions (Kjeldsen et al., 2019), and increased toxicity of accumulated sulfide (Müller et al., 2019) have been proposed as mechanisms leading to declines in cable bacteria activity. Correlation analysis from the present study indicates predation by the Bdellovibrio-affiliated *OM27* clade as another potential mechanism underlying the declines of cable bacteria, and potentially offers a rationale for cable bacteria avoidance of the oxic zone (Malkin et al., 2015). That is, in addition to potential oxidative stress incurred in the oxic zone (Geerlings et al., 2020), my results suggest that predation by *OM27* clade is also likely a serious threat to cable bacteria cathodic cell survival in the oxic zone. Moreover, in a seasonal study of Chesapeake Bay surface sediments, we observed a bloom of the *OM27* clade co-occurring with a bloom of *Ca.* Electrothrix*,* associated with a rapid influx of phytodetritus from a sinking spring bloom (Malkin et al. *in prep*). These observations suggest a potentially strong relationship between marine cable bacteria and *OM27* clade. These results emphasize a need to examine predatory effects on cable bacteria more closely.

Indirect Microbial Association with Cable Bacteria

Through the anodic oxidation of sulfide, cable bacteria established an acidic suboxic zone which facilitates the dissolution of FeS where dissolved iron and excess free sulfides may diffuse towards the surface (Schauer et al., 2014; Seitaj et al., 2015). Diffusing ferrous iron oxidizes and precipitates as iron oxides near the surface which is consistent with previous observations from cores heavily populated with cable bacteria (Schauer et al., 2014; Seitaj et al., 2015; Risgaard-Petersen et al., 2012;

Rao et al., 2016b; Hermans et al., 2020). The removal of sulfide on centimeters scale is a key consequence of cable bacteria metabolism, thereby creating suitable habitat for taxa inhibited by the presence of sulfide. Earlier studies have shown that toxicity of hydrogen sulfide can inhibit sulfate-reducing bacteria (Reis et al., 1992) and nitrifying bacteria (Joye and Hollibaugh, 1995). During this experiment, electrogenic sulfide oxidation by cable bacteria created a 2 cm thick suboxic zone within 20 days of incubation, thereby alleviating potential sulfide toxicity within the sediment. For instance, the removal of H_2S from contaminated sediments likely allowed the enrichment of sulfate-reducing bacteria and in turn, promoted the degradation of hydrocarbons (Marzocchi et al., 2020). Furthermore, recent works have shown that increased levels of SO_4^{2-} driven by electrogenic sulfide oxidation associated with cable bacteria can stimulate sulfate reduction in freshwater sediments (Sandfeld et al., 2020) and reduce CH_4 emissions from rice-vegetated soils (Scholz et al., 2020). Due to their profound influence on the environment, cable bacteria may be considered ecosystem engineers.

Ecosystem Engineering Effects on Sulfur Cycle Players

Some correlations between *Ca.* Electrothrix and other microbes do not have an obvious direct ecological interaction but may be associated with the biogeochemical effects driven by cable bacteria growth. *Desulfocapsa* were positively correlated with *Ca.* Electrothrix in the sediment surface, which I infer may be a consequence of the influence of cable bacteria on iron cycling and pH levels in the sediments. *Desulfocapsa* is an unusual member of the Deltaproteobacteria in that it appears to be specialized for growth specifically by disproportionation of inorganic sulfur compounds such as elemental sulfur, thiosulfate, or sulfite to hydrogen sulfide

and sulfate (Finster et al., 2013), with growth by sulfate reduction occurring only in certain strains (Janssen et al., 1996). Sulfur disproportionation is only favorable at sulfide concentration less than 1 mM and is also heavily dependent of pH (Thamdrup et al., 1993). Cable bacteria may thereby enable the conditions that particularly benefit sulfur disproportionation, specifically by removing sulfide through electrogenic sulfide oxidation, by enhancing iron oxide precipitation near the sediment surface which further provides sulfide scavenging, and by creating alkaline conditions in the oxic zone (Figure 20d & Table 5). Previous studies have identified that enrichment of iron oxides promotes the growth of *Desulfocapsa* by scavenging sulfide, and thereby driving the disproportionation reaction towards thermodynamic favorability (Thamdrup et al., 1993; Janssen et al., 1996). Moreover, in the absence of metal sulfide scavengers, alkaliphilic sulfur bacteria grew by sulfur disproportionation at pH 10 (Poser et al., 2013). Further experimentation would be needed to test this hypothesis on the indirect relationship between cable bacteria and *Desulfocapsa*.

Conversely, *Desulfocapsa* was negatively correlated with *Ca.* Electrothrix at suboxic sediment depths. The mechanism underlying this relationship is not clear but could be attributed to thermodynamic constraints. Under conditions of pH 7 and < 1 mM of sulfide, sulfur disproportionation yields very low energy (Table 5), insufficient for ATP formation which requires at least -20 kJ mol^{-1} (Canfield et al., 2005). With increased acidity but lower concentration of sulfide, sulfur disproportionation becomes an endergonic reaction (Table 5). *Desulfocapsa* may be inhibited at depth since sulfur disproportionation was not thermodynamically

favorable with increased acidity (pH 5-6) from anodic activity of cable bacteria. However, as pH recedes towards neutrality, sulfur disproportionation can become exergonic again at depth (Table 5). Again, this hypothesis on *Desulfocapsa* requires more investigation.

Table 5. Thermodynamics of sulfur disproportionation. Gibb's free energy of reaction (ΔG_r^o) was calculated based on sediment incubation temperature of 16 ˚C and estimated concentration of products and varying pH based on the geochemical effects of cable bacteria. While cable bacteria may decrease the concentration of free sulfides, the increased acidity led to a less thermodynamically favorable reaction of sulfur disproportionation. As sulfides become depleted and pH recedes to neutrality with cable bacteria disappearance, sulfur disproportionation becomes more thermodynamically favorable. An increase in pH also led to higher yield exergonic reaction. Standard-state Gibb's free energy of formation (ΔG_f^o) of chemical species were obtained from Stumm and Morgan, 1996. Note, ATP formation requires a minimum ΔG_r^o value of -20 kJ mol^{-1} (Canfield et al., 2005).

S^o disproportionation	T (˚C)	HS^- (µM)	SO_4^{2-} (mM)	pH	ΔG_r^o (kJ mol^{-1})
$4S^o + 4H_2O \rightarrow 3HS^- + SO_4^{2-} + 5H^+$	16	700	28	7.0	-8.94
		200	28	6.0	9.30
		20	28	7.0	-34.0
		20	28	8.6	-77.4

At suboxic depths, I observed microbes from four SRB families (*Desulfatiglandaceae*, *Desulfobacteraceae*, *Desulfosarcinaceae*, *Desulfobulbaceae*) positively correlated with *Ca.* Electrothrix, which matches my *a priori* prediction. Recent studies have demonstrated that sulfide oxidation carried out by cable bacteria generates sulfate at suboxic depths (Risgaard-Petersen et al., 2012, Rao et al., 2016b), which in turn stimulates sulfate reduction (Scholz et al., 2020; Sandfeld et al., 2020; Marzocchi et al., 2020). By contrast, I also anticipated a negative correlation with methanogens, based on experimental evidence that by stimulating sulfate reduction, cable bacteria activity also may inhibit methanogenesis (Scholz et al. 2020).

However, I did not detect a clear relationship between *Ca.* Electrothrix and microbes of the Archaeal taxa. The lack of association may be attributed to a combination of factors including poor resolution in Archaeal taxonomy and non-steady-state condition as seen by sulfide and ammonium efflux. These conditions could have inhibited such relationships which may exist in steady-state systems.

In contrast to the stimulation of SRB observed at suboxic depths, at the sediment surface, two families of SRB, including microbes affiliated to the genus *Desulfatiglans, SEEP-SRB1, and* the *Sva0081 sediment group,* were negatively correlated with *Ca.* Electrothrix. Similarly, *Desulfuromusa*, an elemental sulfur reducer (Liesack and Finster, 1994), was negatively correlated with *Ca.* Electrothrix. These negative relationships suggest an antagonistic relationship with *Ca.* Electrothrix. One plausible explanation is that cable bacteria may be stimulating the growth of iron reducing bacteria, which in turn are outcompeting the sulfur and sulfate-reducing bacteria (Lovley and Phillips, 1987), which in the uppermost sediment layer, would likely be occurring just below the oxic-anoxic interface. As previously described, cable bacteria strongly influence iron cycling, and promote the precipitation of iron oxides near the sediment surface (Risgaard-Petersen et al., 2012; Rao et al., 2016b). A previous study observed a positive correlation between *Ca.* Electrothrix and iron-reducing bacteria of the genera *Shewanella* and *Geobacter* in a field study at a Danish Fjord (Otte et al. 2018). Although these taxa were not specifically observed to correlate with *Ca.* Electrothrix growth here, it is likely that some existing relationships were not detected, and this hypothesis could be tested through future experimentation.

Ecosystem Engineering Effects on Magnetotactic Bacteria

At the sediment surface (0 – 0.5 cm), there was a significant and positive correlation between *Ca.* Electrothrix and *Magnetovibrio*, which are described as magnetotactic, and microaerophilic or anaerobic chemolithoautotrophs capable of using thiosulfate and sulfide as electron donors coupled with oxygen or nitrous oxide as terminal electron acceptors (Bazylinski et al., 2013). Although the relationship between cable bacteria and these magnetotactic bacteria is not clear, it is possibly linked to the iron cycling and sulfide removal associated with cable bacteria activity. Magnetotactic bacteria have a high growth requirement for iron (Bazylinski and Frankel, 2004), used to produce magnetosomes, which are composed of either magnetite (Fe_3O_4) or greigite (Fe_3S_4) (Simmonds and Edwards, 2007; Yan et al., 2012). Magnetotactic bacteria are typically found in microoxic to suboxic zones, where they commonly co-occur with sulfide oxidizing bacteria (Simmonds and Edwards, 2007; Yan et al., 2012). It is possible *Magnetovibrio* benefit from the ferrous iron made available by cable bacteria activity at suboxic depths and which diffuses towards the oxic-anoxic interface (Risgaard-Petersen et al., 2012; Rao et al., 2016a) and/or benefit from the removal of toxic sulfide associated with cable bacteria activity and their associated iron oxide precipitation at the oxic-anoxic interface.

In the presence of graphite electrodes, *Magnetovibrio* in anoxic sediments can colonize and form biofilms on the anode surface, possibly using it as a "snorkel" for electron transport (Matturo et al., 2017; Marzocchi et al., 2020). It is enticing to wonder if the positive correlation observed between *Magnetovibrio* and cable bacteria could be a result of interspecies electron transfer. Whether ferrous iron liberated by cable bacteria activity stimulates *Magnetovibrio* growth, or whether some other

relationship exists between *Magnetovibrio* and cable bacteria warrants further investigation.

Ecological Implications

In this lab-based sediment incubation study, I inferred plausible relationships that may be occurring between marine cable bacteria and their surrounding microbial community using a manipulative incubation study. The findings I reported here pose the need for not only interrogation in the laboratory setting but further reinforcements with field studies to reveal any ecological relevance. Laboratory experiments are imperfect and can stray from *in situ* condition and real interactions in the field. In particular, the sediment used in this present study was homogenized and packed into cores which resulted in redistribution of resources. In the lab, organic matter was also not replenished to the sediments. Nevertheless, the results I presented here aim to provide a direction for future research efforts.

I found potential interactions with cable bacteria involving direct predation, resource competition, and syntrophic relationship. Additionally, indirect association as a result of geochemical modification imposed by cable bacteria is also plausible. Since cable bacteria grew to dominate the microbial community, the consequences of their high biomass were, hence, not disproportionate to their impacts on the environment. Therefore, in this study, cable bacteria were not classified as keystone species. Overall, due to their strong influence on local sediment biogeochemistry, cable bacteria likely serve as ecosystem engineers.

Appendix

Table A1. Positively and negatively correlated ASVs (*p*-value < 0.05) at the surface (0 - 0.5 cm) and at depth (0.5 - 2.0 cm) with cable bacteria.

Positively Correlated ASVs with Cable Bacteria at the Surface; p < 0.05											
ASV	**Kingdom**	**Phylum**	**Class**	**Order**	**Family**	**Genus**	**Species**	**Spearman's rho**	**p-value**	**fdr**	**follow criteria?**
ASV_0336	Archaea	Halobacterota	Methanosarcinia	Methanosarciniales	Methanosaetaceae	Methanosaeta	NA	0.829	0.042	0.639	
ASV_0451	Archaea	Thermoplasmatota	Thermoplasmata	Marine_Benthic_Group_D_and_DHVEG-1	NA	NA	NA	0.886	0.019	0.639	
ASV_1553	Bacteria	Acidobacteriota	AT-s3-28	NA	NA	NA	NA	0.820	0.046	0.639	yes
ASV_1585	Bacteria	Bacteroidota	Bacteroidia	Chitinophagales	Saprospiraceae	Aureispira	NA	0.880	0.021	0.639	
ASV_0527	Bacteria	Bacteroidota	Bacteroidia	Chitinophagales	Saprospiraceae	NA	NA	0.928	0.008	0.423	
ASV_2522	Bacteria	Bacteroidota	Bacteroidia	Chitinophagales	Saprospiraceae	NA	NA	0.845	0.034	0.639	yes
ASV_2311	Bacteria	Bacteroidota	Bacteroidia	Cytophagales	Cyclobacteriaceae	NA	NA	0.820	0.046	0.639	yes
ASV_1509	Bacteria	Bacteroidota	Bacteroidia	Flavobacteriales	Crocinitomicaceae	Crocinitomix	NA	0.870	0.024	0.639	
ASV_1281	Bacteria	Bacteroidota	Bacteroidia	NA	NA	NA	NA	0.943	0.005	0.323	
ASV_1934	Bacteria	Bacteroidota	Ignavibacteria	Ignavibacteriales	PHOS-HE36	NA	NA	0.841	0.036	0.639	
ASV_0757	Bacteria	Bdellovibrionota	Bdellovibrionia	Bdellovibrionales	Bdellovibrionaceae	OM27_clade	NA	0.928	0.008	0.423	yes
ASV_0838	Bacteria	Bdellovibrionota	Bdellovibrionia	Bdellovibrionales	Bdellovibrionaceae	OM27_clade	NA	0.829	0.042	0.639	yes
ASV_0864	Bacteria	Bdellovibrionota	Bdellovibrionia	Bdellovibrionales	Bdellovibrionaceae	OM27_clade	NA	0.841	0.036	0.639	
ASV_3913	Bacteria	Bdellovibrionota	Bdellovibrionia	Bdellovibrionales	Bdellovibrionaceae	OM27_clade	NA	0.845	0.034	0.639	yes
ASV_1012	Bacteria	Chloroflexi	Anaerolineae	Anaerolineales	Anaerolineaceae	NA	NA	0.820	0.046	0.639	
ASV_0703	Bacteria	Chloroflexi	Anaerolineae	Ardenticatenales	NA	NA	NA	0.943	0.005	0.323	
ASV_2219	Bacteria	Deinococcota	Deinococci	Deinococcales	Trueperaceae	Truepera	NA	0.899	0.015	0.639	
ASV_1061	Bacteria	Desulfobacterota	Desulfobacteria	Desulfatiglandales	Desulfatiglandaceae	Desulfatiglans	NA	0.928	0.008	0.423	
ASV_5587	Bacteria	Desulfobacterota	Desulfobacteria	Desulfatiglandales	Desulfatiglandaceae	Desulfatiglans	NA	0.845	0.034	0.639	yes
ASV_0652	Bacteria	Desulfobacterota	Desulfobacteria	Desulfobacterales	Desulfosarcinaceae	Desulfosarcina	NA	0.943	0.005	0.323	
ASV_0014	Bacteria	Desulfobacterota	Desulfobulbia	Desulfobulbales	Desulfocapsaceae	Desulfocapsa	NA	0.812	0.050	0.639	yes
ASV_0066	Bacteria	Desulfobacterota	Desulfobulbia	Desulfobulbales	Desulfocapsaceae	Desulfocapsa	NA	0.943	0.005	0.323	yes
ASV_0060	Bacteria	Desulfobacterota	Desulfobulbia	Desulfobulbales	Desulfurivibrionaceae	MSBL7	NA	0.812	0.050	0.639	yes
ASV_1638	Bacteria	Desulfobacterota	Desulfuromonadia	Bradymonadales	NA	NA	NA	0.941	0.005	0.323	yes
ASV_1736	Bacteria	Marinimicrobia_(SAR406_clade)	NA	NA	NA	NA	NA	0.845	0.034	0.639	yes

Positively Correlated ASVs with Cable Bacteria at the Surface; p < 0.05 (continued)											
ASV	Kingdom	Phylum	Class	Order	Family	Genus	Species	Spearman's rho	p-value	fdr	follow criteria?
ASV_1040	Bacteria	Myxococcota	Polyangia	Haliangiales	Haliangiaceae	Haliangium	NA	0.943	0.005	0.323	
ASV_1463	Bacteria	Myxococcota	Polyangia	Haliangiales	Haliangiaceae	Haliangium	NA	0.941	0.005	0.323	yes
ASV_0987	Bacteria	Planctomycetota	Planctomycetes	Planctomycetales	Rubinisphaeraceae	Planctomicrobium	NA	0.886	0.019	0.639	
ASV_0150	Bacteria	Proteobacteria	Alphaproteobacteria	Rhodospirillales	Magnetospiraceae	Magnetovibrio	NA	0.943	0.005	0.323	yes
ASV_0221	Bacteria	Proteobacteria	Alphaproteobacteria	Rhodospirillales	Magnetospiraceae	Magnetovibrio	NA	0.943	0.005	0.323	
ASV_0466	Bacteria	Proteobacteria	Alphaproteobacteria	Rhodospirillales	Magnetospiraceae	Magnetovibrio	NA	1.000	0.000	0.000	yes
ASV_0741	Bacteria	Proteobacteria	Alphaproteobacteria	Rhodospirillales	Magnetospiraceae	Magnetovibrio	NA	1.000	0.000	0.000	yes
ASV_0572	Bacteria	Proteobacteria	Gammaproteobacteria	Burkholderiales	Nitrosomonadaceae	Nitrosomonas	NA	0.829	0.042	0.639	yes
ASV_1220	Bacteria	Proteobacteria	Gammaproteobacteria	Chromatiales	Chromatiaceae	Candidatus_Thiobios	NA	0.812	0.050	0.639	
ASV_0687	Bacteria	Proteobacteria	Gammaproteobacteria	Ectothiorhodospirales	Thioalkalispiraceae	Thioalkalispira-Sulfurivermis	NA	0.986	0.000	0.102	yes
ASV_2934	Bacteria	Proteobacteria	Gammaproteobacteria	Ectothiorhodospirales	Thioalkalispiraceae	Thiohalophilus	NA	0.841	0.036	0.639	
ASV_0213	Bacteria	Proteobacteria	Gammaproteobacteria	Gammaproteobacteria _Incertae_Sedis	Unknown_Family	NA	NA	0.943	0.005	0.323	yes
ASV_0377	Bacteria	Proteobacteria	Gammaproteobacteria	NA	NA	NA	NA	0.820	0.046	0.639	yes
ASV_1480	Bacteria	Proteobacteria	Gammaproteobacteria	NA	NA	NA	NA	0.886	0.019	0.639	yes
ASV_1123	Bacteria	Proteobacteria	Gammaproteobacteria	Steroidobacterales	Woeseiaceae	Woeseia	NA	0.943	0.005	0.323	
ASV_2894	Bacteria	Verrucomicrobiota	Chlamydiae	Chlamydiales	NA	NA	NA	0.841	0.036	0.639	
ASV_1227	Bacteria	Verrucomicrobiota	Verrucomicrobiae	Opitutales	Opitutaceae	Diplosphaera	NA	0.820	0.046	0.639	yes
ASV_1970	Bacteria	Zixibacteria	NA	NA	NA	NA	NA	0.880	0.021	0.639	

Negatively Correlated ASVs with Cable Bacteria at the Surface; p < 0.05											
ASV	Kingdom	Phylum	Class	Order	Family	Genus	Species	Spearman's rho	p-value	fdr	follow criteria?
ASV_1924	Archaea	Asgardarchaeota	Heimdallarchaeia	NA	NA	NA	NA	-0.941	0.005	0.323	yes
ASV_0315	Archaea	Asgardarchaeota	Lokiarchaeia	NA	NA	NA	NA	-0.812	0.050	0.639	
ASV_0385	Archaea	Asgardarchaeota	Lokiarchaeia	NA	NA	NA	NA	-0.845	0.034	0.639	
ASV_0449	Archaea	Thermoplasmatota	Thermoplasmata	Marine_Benthic_Group_D_and_DHVEG-1	NA	NA	NA	-0.941	0.005	0.323	yes
ASV_1033	Archaea	Thermoplasmatota	Thermoplasmata	Marine_Benthic_Group_D_and_DHVEG-1	NA	NA	NA	-0.845	0.034	0.639	
ASV_1224	Archaea	Thermoplasmatota	Thermoplasmata	Marine_Benthic_Group_D_and_DHVEG-1	NA	NA	NA	-0.941	0.005	0.323	yes
ASV_1462	Archaea	Thermoplasmatota	Thermoplasmata	Marine_Benthic_Group_D_and_DHVEG-1	NA	NA	NA	-0.845	0.034	0.639	
ASV_0523	Bacteria	Acidobacteriota	Aminicenantia	Aminicenantales	NA	NA	NA	-0.941	0.005	0.323	yes
ASV_1089	Bacteria	Acidobacteriota	Aminicenantia	Aminicenantales	NA	NA	NA	-0.845	0.034	0.639	
ASV_2025	Bacteria	Acidobacteriota	Aminicenantia	Aminicenantales	NA	NA	NA	-0.845	0.034	0.639	
ASV_2548	Bacteria	Acidobacteriota	Aminicenantia	Aminicenantales	NA	NA	NA	-0.941	0.005	0.323	yes
ASV_1289	Bacteria	Acidobacteriota	AT-s3-28	NA	NA	NA	NA	-0.845	0.034	0.639	
ASV_2541	Bacteria	Acidobacteriota	Holophagae	Acanthopleuribacteraleles	Acanthopleuribacteraceae	Acanthopleuribacter	NA	-0.845	0.034	0.639	
ASV_1302	Bacteria	Acidobacteriota	Subgroup_22	NA	NA	NA	NA	-0.941	0.005	0.323	yes
ASV_1572	Bacteria	Acidobacteriota	Subgroup_22	NA	NA	NA	NA	-0.941	0.005	0.323	yes
ASV_3280	Bacteria	Acidobacteriota	Subgroup_22	NA	NA	NA	NA	-0.845	0.034	0.639	
ASV_0469	Bacteria	Acidobacteriota	Vicinamibacteria	Subgroup_9	NA	NA	NA	-0.812	0.050	0.639	
ASV_2164	Bacteria	Actinobacteriota	Actinobacteria	PeM15	NA	NA	NA	-0.845	0.034	0.639	
ASV_0538	Bacteria	Bacteroidota	Bacteroidia	Bacteroidales	Bacteroidetes_BD2-2	NA	NA	-0.820	0.046	0.639	
ASV_0745	Bacteria	Bacteroidota	Bacteroidia	Bacteroidales	Bacteroidetes_BD2-2	NA	NA	-0.845	0.034	0.639	
ASV_0828	Bacteria	Bacteroidota	Bacteroidia	Bacteroidales	Bacteroidetes_BD2-2	NA	NA	-0.820	0.046	0.639	
ASV_1198	Bacteria	Bacteroidota	Bacteroidia	Bacteroidales	Bacteroidetes_BD2-2	NA	NA	-0.820	0.046	0.639	
ASV_2372	Bacteria	Bacteroidota	Bacteroidia	Bacteroidales	Bacteroidetes_BD2-2	NA	NA	-0.845	0.034	0.639	
ASV_0666	Bacteria	Bacteroidota	Bacteroidia	Bacteroidales	Bacteroidetes_vadinHA17	NA	NA	-0.941	0.005	0.323	yes
ASV_1400	Bacteria	Bacteroidota	Bacteroidia	Bacteroidales	Bacteroidetes_vadinHA17	NA	NA	-0.845	0.034	0.639	
ASV_2408	Bacteria	Bacteroidota	Bacteroidia	Bacteroidales	Bacteroidetes_vadinHA17	NA	NA	-0.845	0.034	0.639	

Negatively Correlated ASVs with Cable Bacteria at the Surface; p < 0.05 (continued)											
ASV	Kingdom	Phylum	Class	Order	Family	Genus	Species	Spearman's rho	p-value	fdr	follow criteria?
ASV_0754	Bacteria	Bacteroidota	Bacteroidia	Bacteroidales	Marinilabiliaceae	NA	NA	-0.820	0.046	0.639	
ASV_1261	Bacteria	Bacteroidota	Bacteroidia	Bacteroidales	NA	NA	NA	-0.845	0.034	0.639	
ASV_1318	Bacteria	Bacteroidota	Bacteroidia	Bacteroidales	NA	NA	NA	-0.845	0.034	0.639	
ASV_1107	Bacteria	Bacteroidota	Bacteroidia	Chitinophagales	Saprospiraceae	Phaeodactylibacter	NA	-0.986	0.000	0.102	yes
ASV_1763	Bacteria	Bacteroidota	Bacteroidia	Cytophagales	Cyclobacteriaceae	Algoriphagus	NA	-0.845	0.034	0.639	
ASV_0787	Bacteria	Bacteroidota	Bacteroidia	Cytophagales	Cyclobacteriaceae	NA	NA	-0.812	0.050	0.639	
ASV_1311	Bacteria	Bacteroidota	Bacteroidia	Flavobacteriales	Flavobacteriaceae	Maribacter	NA	-0.941	0.005	0.323	yes
ASV_1104	Bacteria	Bacteroidota	Bacteroidia	Flavobacteriales	Flavobacteriaceae	NA	NA	-0.880	0.021	0.639	yes
ASV_0697	Bacteria	Bacteroidota	Bacteroidia	NA	NA	NA	NA	-0.886	0.019	0.639	yes
ASV_0792	Bacteria	Bacteroidota	Bacteroidia	Sphingobacteriales	Lentimicrobiaceae	NA	NA	-0.820	0.046	0.639	
ASV_0948	Bacteria	Bacteroidota	Bacteroidia	Sphingobacteriales	Lentimicrobiaceae	NA	NA	-0.941	0.005	0.323	yes
ASV_1225	Bacteria	Bacteroidota	Bacteroidia	Sphingobacteriales	Lentimicrobiaceae	NA	NA	-0.845	0.034	0.639	
ASV_1631	Bacteria	Bacteroidota	Bacteroidia	Sphingobacteriales	Lentimicrobiaceae	NA	NA	-0.845	0.034	0.639	
ASV_2119	Bacteria	Bacteroidota	Bacteroidia	Sphingobacteriales	Lentimicrobiaceae	NA	NA	-0.845	0.034	0.639	
ASV_2190	Bacteria	Bacteroidota	Bacteroidia	Sphingobacteriales	Lentimicrobiaceae	NA	NA	-0.880	0.021	0.639	yes
ASV_2368	Bacteria	Bacteroidota	Bacteroidia	Sphingobacteriales	Lentimicrobiaceae	NA	NA	-0.845	0.034	0.639	
ASV_0120	Bacteria	Bacteroidota	Ignavibacteria	Ignavibacteriales	Ignavibacteriaceae	Ignavibacterium	NA	-0.943	0.005	0.323	
ASV_1146	Bacteria	Bacteroidota	Ignavibacteria	Ignavibacteriales	NA	NA	NA	-0.880	0.021	0.639	yes
ASV_2090	Bacteria	Bacteroidota	Ignavibacteria	Ignavibacteriales	NA	NA	NA	-0.845	0.034	0.639	
ASV_0184	Bacteria	Bacteroidota	Kryptonia	Kryptoniales	BSV26	NA	NA	-0.829	0.042	0.639	
ASV_0898	Bacteria	Calditrichota	Calditrichia	Calditrichales	Calditrichaceae	JdFR-76	NA	-0.829	0.042	0.639	
ASV_0645	Bacteria	Calditrichota	Calditrichia	Calditrichales	Calditrichaceae	NA	NA	-0.886	0.019	0.639	
ASV_1119	Bacteria	Calditrichota	Calditrichia	Calditrichales	Calditrichaceae	NA	NA	-0.845	0.034	0.639	
ASV_1294	Bacteria	Calditrichota	Calditrichia	Calditrichales	Calditrichaceae	NA	NA	-0.845	0.034	0.639	
ASV_0723	Bacteria	Calditrichota	Calditrichia	Calditrichales	Calditrichaceae	SM23-31	NA	-0.845	0.034	0.639	
ASV_1187	Bacteria	Calditrichota	Calditrichia	Calditrichales	Calditrichaceae	SM23-31	NA	-0.812	0.050	0.639	yes
ASV_1804	Bacteria	Calditrichota	Calditrichia	Calditrichales	Calditrichaceae	SM23-31	NA	-0.845	0.034	0.639	
ASV_0746	Bacteria	Campilobacterota	Campylobacteria	Campylobacterales	Sulfurimonadaceae	Sulfurimonas	NA	-0.820	0.046	0.639	
ASV_1135	Bacteria	Campilobacterota	Campylobacteria	Campylobacterales	Sulfurimonadaceae	Sulfurimonas	NA	-0.820	0.046	0.639	
ASV_2699	Bacteria	Campilobacterota	Campylobacteria	Campylobacterales	Sulfurimonadaceae	Sulfurimonas	NA	-0.845	0.034	0.639	
ASV_1495	Bacteria	Chloroflexi	Anaerolineae	Anaerolineales	Anaerolineaceae	Anaerolineaceae_UC G-001	NA	-0.812	0.050	0.639	
ASV_0446	Bacteria	Chloroflexi	Anaerolineae	Anaerolineales	Anaerolineaceae	NA	NA	-0.820	0.046	0.639	
ASV_1103	Bacteria	Chloroflexi	Anaerolineae	Anaerolineales	Anaerolineaceae	NA	NA	-0.820	0.046	0.639	
ASV_2577	Bacteria	Chloroflexi	Anaerolineae	SBR1031	A4b	NA	NA	-0.845	0.034	0.639	

Negatively Correlated ASVs with Cable Bacteria at the Surface; p < 0.05 (continued)											
ASV	Kingdom	Phylum	Class	Order	Family	Genus	Species	Spearman's rho	p-value	fdr	follow criteria?
ASV_1571	Bacteria	Cloacimonadota	Cloacimonadia	Cloacimonadales	NA	NA	NA	-0.845	0.034	0.639	
ASV_0428	Bacteria	Desulfobacterota	Desulfobacteria	Desulfatiglandales	Desulfatiglandaceae	Desulfatiglans	NA	-0.829	0.042	0.639	yes
ASV_1022	Bacteria	Desulfobacterota	Desulfobacteria	Desulfatiglandales	Desulfatiglandaceae	Desulfatiglans	NA	-0.829	0.042	0.639	yes
ASV_1251	Bacteria	Desulfobacterota	Desulfobacteria	Desulfatiglandales	Desulfatiglandaceae	Desulfatiglans	NA	-0.845	0.034	0.639	
ASV_1827	Bacteria	Desulfobacterota	Desulfobacteria	Desulfatiglandales	Desulfatiglandaceae	Desulfatiglans	NA	-0.986	0.000	0.102	yes
ASV_0077	Bacteria	Desulfobacterota	Desulfobacteria	Desulfobacterales	Desulfosarcinaceae	NA	NA	-0.829	0.042	0.639	
ASV_0124	Bacteria	Desulfobacterota	Desulfobacteria	Desulfobacterales	Desulfosarcinaceae	NA	NA	-0.886	0.019	0.639	
ASV_0551	Bacteria	Desulfobacterota	Desulfobacteria	Desulfobacterales	Desulfosarcinaceae	NA	NA	-0.941	0.005	0.323	yes
ASV_0591	Bacteria	Desulfobacterota	Desulfobacteria	Desulfobacterales	Desulfosarcinaceae	NA	NA	-0.829	0.042	0.639	yes
ASV_0748	Bacteria	Desulfobacterota	Desulfobacteria	Desulfobacterales	Desulfosarcinaceae	NA	NA	-0.845	0.034	0.639	
ASV_1148	Bacteria	Desulfobacterota	Desulfobacteria	Desulfobacterales	Desulfosarcinaceae	NA	NA	-0.941	0.005	0.323	yes
ASV_1904	Bacteria	Desulfobacterota	Desulfobacteria	Desulfobacterales	Desulfosarcinaceae	NA	NA	-0.880	0.021	0.639	yes
ASV_2239	Bacteria	Desulfobacterota	Desulfobacteria	Desulfobacterales	Desulfosarcinaceae	NA	NA	-0.941	0.005	0.323	yes
ASV_2683	Bacteria	Desulfobacterota	Desulfobacteria	Desulfobacterales	Desulfosarcinaceae	NA	NA	-0.986	0.000	0.102	yes
ASV_2752	Bacteria	Desulfobacterota	Desulfobacteria	Desulfobacterales	Desulfosarcinaceae	NA	NA	-0.829	0.042	0.639	
ASV_0142	Bacteria	Desulfobacterota	Desulfobacteria	Desulfobacterales	Desulfosarcinaceae	SEEP-SRB1	NA	-0.829	0.042	0.639	yes
ASV_0536	Bacteria	Desulfobacterota	Desulfobacteria	Desulfobacterales	Desulfosarcinaceae	SEEP-SRB1	NA	-0.941	0.005	0.323	yes
ASV_0597	Bacteria	Desulfobacterota	Desulfobacteria	Desulfobacterales	Desulfosarcinaceae	SEEP-SRB1	NA	-0.928	0.008	0.423	yes
ASV_0004	Bacteria	Desulfobacterota	Desulfobacteria	Desulfobacterales	Desulfosarcinaceae	Sva0081_sediment_group	NA	-0.829	0.042	0.639	yes
ASV_0140	Bacteria	Desulfobacterota	Desulfobacteria	Desulfobacterales	Desulfosarcinaceae	Sva0081_sediment_group	NA	-0.886	0.019	0.639	
ASV_0206	Bacteria	Desulfobacterota	Desulfobacteria	Desulfobacterales	Desulfosarcinaceae	Sva0081_sediment_group	NA	-0.928	0.008	0.423	yes
ASV_0585	Bacteria	Desulfobacterota	Desulfobulbia	Desulfobulbales	Desulfocapsaceae	NA	NA	-0.941	0.005	0.323	yes
ASV_0521	Bacteria	Desulfobacterota	Desulfuromonadia	Desulfuromonadia_or	Geopsychrobacteracea e	Desulfuromusa	NA	-0.812	0.050	0.639	
ASV_1545	Bacteria	Desulfobacterota	Desulfuromonadia	Desulfuromonadia_or	Geopsychrobacteracea e	Desulfuromusa	NA	-0.870	0.024	0.639	yes
ASV_2928	Bacteria	Desulfobacterota	Syntrophia	Syntrophales	NA	NA	NA	-0.845	0.034	0.639	
ASV_1060	Bacteria	Desulfobacterota	Syntrophia	Syntrophales	Syntrophaceae	Syntrophus	NA	-0.845	0.034	0.639	
ASV_0069	Bacteria	Desulfobacterota	Syntrophobacteria	Syntrophobacterales	NA	NA	NA	-0.829	0.042	0.639	yes
ASV_0974	Bacteria	Desulfobacterota	Syntrophobacteria	Syntrophobacterales	NA	NA	NA	-0.928	0.008	0.423	yes
ASV_1404	Bacteria	Fermentibacterota	Fermentibacteria	Fermentibacterales	Fermentibacteraceae	NA	NA	-0.941	0.005	0.323	yes

Negatively Correlated ASVs with Cable Bacteria at the Surface; p < 0.05 (continued)											
ASV	Kingdom	Phylum	Class	Order	Family	Genus	Species	Spearman's rho	p-value	fdr	follow criteria?
ASV_1532	Bacteria	Fermentibacterota	Fermentibacteria	Fermentibacterales	Fermentibacteraceae	NA	NA	-0.845	0.034	0.639	
ASV_1382	Bacteria	Gemmatimonadota	Gemmatimonadetes	Gemmatimonadales	Gemmatimonadaceae	NA	NA	-0.845	0.034	0.639	
ASV_1238	Bacteria	Gemmatimonadota	MD2902-B12	NA	NA	NA	NA	-0.845	0.034	0.639	
ASV_1164	Bacteria	Latescibacterota	Latescibacteria	Latescibacterales	Latescibacteraceae	NA	NA	-0.880	0.021	0.639	yes
ASV_0641	Bacteria	Latescibacterota	NA	NA	NA	NA	NA	-0.941	0.005	0.323	yes
ASV_0771	Bacteria	Latescibacterota	NA	NA	NA	NA	NA	-1.000	0.000	0.000	yes
ASV_0878	Bacteria	Latescibacterota	NA	NA	NA	NA	NA	-0.928	0.008	0.423	yes
ASV_2411	Bacteria	LCP-89	NA	NA	NA	NA	NA	-0.845	0.034	0.639	
ASV_2731	Bacteria	Marinimicrobia_(SAR406_clade)	NA	NA	NA	NA	NA	-0.880	0.021	0.639	yes
ASV_1372	Bacteria	Myxococcota	Polyangia	PS-B29	NA	NA	NA	-0.845	0.034	0.639	
ASV_0938	Bacteria	Myxococcota	Polyangia	VHS-B3-70	NA	NA	NA	-0.880	0.021	0.639	yes
ASV_2640	Bacteria	Myxococcota	Polyangia	VHS-B3-70	NA	NA	NA	-0.880	0.021	0.639	yes
ASV_1749	Bacteria	Planctomycetota	OM190	NA	NA	NA	NA	-0.845	0.034	0.639	
ASV_1525	Bacteria	Planctomycetota	Phycisphaerae	DG-20	NA	NA	NA	-0.845	0.034	0.639	
ASV_1761	Bacteria	Planctomycetota	Phycisphaerae	MSBL9	SG8-4	NA	NA	-0.941	0.005	0.323	yes
ASV_2304	Bacteria	Planctomycetota	Phycisphaerae	MSBL9	SG8-4	NA	NA	-0.880	0.021	0.639	yes
ASV_0688	Bacteria	Planctomycetota	Phycisphaerae	Phycisphaerales	Phycisphaeraceae	Urania-1B-19_marine_sediment_group	NA	-0.899	0.015	0.639	
ASV_1017	Bacteria	Planctomycetota	Planctomycetes	Pirellulales	Pirellulaceae	NA	NA	-0.845	0.034	0.639	
ASV_0476	Bacteria	Proteobacteria	Alphaproteobacteria	Rhodobacterales	Rhodobacteraceae	NA	NA	-0.943	0.005	0.323	yes
ASV_2848	Bacteria	Proteobacteria	Alphaproteobacteria	Rhodobacterales	Rhodobacteraceae	NA	NA	-0.941	0.005	0.323	yes
ASV_1840	Bacteria	Proteobacteria	Alphaproteobacteria	Rhodobacterales	Rhodobacteraceae	Sulfitobacter	litoralis	-0.845	0.034	0.639	
ASV_0021	Bacteria	Proteobacteria	Gammaproteobacteria	B2M28	NA	NA	NA	-0.829	0.042	0.639	
ASV_0047	Bacteria	Proteobacteria	Gammaproteobacteria	B2M28	NA	NA	NA	-0.886	0.019	0.639	
ASV_0053	Bacteria	Proteobacteria	Gammaproteobacteria	B2M28	NA	NA	NA	-0.886	0.019	0.639	
ASV_0078	Bacteria	Proteobacteria	Gammaproteobacteria	B2M28	NA	NA	NA	-0.943	0.005	0.323	yes
ASV_0173	Bacteria	Proteobacteria	Gammaproteobacteria	B2M28	NA	NA	NA	-1.000	0.000	0.000	yes
ASV_0226	Bacteria	Proteobacteria	Gammaproteobacteria	B2M28	NA	NA	NA	-0.943	0.005	0.323	yes
ASV_0296	Bacteria	Proteobacteria	Gammaproteobacteria	B2M28	NA	NA	NA	-0.899	0.015	0.639	
ASV_0361	Bacteria	Proteobacteria	Gammaproteobacteria	B2M28	NA	NA	NA	-0.812	0.050	0.639	

Negatively Correlated ASVs with Cable Bacteria at the Surface; p < 0.05 (continued)											
ASV	Kingdom	Phylum	Class	Order	Family	Genus	Species	Spearman's rho	p-value	fdr	follow criteria?
ASV_0369	Bacteria	Proteobacteria	Gammaproteobacteria	B2M28	NA	NA	NA	-0.812	0.050	0.639	
ASV_0412	Bacteria	Proteobacteria	Gammaproteobacteria	B2M28	NA	NA	NA	-0.829	0.042	0.639	
ASV_0131	Bacteria	Proteobacteria	Gammaproteobacteria	Cellvibrionales	Halieaceae	Halioglobus	NA	-0.943	0.005	0.323	
ASV_0347	Bacteria	Proteobacteria	Gammaproteobacteria	Cellvibrionales	Halieaceae	Halioglobus	NA	-0.829	0.042	0.639	
ASV_2228	Bacteria	Proteobacteria	Gammaproteobacteria	Cellvibrionales	Porticoccaceae	Porticoccus	NA	-0.880	0.021	0.639	yes
ASV_0127	Bacteria	Proteobacteria	Gammaproteobacteria	Chromatiales	Sedimenticolaceae	NA	NA	-1.000	0.000	0.000	yes
ASV_1295	Bacteria	Proteobacteria	Gammaproteobacteria	Chromatiales	Sedimenticolaceae	NA	NA	-0.880	0.021	0.639	yes
ASV_1365	Bacteria	Proteobacteria	Gammaproteobacteria	Chromatiales	Sedimenticolaceae	NA	NA	-0.941	0.005	0.323	yes
ASV_0867	Bacteria	Proteobacteria	Gammaproteobacteria	Chromatiales	Sedimenticolaceae	Sedimenticola	NA	-0.829	0.042	0.639	
ASV_0345	Bacteria	Proteobacteria	Gammaproteobacteria	Ectothiorhodospirales	Ectothiorhodospiraceae	Thiogranum	NA	-0.941	0.005	0.323	yes
ASV_0024	Bacteria	Proteobacteria	Gammaproteobacteria	NA	NA	NA	NA	-0.829	0.042	0.639	
ASV_0095	Bacteria	Proteobacteria	Gammaproteobacteria	NA	NA	NA	NA	-0.829	0.042	0.639	
ASV_0243	Bacteria	Proteobacteria	Gammaproteobacteria	NA	NA	NA	NA	-0.829	0.042	0.639	
ASV_0289	Bacteria	Proteobacteria	Gammaproteobacteria	NA	NA	NA	NA	-0.829	0.042	0.639	
ASV_1550	Bacteria	Proteobacteria	Gammaproteobacteria	NA	NA	NA	NA	-0.880	0.021	0.639	yes
ASV_3957	Bacteria	Proteobacteria	Gammaproteobacteria	NA	NA	NA	NA	-0.845	0.034	0.639	
ASV_1547	Bacteria	Proteobacteria	Gammaproteobacteria	Oceanospirillales	Nitrincolaceae	Neptunomonas	NA	-0.820	0.046	0.639	
ASV_0057	Bacteria	Proteobacteria	Gammaproteobacteria	Thiomicrospirales	Thiomicrospiraceae	Thiomicrorhabdus	NA	-0.943	0.005	0.323	
ASV_1369	Bacteria	Proteobacteria	Gammaproteobacteria	Thiomicrospirales	Thiomicrospiraceae	Thiomicrorhabdus	NA	-0.845	0.034	0.639	
ASV_1780	Bacteria	Proteobacteria	Gammaproteobacteria	Thiotrichales	Thiotrichaceae	NA	NA	-0.845	0.034	0.639	
ASV_0431	Bacteria	Spirochaetota	Leptospirae	Leptospirales	Leptospiraceae	RBG-16-49-21	NA	-0.820	0.046	0.639	
ASV_0751	Bacteria	Spirochaetota	Leptospirae	Leptospirales	Leptospiraceae	RBG-16-49-21	NA	-0.845	0.034	0.639	
ASV_1169	Bacteria	Spirochaetota	Spirochaetia	Spirochaetales	Spirochaetaceae	Spirochaeta	NA	-0.880	0.021	0.639	yes
ASV_0848	Bacteria	Spirochaetota	Spirochaetia	Spirochaetales	Spirochaetaceae	Spirochaeta_2	NA	-0.845	0.034	0.639	
ASV_1670	Bacteria	Spirochaetota	Spirochaetia	Spirochaetales	Spirochaetaceae	Spirochaeta_2	NA	-0.820	0.046	0.639	
ASV_0998	Bacteria	Sva0485	NA	NA	NA	NA	NA	-0.845	0.034	0.639	
ASV_1241	Bacteria	Sva0485	NA	NA	NA	NA	NA	-0.845	0.034	0.639	
ASV_1242	Bacteria	Synergistota	Synergistia	Synergistales	Synergistaceae	Thermovirga	NA	-0.841	0.036	0.639	
ASV_2256	Bacteria	Verrucomicrobiota	Kiritimatiellae	WCHB1-41	NA	NA	NA	-0.845	0.034	0.639	
ASV_2266	Bacteria	Verrucomicrobiota	Lentisphaeria	NA	NA	NA	NA	-0.845	0.034	0.639	
ASV_2226	Bacteria	Verrucomicrobiota	Verrucomicrobiae	S-BQ2-57_soil_group	NA	NA	NA	-0.845	0.034	0.639	

Positively Correlated ASVs with Cable Bacteria at Depth; p < 0.05											
ASV	**Kingdom**	**Phylum**	**Class**	**Order**	**Family**	**Genus**	**Species**	**Spearman's rho**	**p-value**	**fdr**	**follow criteria?**
ASV_0410	Archaea	Asgardarchaeota	Lokiarchaeia	NA	NA	NA	NA	0.505	0.020	0.682	yes
ASV_5292	Archaea	Crenarchaeota	Bathyarchaeia	NA	NA	NA	NA	0.463	0.035	0.682	
ASV_5466	Archaea	Crenarchaeota	Nitrososphaeria	Nitrosopumilales	Nitrosopumilaceae	Candidatus_Nitrosopumilus	NA	0.463	0.035	0.682	
ASV_4442	Archaea	Halobacterota	Methanomicrobia	Methanomicrobiales	NA	NA	NA	0.463	0.035	0.682	
ASV_4580	Archaea	Halobacterota	Methanomicrobia	Methanomicrobiales	NA	NA	NA	0.463	0.035	0.682	
ASV_0132	Archaea	Thermoplasmatota	Thermoplasmata	Marine_Benthic_Group_D_and_DHVEG-1	NA	NA	NA	0.456	0.038	0.682	
ASV_0496	Archaea	Thermoplasmatota	Thermoplasmata	Marine_Benthic_Group_D_and_DHVEG-1	NA	NA	NA	0.506	0.019	0.682	yes
ASV_0556	Archaea	Thermoplasmatota	Thermoplasmata	Marine_Benthic_Group_D_and_DHVEG-1	NA	NA	NA	0.619	0.003	0.376	yes
ASV_2739	Archaea	Thermoplasmatota	Thermoplasmata	Marine_Benthic_Group_D_and_DHVEG-1	NA	NA	NA	0.463	0.035	0.682	
ASV_2975	Archaea	Thermoplasmatota	Thermoplasmata	Marine_Benthic_Group_D_and_DHVEG-1	NA	NA	NA	0.510	0.018	0.682	
ASV_0562	Archaea	Thermoplasmatota	Thermoplasmata	Methanomassiliicoccales	Methanomassiliicoccaceae	NA	NA	0.619	0.003	0.376	
ASV_4159	Archaea	Thermoplasmatota	Thermoplasmata	SG8-5	NA	NA	NA	0.463	0.035	0.682	
ASV_1122	Bacteria	Acidobacteriota	Aminicenantia	Aminicenantales	NA	NA	NA	0.651	0.001	0.299	
ASV_4577	Bacteria	Acidobacteriota	Aminicenantia	Aminicenantales	NA	NA	NA	0.463	0.035	0.682	
ASV_3134	Bacteria	Acidobacteriota	Subgroup_22	NA	NA	NA	NA	0.463	0.035	0.682	
ASV_1983	Bacteria	Acidobacteriota	Thermoanaerobaculia	Thermoanaerobaculales	Thermoanaerobaculaceae	Subgroup_23	NA	0.463	0.035	0.682	
ASV_0366	Bacteria	Acidobacteriota	Vicinamibacteria	Subgroup_17	NA	NA	NA	0.501	0.021	0.682	
ASV_3556	Bacteria	Acidobacteriota	Vicinamibacteria	Subgroup_9	NA	NA	NA	0.463	0.035	0.682	
ASV_2164	Bacteria	Actinobacteriota	Actinobacteria	PeM15	NA	NA	NA	0.540	0.012	0.649	
ASV_0528	Bacteria	Bacteroidota	Bacteroidia	Bacteroidales	Bacteroidetes_BD2-2	NA	NA	0.676	0.001	0.299	yes
ASV_0542	Bacteria	Bacteroidota	Bacteroidia	Bacteroidales	Bacteroidetes_BD2-2	NA	NA	0.462	0.035	0.682	
ASV_0745	Bacteria	Bacteroidota	Bacteroidia	Bacteroidales	Bacteroidetes_BD2-2	NA	NA	0.549	0.010	0.611	
ASV_4578	Bacteria	Bacteroidota	Bacteroidia	Bacteroidales	Marinifilaceae	NA	NA	0.463	0.035	0.682	
ASV_4439	Bacteria	Bacteroidota	Bacteroidia	Bacteroidales	NA	NA	NA	0.463	0.035	0.682	
ASV_0601	Bacteria	Bacteroidota	Bacteroidia	Bacteroidales	Prolixibacteraceae	NA	NA	0.602	0.004	0.452	
ASV_2939	Bacteria	Bacteroidota	Bacteroidia	Bacteroidales	Prolixibacteraceae	WCHB1-32	NA	0.575	0.006	0.528	

Positively Correlated ASVs with Cable Bacteria at Depth; p < 0.05 (continued)											
ASV	Kingdom	Phylum	Class	Order	Family	Genus	Species	Spearman's rho	p-value	fdr	follow criteria?
ASV_5615	Bacteria	Bacteroidota	Bacteroidia	Chitinophagales	Saprospiraceae	NA	NA	0.463	0.035	0.682	
ASV_3828	Bacteria	Bacteroidota	Bacteroidia	Sphingobacteriales	Lentimicrobiaceae	NA	NA	0.463	0.035	0.682	
ASV_3643	Bacteria	Bacteroidota	Kapabacteria	Kapabacteriales	NA	NA	NA	0.463	0.035	0.682	
ASV_4427	Bacteria	Bacteroidota	Kryptonia	Kryptoniales	MSB-3C8	NA	NA	0.441	0.045	0.682	
ASV_0578	Bacteria	Calditrichota	Calditrichia	Calditrichales	Calditrichaceae	NA	NA	0.661	0.001	0.299	yes
ASV_2559	Bacteria	Calditrichota	Calditrichia	Calditrichales	Calditrichaceae	NA	NA	0.463	0.035	0.682	
ASV_3260	Bacteria	Calditrichota	Calditrichia	Calditrichales	Calditrichaceae	NA	NA	0.445	0.043	0.682	
ASV_4804	Bacteria	Calditrichota	Calditrichia	Calditrichales	Calditrichaceae	NA	NA	0.576	0.006	0.528	
ASV_4734	Bacteria	Calditrichota	Calditrichia	Calditrichales	Calditrichaceae	SM23-31	NA	0.463	0.035	0.682	
ASV_0825	Bacteria	Campilobacterota	Campylobacteria	Campylobacterales	Arcobacteraceae	NA	NA	0.461	0.035	0.682	
ASV_0135	Bacteria	Chloroflexi	Anaerolineae	Anaerolineales	Anaerolineaceae	NA	NA	0.487	0.025	0.682	yes
ASV_0462	Bacteria	Chloroflexi	Anaerolineae	Anaerolineales	Anaerolineaceae	NA	NA	0.477	0.029	0.682	
ASV_0515	Bacteria	Chloroflexi	Anaerolineae	Anaerolineales	Anaerolineaceae	NA	NA	0.655	0.001	0.299	
ASV_4441	Bacteria	Chloroflexi	Anaerolineae	Ardenticatenales	NA	NA	NA	0.463	0.035	0.682	
ASV_4440	Bacteria	Chloroflexi	Anaerolineae	NA	NA	NA	NA	0.463	0.035	0.682	
ASV_1737	Bacteria	Chloroflexi	Anaerolineae	SBR1031	NA	NA	NA	0.467	0.033	0.682	
ASV_0119	Bacteria	Chloroflexi	Dehalococcoidia	FS117-23B-02	NA	NA	NA	0.643	0.002	0.299	
ASV_4158	Bacteria	Chloroflexi	Dehalococcoidia	Sh765B-AG-111	NA	NA	NA	0.463	0.035	0.682	
ASV_1442	Bacteria	Cloacimonadota	Cloacimonadia	Cloacimonadales	MSBL8	NA	NA	0.636	0.002	0.322	
ASV_0676	Bacteria	Cyanobacteria	Cyanobacteriia	Synechococcales	Cyanobiaceae	Cyanobium_PCC-6307	NA	0.522	0.015	0.682	
ASV_2746	Bacteria	Cyanobacteria	Cyanobacteriia	Synechococcales	Cyanobiaceae	Cyanobium_PCC-6307	NA	0.543	0.011	0.625	
ASV_0103	Bacteria	Desulfobacterota	Desulfobacteria	Desulfatiglandales	Desulfatiglandaceae	Desulfatiglans	NA	0.544	0.011	0.625	yes
ASV_0453	Bacteria	Desulfobacterota	Desulfobacteria	Desulfatiglandales	Desulfatiglandaceae	Desulfatiglans	NA	0.707	3.43E-04	0.218	yes
ASV_0561	Bacteria	Desulfobacterota	Desulfobacteria	Desulfatiglandales	Desulfatiglandaceae	Desulfatiglans	NA	0.444	0.044	0.682	
ASV_4582	Bacteria	Desulfobacterota	Desulfobacteria	Desulfatiglandales	Desulfatiglandaceae	Desulfatiglans	NA	0.543	0.011	0.625	
ASV_1278	Bacteria	Desulfobacterota	Desulfobacteria	Desulfobacterales	Desulfobacteraceae	Desulfobacter	NA	0.505	0.020	0.682	
ASV_1147	Bacteria	Desulfobacterota	Desulfobacteria	Desulfobacterales	Desulfosarcinaceae	NA	NA	0.505	0.020	0.682	
ASV_1518	Bacteria	Desulfobacterota	Desulfobacteria	Desulfobacterales	Desulfosarcinaceae	NA	NA	0.621	0.003	0.376	
ASV_2508	Bacteria	Desulfobacterota	Desulfobacteria	Desulfobacterales	Desulfosarcinaceae	NA	NA	0.498	0.021	0.682	
ASV_2683	Bacteria	Desulfobacterota	Desulfobacteria	Desulfobacterales	Desulfosarcinaceae	NA	NA	0.599	0.004	0.452	yes
ASV_3642	Bacteria	Desulfobacterota	Desulfobacteria	Desulfobacterales	Desulfosarcinaceae	NA	NA	0.463	0.035	0.682	
ASV_5078	Bacteria	Desulfobacterota	Desulfobacteria	Desulfobacterales	Desulfosarcinaceae	NA	NA	0.463	0.035	0.682	

Positively Correlated ASVs with Cable Bacteria at Depth; p < 0.05 (continued)											
ASV	Kingdom	Phylum	Class	Order	Family	Genus	Species	Spearman's rho	p-value	fdr	follow criteria?
ASV_3457	Bacteria	Desulfobacterota	Desulfobacteria	Desulfobacterales	NA	NA	NA	0.792	1.90E-05	0.042	yes
ASV_0441	Bacteria	Desulfobacterota	Desulfobulbia	Desulfobulbales	Desulfobulbaceae	NA	NA	0.891	6.09E-08	2.71E-04	yes
ASV_1067	Bacteria	Desulfobacterota	Desulfobulbia	Desulfobulbales	Desulfobulbaceae	NA	NA	0.684	0.001	0.276	yes
ASV_1696	Bacteria	Desulfobacterota	Desulfobulbia	Desulfobulbales	Desulfobulbaceae	NA	NA	0.607	0.004	0.448	
ASV_5464	Bacteria	Desulfobacterota	Desulfobulbia	Desulfobulbales	Desulfocapsaceae	NA	NA	0.463	0.035	0.682	
ASV_2625	Bacteria	Desulfobacterota	Desulfuromonadia	Bradymonadales	NA	NA	NA	0.543	0.011	0.625	
ASV_4138	Bacteria	Desulfobacterota	NA	NA	NA	NA	NA	0.668	0.001	0.299	yes
ASV_1336	Bacteria	Desulfobacterota	Syntrophia	Syntrophales	NA	NA	NA	0.712	2.92E-04	0.216	
ASV_2035	Bacteria	Desulfobacterota	Syntrophia	Syntrophales	NA	NA	NA	0.460	0.036	0.682	
ASV_5288	Bacteria	Elusimicrobiota	Lineage_IIb	NA	NA	NA	NA	0.463	0.035	0.682	
ASV_5751	Bacteria	Elusimicrobiota	NA	NA	NA	NA	NA	0.463	0.035	0.682	
ASV_2098	Bacteria	Fermentibacterota	Fermentibacteria	Fermentibacterales	Fermentibacteraceae	NA	NA	0.588	0.005	0.497	
ASV_5618	Bacteria	Firmicutes	Clostridia	Christensenellales	Christensenellaceae	NA	NA	0.463	0.035	0.682	
ASV_5289	Bacteria	Gemmatimonadota	BD2-11_terrestrial_group	NA	NA	NA	NA	0.463	0.035	0.682	
ASV_5465	Bacteria	Gemmatimonadota	BD2-11_terrestrial_group	NA	NA	NA	NA	0.463	0.035	0.682	
ASV_2856	Bacteria	Gemmatimonadota	MD2902-B12	NA	NA	NA	NA	0.511	0.018	0.682	
ASV_4898	Bacteria	Latescibacterota	Latescibacteria	Latescibacterales	Latescibacteraceae	Candidatus_Latesciba cter	NA	0.463	0.035	0.682	
ASV_2418	Bacteria	Latescibacterota	Latescibacteria	Latescibacterales	Latescibacteraceae	NA	NA	0.463	0.035	0.682	
ASV_0447	Bacteria	Latescibacterota	NA	NA	NA	NA	NA	0.458	0.037	0.682	
ASV_0450	Bacteria	Latescibacterota	NA	NA	NA	NA	NA	0.506	0.019	0.682	
ASV_3133	Bacteria	Latescibacterota	NA	NA	NA	NA	NA	0.463	0.035	0.682	
ASV_3466	Bacteria	Latescibacterota	NA	NA	NA	NA	NA	0.463	0.035	0.682	
ASV_4579	Bacteria	Latescibacterota	NA	NA	NA	NA	NA	0.463	0.035	0.682	
ASV_4581	Bacteria	Latescibacterota	NA	NA	NA	NA	NA	0.463	0.035	0.682	
ASV_3555	Bacteria	LCP-89	NA	NA	NA	NA	NA	0.463	0.035	0.682	
ASV_4732	Bacteria	LCP-89	NA	NA	NA	NA	NA	0.463	0.035	0.682	
ASV_1392	Bacteria	Myxococcota	Polyangia	VHS-B3-70	NA	NA	NA	0.755	7.73E-05	0.086	yes
ASV_1852	Bacteria	NB1-j	NA	NA	NA	NA	NA	0.572	0.007	0.528	
ASV_3301	Bacteria	NB1-j	NA	NA	NA	NA	NA	0.463	0.035	0.682	
ASV_1030	Bacteria	Nitrospinota	Nitrospinia	Nitrospinales	Nitrospinaceae	Nitrospina	NA	0.684	0.001	0.276	yes
ASV_1073	Bacteria	Planctomycetota	NA	NA	NA	NA	NA	0.574	0.007	0.528	

Positively Correlated ASVs with Cable Bacteria at Depth; p < 0.05 (continued)											
ASV	Kingdom	Phylum	Class	Order	Family	Genus	Species	Spearman's rho	p-value	fdr	follow criteria?
ASV_3271	Bacteria	Planctomycetota	OM190	NA	NA	NA	NA	0.448	0.042	0.682	
ASV_3736	Bacteria	Planctomycetota	Phycisphaerae	CCM11a	NA	NA	NA	0.463	0.035	0.682	
ASV_4290	Bacteria	Planctomycetota	Phycisphaerae	CCM11a	NA	NA	NA	0.463	0.035	0.682	
ASV_1525	Bacteria	Planctomycetota	Phycisphaerae	DG-20	NA	NA	NA	0.498	0.022	0.682	
ASV_3641	Bacteria	Planctomycetota	Phycisphaerae	mle1-8	NA	NA	NA	0.463	0.035	0.682	
ASV_0156	Bacteria	Planctomycetota	Phycisphaerae	MSBL9	SG8-4	NA	NA	0.451	0.040	0.682	
ASV_0223	Bacteria	Planctomycetota	Phycisphaerae	MSBL9	SG8-4	NA	NA	0.653	0.001	0.299	yes
ASV_0674	Bacteria	Planctomycetota	Phycisphaerae	MSBL9	SG8-4	NA	NA	0.585	0.005	0.497	
ASV_0952	Bacteria	Planctomycetota	Phycisphaerae	MSBL9	SG8-4	NA	NA	0.519	0.016	0.682	
ASV_2355	Bacteria	Planctomycetota	Phycisphaerae	MSBL9	SG8-4	NA	NA	0.463	0.035	0.682	
ASV_2709	Bacteria	Planctomycetota	Phycisphaerae	MSBL9	SG8-4	NA	NA	0.495	0.022	0.682	
ASV_3925	Bacteria	Planctomycetota	Phycisphaerae	MSBL9	SG8-4	NA	NA	0.463	0.035	0.682	
ASV_5752	Bacteria	Planctomycetota	Phycisphaerae	NA	NA	NA	NA	0.463	0.035	0.682	
ASV_4897	Bacteria	Planctomycetota	Phycisphaerae	Phycisphaerales	AKAU3564_sediment_ group	NA	NA	0.463	0.035	0.682	
ASV_5613	Bacteria	Planctomycetota	Phycisphaerae	Phycisphaerales	Phycisphaeraceae	CL500-3	NA	0.463	0.035	0.682	
ASV_1172	Bacteria	Planctomycetota	Pla3_lineage	NA	NA	NA	NA	0.604	0.004	0.452	
ASV_2370	Bacteria	Planctomycetota	Pla3_lineage	NA	NA	NA	NA	0.477	0.029	0.682	
ASV_3303	Bacteria	Planctomycetota	Pla4_lineage	NA	NA	NA	NA	0.463	0.035	0.682	
ASV_2236	Bacteria	Planctomycetota	Planctomycetes	Pirellulales	Pirellulaceae	NA	NA	0.511	0.018	0.682	
ASV_2820	Bacteria	Planctomycetota	Planctomycetes	Pirellulales	Pirellulaceae	Pir4_lineage	NA	0.463	0.035	0.682	
ASV_3135	Bacteria	Planctomycetota	Planctomycetes	Pirellulales	Pirellulaceae	Rhodopirellula	NA	0.463	0.035	0.682	
ASV_4900	Bacteria	Planctomycetota	Planctomycetes	Pirellulales	Pirellulaceae	Rhodopirellula	NA	0.463	0.035	0.682	
ASV_3039	Bacteria	Planctomycetota	Planctomycetes	Planctomycetales	Gimesiaceae	NA	NA	0.463	0.035	0.682	
ASV_2629	Bacteria	Poribacteria	NA	NA	NA	NA	NA	0.463	0.035	0.682	
ASV_1245	Bacteria	Proteobacteria	Alphaproteobacteria	Rhodospirillales	Magnetospiraceae	NA	NA	0.511	0.018	0.682	
ASV_0485	Bacteria	Proteobacteria	Gammaproteobacteria	Burkholderiales	Nitrosomonadaceae	NA	NA	0.470	0.031	0.682	
ASV_0917	Bacteria	Proteobacteria	Gammaproteobacteria	Chromatiales	Chromatiaceae	Candidatus_Thiobios	NA	0.539	0.012	0.651	
ASV_0509	Bacteria	Proteobacteria	Gammaproteobacteria	Chromatiales	Sedimenticolaceae	Sedimenticola	NA	0.585	0.005	0.497	yes
ASV_0080	Bacteria	Proteobacteria	Gammaproteobacteria	Ectothiorhodospirales	Ectothiorhodospiracea e	Thiogranum	NA	0.643	0.002	0.299	yes
ASV_4443	Bacteria	Proteobacteria	Gammaproteobacteria	Ectothiorhodospirales	Ectothiorhodospiracea e	Thiogranum	NA	0.463	0.035	0.682	
ASV_0354	Bacteria	Proteobacteria	Gammaproteobacteria	NA	NA	NA	NA	0.477	0.029	0.682	

Positively Correlated ASVs with Cable Bacteria at Depth; p < 0.05 (continued)											
ASV	Kingdom	Phylum	Class	Order	Family	Genus	Species	Spearman's rho	p-value	fdr	follow criteria?
ASV_0331	Bacteria	Proteobacteria	Gammaproteobacteria	Oceanospirillales	Pseudohongiellaceae	Pseudohongiella	NA	0.481	0.027	0.682	
ASV_1971	Bacteria	Proteobacteria	Gammaproteobacteria	Steroidobacterales	Woeseiaceae	Woeseia	NA	0.463	0.035	0.682	
ASV_0018	Bacteria	Proteobacteria	Gammaproteobacteria	Thiotrichales	Thiotrichaceae	NA	NA	0.560	0.008	0.575	yes
ASV_0319	Bacteria	Proteobacteria	Gammaproteobacteria	Thiotrichales	Thiotrichaceae	NA	NA	0.485	0.026	0.682	
ASV_0751	Bacteria	Spirochaetota	Leptospirae	Leptospirales	Leptospiraceae	RBG-16-49-21	NA	0.497	0.022	0.682	yes
ASV_0439	Bacteria	Spirochaetota	Spirochaetia	Spirochaetales	Spirochaetaceae	NA	NA	0.506	0.019	0.682	
ASV_0534	Bacteria	Spirochaetota	Spirochaetia	Spirochaetales	Spirochaetaceae	NA	NA	0.567	0.007	0.568	
ASV_5750	Bacteria	Spirochaetota	Spirochaetia	Spirochaetales	Spirochaetaceae	NA	NA	0.463	0.035	0.682	
ASV_0072	Bacteria	Spirochaetota	Spirochaetia	Spirochaetales	Spirochaetaceae	Sediminispirochaeta	NA	0.527	0.014	0.682	
ASV_1725	Bacteria	Spirochaetota	Spirochaetia	Spirochaetales	Spirochaetaceae	Sediminispirochaeta	NA	0.607	0.004	0.448	
ASV_0821	Bacteria	Spirochaetota	Spirochaetia	Spirochaetales	Spirochaetaceae	Spirochaeta	NA	0.641	0.002	0.299	
ASV_0991	Bacteria	Spirochaetota	Spirochaetia	Spirochaetales	Spirochaetaceae	Spirochaeta	NA	0.459	0.036	0.682	
ASV_3733	Bacteria	Spirochaetota	Spirochaetia	Spirochaetales	Spirochaetaceae	Spirochaeta	NA	0.466	0.033	0.682	
ASV_4040	Bacteria	Sumerlaeota	Sumerlaeia	Sumerlaeales	Sumerlaeaceae	Sumerlaea	NA	0.463	0.035	0.682	
ASV_0643	Bacteria	Sva0485	NA	NA	NA	NA	NA	0.548	0.010	0.611	yes
ASV_3465	Bacteria	Sva0485	NA	NA	NA	NA	NA	0.463	0.035	0.682	
ASV_0229	Bacteria	Verrucomicrobiota	Kiritimatiellae	Kiritimatiellales	Kiritimatiellaceae	R76-B128	NA	0.435	0.049	0.682	
ASV_4160	Bacteria	Verrucomicrobiota	Kiritimatiellae	WCHB1-41	NA	NA	NA	0.463	0.035	0.682	
ASV_5617	Bacteria	Verrucomicrobiota	Kiritimatiellae	WCHB1-41	NA	NA	NA	0.463	0.035	0.682	
ASV_5290	Bacteria	Verrucomicrobiota	Lentisphaeria	Oligosphaerales	Lenti-02	NA	NA	0.463	0.035	0.682	
ASV_2167	Bacteria	Verrucomicrobiota	Omnitrophia	Omnitrophales	Omnitrophaceae	Candidatus_Omnitrophus	NA	0.572	0.007	0.528	
ASV_0728	Bacteria	Verrucomicrobiota	Verrucomicrobiae	Opitutales	Opitutaceae	NA	NA	0.624	0.003	0.374	
ASV_4733	Bacteria	Verrucomicrobiota	Verrucomicrobiae	Opitutales	Puniceicoccaceae	Lentimonas	NA	0.463	0.035	0.682	
ASV_5614	Bacteria	Verrucomicrobiota	Verrucomicrobiae	Pedosphaerales	Pedosphaeraceae	NA	NA	0.463	0.035	0.682	

Negatively Correlated ASVs with Cable Bacteria at Depth; p < 0.05											
ASV	Kingdom	Phylum	Class	Order	Family	Genus	Species	Spearman's rho	p-value	fdr	follow criteria?
ASV_0672	Archaea	Asgardarchaeota	Heimdallarchaeia	NA	NA	NA	NA	-0.528	0.014	0.682	
ASV_0837	Archaea	Halobacterota	Methanosarcinia	Methanosarciniales	Methanosarcinaceae	NA	NA	-0.458	0.037	0.682	
ASV_0398	Archaea	Thermoplasmatota	Thermoplasmata	Marine_Benthic_Group_D_and_DHVEG-1	NA	NA	NA	-0.558	0.009	0.575	
ASV_0549	Bacteria	Acidobacteriota	Subgroup_21	NA	NA	NA	NA	-0.507	0.019	0.682	yes
ASV_1951	Bacteria	Acidobacteriota	Subgroup_22	NA	NA	NA	NA	-0.469	0.032	0.682	
ASV_0469	Bacteria	Acidobacteriota	Vicinamibacteria	Subgroup_9	NA	NA	NA	-0.521	0.015	0.682	
ASV_1091	Bacteria	Acidobacteriota	Vicinamibacteria	Subgroup_9	NA	NA	NA	-0.554	0.009	0.575	
ASV_0512	Bacteria	Bacteroidota	Bacteroidia	Bacteroidales	Bacteroidetes_BD2-2	NA	NA	-0.469	0.032	0.682	
ASV_0538	Bacteria	Bacteroidota	Bacteroidia	Bacteroidales	Bacteroidetes_BD2-2	NA	NA	-0.469	0.032	0.682	yes
ASV_1133	Bacteria	Bacteroidota	Bacteroidia	Bacteroidales	Bacteroidetes_BD2-2	NA	NA	-0.470	0.032	0.682	
ASV_2408	Bacteria	Bacteroidota	Bacteroidia	Bacteroidales	Bacteroidetes_vadinHA17	NA	NA	-0.469	0.032	0.682	
ASV_1455	Bacteria	Bacteroidota	Bacteroidia	Bacteroidales	Marinifilaceae	Marinifilum	NA	-0.554	0.009	0.575	
ASV_0754	Bacteria	Bacteroidota	Bacteroidia	Bacteroidales	Marinilabiliaceae	NA	NA	-0.625	0.002	0.374	yes
ASV_1698	Bacteria	Bacteroidota	Bacteroidia	Flavobacteriales	Flavobacteriaceae	NA	NA	-0.469	0.032	0.682	
ASV_0697	Bacteria	Bacteroidota	Bacteroidia	NA	NA	NA	NA	-0.467	0.033	0.682	
ASV_0953	Bacteria	Bacteroidota	Bacteroidia	Sphingobacteriales	Lentimicrobiaceae	NA	NA	-0.641	0.002	0.299	
ASV_1431	Bacteria	Bacteroidota	Ignavibacteria	Ignavibacteriales	Ignavibacteriaceae	Ignavibacterium	NA	-0.455	0.038	0.682	
ASV_3195	Bacteria	Bacteroidota	Ignavibacteria	Ignavibacteriales	Ignavibacteriaceae	Ignavibacterium	NA	-0.469	0.032	0.682	
ASV_1181	Bacteria	Bacteroidota	Ignavibacteria	Ignavibacteriales	Melioribacteraceae	IheB3-7	NA	-0.511	0.018	0.682	
ASV_0838	Bacteria	Bdellovibrionota	Bdellovibrionia	Bdellovibrionales	Bdellovibrionaceae	OM27_clade	NA	-0.554	0.009	0.575	
ASV_0452	Bacteria	Calditrichota	Calditrichia	Calditrichales	Calditrichaceae	Calorithrix	NA	-0.458	0.037	0.682	
ASV_0390	Bacteria	Calditrichota	Calditrichia	Calditrichales	Calditrichaceae	NA	NA	-0.641	0.002	0.299	
ASV_0481	Bacteria	Calditrichota	Calditrichia	Calditrichales	Calditrichaceae	NA	NA	-0.516	0.017	0.682	
ASV_0614	Bacteria	Calditrichota	Calditrichia	Calditrichales	Calditrichaceae	NA	NA	-0.479	0.028	0.682	
ASV_0640	Bacteria	Calditrichota	Calditrichia	Calditrichales	Calditrichaceae	NA	NA	-0.503	0.020	0.682	
ASV_0759	Bacteria	Calditrichota	Calditrichia	Calditrichales	Calditrichaceae	NA	NA	-0.466	0.033	0.682	
ASV_0942	Bacteria	Calditrichota	Calditrichia	Calditrichales	Calditrichaceae	NA	NA	-0.597	0.004	0.452	
ASV_0962	Bacteria	Calditrichota	Calditrichia	Calditrichales	Calditrichaceae	NA	NA	-0.554	0.009	0.575	
ASV_1018	Bacteria	Calditrichota	Calditrichia	Calditrichales	Calditrichaceae	NA	NA	-0.441	0.045	0.682	
ASV_1140	Bacteria	Calditrichota	Calditrichia	Calditrichales	Calditrichaceae	NA	NA	-0.597	0.004	0.452	
ASV_1371	Bacteria	Calditrichota	Calditrichia	Calditrichales	Calditrichaceae	NA	NA	-0.554	0.009	0.575	
ASV_0174	Bacteria	Campilobacterota	Campylobacteria	Campylobacterales	Sulfurimonadaceae	Sulfurimonas	NA	-0.480	0.028	0.682	

Negatively Correlated ASVs with Cable Bacteria at Depth; p < 0.05 (continued)											
ASV	Kingdom	Phylum	Class	Order	Family	Genus	Species	Spearman's rho	p-value	fdr	follow criteria?
ASV_0721	Bacteria	Chloroflexi	Anaerolineae	Anaerolineales	Anaerolineaceae	NA	NA	-0.454	0.039	0.682	
ASV_0936	Bacteria	Chloroflexi	Anaerolineae	Anaerolineales	Anaerolineaceae	NA	NA	-0.527	0.014	0.682	
ASV_0294	Bacteria	Chloroflexi	Anaerolineae	Ardenticatenales	NA	NA	NA	-0.699	4.22E-04	0.234	yes
ASV_0424	Bacteria	Chloroflexi	Anaerolineae	SBR1031	NA	NA	NA	-0.602	0.004	0.452	yes
ASV_0165	Bacteria	Cyanobacteria	Cyanobacteriia	Synechococcales	Cyanobiaceae	Cyanobium_PCC-6307	NA	-0.433	0.050	0.682	
ASV_0155	Bacteria	Desulfobacterota	Desulfobacteria	Desulfatiglandales	Desulfatiglandaceae	Desulfatiglans	NA	-0.583	0.006	0.504	
ASV_0303	Bacteria	Desulfobacterota	Desulfobacteria	Desulfatiglandales	Desulfatiglandaceae	Desulfatiglans	NA	-0.524	0.015	0.682	
ASV_0309	Bacteria	Desulfobacterota	Desulfobacteria	Desulfatiglandales	Desulfatiglandaceae	Desulfatiglans	NA	-0.436	0.048	0.682	yes
ASV_0635	Bacteria	Desulfobacterota	Desulfobacteria	Desulfatiglandales	Desulfatiglandaceae	Desulfatiglans	NA	-0.461	0.035	0.682	
ASV_0648	Bacteria	Desulfobacterota	Desulfobacteria	Desulfatiglandales	Desulfatiglandaceae	Desulfatiglans	NA	-0.641	0.002	0.299	
ASV_0658	Bacteria	Desulfobacterota	Desulfobacteria	Desulfatiglandales	Desulfatiglandaceae	Desulfatiglans	NA	-0.435	0.049	0.682	
ASV_0841	Bacteria	Desulfobacterota	Desulfobacteria	Desulfatiglandales	Desulfatiglandaceae	Desulfatiglans	NA	-0.537	0.012	0.658	
ASV_0986	Bacteria	Desulfobacterota	Desulfobacteria	Desulfatiglandales	Desulfatiglandaceae	Desulfatiglans	NA	-0.641	0.002	0.299	
ASV_1482	Bacteria	Desulfobacterota	Desulfobacteria	Desulfatiglandales	Desulfatiglandaceae	Desulfatiglans	NA	-0.524	0.015	0.682	
ASV_0664	Bacteria	Desulfobacterota	Desulfobacteria	Desulfobacterales	Desulfosarcinaceae	Incertae_Sedis	NA	-0.447	0.042	0.682	
ASV_0774	Bacteria	Desulfobacterota	Desulfobacteria	Desulfobacterales	Desulfosarcinaceae	LCP-80	NA	-0.469	0.032	0.682	
ASV_1134	Bacteria	Desulfobacterota	Desulfobacteria	Desulfobacterales	Desulfosarcinaceae	NA	NA	-0.486	0.026	0.682	
ASV_0706	Bacteria	Desulfobacterota	Desulfobacteria	Desulfobacterales	Desulfosarcinaceae	SEEP-SRB1	NA	-0.469	0.032	0.682	
ASV_1381	Bacteria	Desulfobacterota	Desulfobacteria	Desulfobacterales	Desulfosarcinaceae	Sva0081_sediment_group	NA	-0.469	0.032	0.682	
ASV_1707	Bacteria	Desulfobacterota	Desulfobacteria	Desulfobacterales	Desulfosarcinaceae	Sva0081_sediment_group	NA	-0.437	0.047	0.682	
ASV_3413	Bacteria	Desulfobacterota	Desulfobacteria	Desulfobacterales	Desulfosarcinaceae	Sva0081_sediment_group	NA	-0.554	0.009	0.575	
ASV_0066	Bacteria	Desulfobacterota	Desulfobulbia	Desulfobulbales	Desulfocapsaceae	Desulfocapsa	NA	-0.779	3.146E-05	0.047	yes
ASV_0585	Bacteria	Desulfobacterota	Desulfobulbia	Desulfobulbales	Desulfocapsaceae	NA	NA	-0.641	0.002	0.299	
ASV_1007	Bacteria	Desulfobacterota	Desulfobulbia	Desulfobulbales	Desulfocapsaceae	NA	NA	-0.511	0.018	0.682	
ASV_1610	Bacteria	Desulfobacterota	Desulfobulbia	Desulfobulbales	NA	NA	NA	-0.469	0.032	0.682	
ASV_0699	Bacteria	Desulfobacterota	Syntrophia	Syntrophales	NA	NA	NA	-0.573	0.007	0.528	
ASV_0767	Bacteria	Desulfobacterota	Syntrophia	Syntrophales	NA	NA	NA	-0.441	0.045	0.682	
ASV_0260	Bacteria	Desulfobacterota	Syntrophobacteria	Syntrophobacterales	NA	NA	NA	-0.595	0.004	0.459	
ASV_1532	Bacteria	Fermentibacterota	Fermentibacteria	Fermentibacterales	Fermentibacteraceae	NA	NA	-0.554	0.009	0.575	
ASV_1844	Bacteria	Firmicutes	Clostridia	Lachnospirales	Lachnospiraceae	NA	NA	-0.511	0.018	0.682	

Negatively Correlated ASVs with Cable Bacteria at Depth; p < 0.05 (continued)											
ASV	Kingdom	Phylum	Class	Order	Family	Genus	Species	Spearman's rho	p-value	fdr	follow criteria?
ASV_0739	Bacteria	Gemmatimonadota	BD2-11_terrestrial_group	NA	NA	NA	NA	-0.470	0.032	0.682	
ASV_1025	Bacteria	Gemmatimonadota	BD2-11_terrestrial_group	NA	NA	NA	NA	-0.532	0.013	0.682	
ASV_1329	Bacteria	Gemmatimonadota	BD2-11_terrestrial_group	NA	NA	NA	NA	-0.511	0.018	0.682	
ASV_1382	Bacteria	Gemmatimonadota	Gemmatimonadetes	Gemmatimonadales	Gemmatimonadaceae	NA	NA	-0.554	0.009	0.575	
ASV_0624	Bacteria	Hydrogenedentes	Hydrogenedentia	Hydrogenedentiales	Hydrogenedensaceae	NA	NA	-0.467	0.033	0.682	
ASV_0380	Bacteria	Latescibacterota	Latescibacteria	Latescibacterales	Latescibacteraceae	Candidatus_Latescibacter	NA	-0.474	0.030	0.682	
ASV_0980	Bacteria	Latescibacterota	Latescibacteria	Latescibacterales	Latescibacteraceae	Candidatus_Latescibacter	NA	-0.529	0.014	0.682	
ASV_0877	Bacteria	Latescibacterota	NA	NA	NA	NA	NA	-0.490	0.024	0.682	
ASV_0806	Bacteria	Modulibacteria	Moduliflexia	Moduliflexales	Moduliflexaceae	NA	NA	-0.436	0.048	0.682	
ASV_0871	Bacteria	Myxococcota	Polyangia	NA	NA	NA	NA	-0.438	0.047	0.682	
ASV_1201	Bacteria	Myxococcota	Polyangia	Nannocystales	Nannocystaceae	NA	NA	-0.529	0.014	0.682	
ASV_0075	Bacteria	Myxococcota	Polyangia	Polyangiales	Sandaracinaceae	NA	NA	-0.480	0.028	0.682	
ASV_1457	Bacteria	Myxococcota	Polyangia	Polyangiales	Sandaracinaceae	Sandaracinus	NA	-0.585	0.005	0.497	
ASV_0902	Bacteria	Myxococcota	Polyangia	VHS-B3-70	NA	NA	NA	-0.641	0.002	0.299	
ASV_1106	Bacteria	Myxococcota	Polyangia	VHS-B3-70	NA	NA	NA	-0.455	0.038	0.682	yes
ASV_0407	Bacteria	Nitrospinota	Nitrospinia	Nitrospinales	Nitrospinaceae	Nitrospina	NA	-0.579	0.006	0.519	
ASV_1100	Bacteria	Planctomycetota	NA	NA	NA	NA	NA	-0.469	0.032	0.682	yes
ASV_1256	Bacteria	Planctomycetota	NA	NA	NA	NA	NA	-0.511	0.018	0.682	
ASV_1002	Bacteria	Planctomycetota	Phycisphaerae	MSBL9	SG8-4	NA	NA	-0.481	0.027	0.682	
ASV_1068	Bacteria	Planctomycetota	Planctomycetes	Pirellulales	Pirellulaceae	Rhodopirellula	NA	-0.624	0.002	0.374	
ASV_0905	Bacteria	Planctomycetota	Planctomycetes	Pirellulales	Pirellulaceae	Rubripirellula	NA	-0.469	0.032	0.682	
ASV_1727	Bacteria	Planctomycetota	Planctomycetes	Pirellulales	Pirellulaceae	Rubripirellula	NA	-0.469	0.032	0.682	
ASV_0265	Bacteria	Proteobacteria	Alphaproteobacteria	Rhizobiales	Hyphomicrobiaceae	Filomicrobium	NA	-0.450	0.041	0.682	
ASV_1830	Bacteria	Proteobacteria	Alphaproteobacteria	Rhodobacterales	Rhodobacteraceae	Tateyamaria	NA	-0.469	0.032	0.682	
ASV_0226	Bacteria	Proteobacteria	Gammaproteobacteria	B2M28	NA	NA	NA	-0.456	0.038	0.682	
ASV_0475	Bacteria	Proteobacteria	Gammaproteobacteria	Ectothiorhodospirales	Ectothiorhodospiraceae	Thiogranum	NA	-0.579	0.006	0.519	yes

Negatively Correlated ASVs with Cable Bacteria at Depth; p < 0.05 (continued)											
ASV	**Kingdom**	**Phylum**	**Class**	**Order**	**Family**	**Genus**	**Species**	**Spearman's rho**	**p-value**	**fdr**	**follow criteria?**
ASV_0275	Bacteria	Proteobacteria	Gammaproteobacteria	Gammaproteobacteria _Incertae_Sedis	Unknown_Family	NA	NA	-0.726	1.94E-04	0.173	yes
ASV_0219	Bacteria	Proteobacteria	Gammaproteobacteria	NA	NA	NA	NA	-0.457	0.037	0.682	
ASV_0983	Bacteria	Proteobacteria	Gammaproteobacteria	NA	NA	NA	NA	-0.474	0.030	0.682	
ASV_3102	Bacteria	Proteobacteria	Gammaproteobacteria	Steroidobacterales	Woeseiaceae	Woeseia	NA	-0.554	0.009	0.575	
ASV_0518	Bacteria	Proteobacteria	Gammaproteobacteria	Thiotrichales	Thiotrichaceae	NA	NA	-0.592	0.005	0.474	
ASV_1173	Bacteria	SAR324_clade(Marine_group_B)	NA	NA	NA	NA	NA	-0.469	0.032	0.682	
ASV_1491	Bacteria	Spirochaetota	Leptospirae	Leptospirales	Leptospiraceae	RBG-16-49-21	NA	-0.554	0.009	0.575	
ASV_1094	Bacteria	Spirochaetota	Spirochaetia	Spirochaetales	Spirochaetaceae	Sediminispirochaeta	NA	-0.455	0.038	0.682	
ASV_1076	Bacteria	Spirochaetota	Spirochaetia	Spirochaetales	Spirochaetaceae	Spirochaeta	NA	-0.648	0.002	0.299	
ASV_0308	Bacteria	Sva0485	NA	NA	NA	NA	NA	-0.462	0.035	0.682	
ASV_0461	Bacteria	Sva0485	NA	NA	NA	NA	NA	-0.548	0.010	0.611	
ASV_0769	Bacteria	Sva0485	NA	NA	NA	NA	NA	-0.483	0.027	0.682	
ASV_0998	Bacteria	Sva0485	NA	NA	NA	NA	NA	-0.597	0.004	0.452	
ASV_0663	Bacteria	Synergistota	Synergistia	Synergistales	Synergistaceae	NA	NA	-0.558	0.009	0.575	

Table A2. Positively and negatively correlated genera (*p*-value < 0.05) at the surface (0 - 0.5 cm) and at depth (0.5 - 2.0 cm) with cable bacteria.

Positively Correlated Genera with Cable Bacteria at the Surface; p < 0.05									
Kingdom	**Phylum**	**Class**	**Order**	**Family**	**Genus**	**Spearman's rho**	**p-value**	**fdr**	**follow criteria?**
Bacteria	Bacteroidota	Bacteroidia	Chitinophagales	Saprospiraceae	Aureispira	0.899	0.015	0.459	yes
Bacteria	Bacteroidota	Bacteroidia	Chitinophagales	Saprospiraceae	Portibacter	0.886	0.019	0.459	yes
Bacteria	Bacteroidota	Bacteroidia	Flavobacteriales	Crocinitomicaceae	Crocinitomix	0.829	0.042	0.502	yes
Bacteria	Bdellovibrionota	Bdellovibrionia	Bdellovibrionales	Bdellovibrionaceae	OM27_clade	0.829	0.042	0.502	yes
Bacteria	Deinococcota	Deinococci	Deinococcales	Trueperaceae	Truepera	0.899	0.015	0.459	yes
Bacteria	Myxococcota	Polyangia	Haliangiales	Haliangiaceae	Haliangium	0.943	0.005	0.223	yes
Bacteria	Proteobacteria	Alphaproteobacteria	Rhodospirillales	Magnetospiraceae	Magnetovibrio	0.943	0.005	0.223	yes
Bacteria	Verrucomicrobiota	Verrucomicrobiae	Opitutales	Opitutaceae	Diplosphaera	0.820	0.046	0.502	yes

Negatively Correlated Genera with Cable Bacteria at the Surface; p < 0.05									
Kingdom	**Phylum**	**Class**	**Order**	**Family**	**Genus**	**Spearman's rho**	**p-value**	**fdr**	**follow criteria?**
Bacteria	Bacteroidota	Bacteroidia	Flavobacteriales	Flavobacteriaceae	Maribacter	-0.941	0.005	0.223	yes
Bacteria	Calditrichota	Calditrichia	Calditrichales	Calditrichaceae	JdFR-76	-0.829	0.042	0.502	yes
Bacteria	Desulfobacterota	Desulfobacteria	Desulfatiglandales	Desulfatiglandaceae	Desulfatiglans	-0.829	0.042	0.502	yes
Bacteria	Desulfobacterota	Desulfobacteria	Desulfobacterales	Desulfosarcinaceae	SEEP-SRB1	-0.886	0.019	0.459	yes
Bacteria	Desulfobacterota	Desulfobacteria	Desulfobacterales	Desulfosarcinaceae	Sva0081_sediment_group	-0.943	0.005	0.223	yes
Bacteria	Desulfobacterota	Desulfovibrionia	Desulfovibrionales	Desulfovibrionaceae	Desulfovibrio	-0.845	0.034	0.502	
Bacteria	Desulfobacterota	Desulfuromonadia	Desulfuromonadia_or	Geopsychrobacteraceae	Desulfuromusa	-0.812	0.050	0.520	yes
Bacteria	Proteobacteria	Gammaproteobacteria	Cellvibrionales	Halieaceae	Halioglobus	-0.829	0.042	0.502	yes
Bacteria	Proteobacteria	Gammaproteobacteria	Chromatiales	Sedimenticolaceae	Sedimenticola	-0.943	0.005	0.223	yes
Bacteria	Proteobacteria	Gammaproteobacteria	Ectothiorhodospirales	Ectothiorhodospiraceae	Thiogranum	-0.829	0.042	0.502	yes
Bacteria	Proteobacteria	Gammaproteobacteria	Oceanospirillales	Nitrincolaceae	Neptunomonas	-0.820	0.046	0.502	
Bacteria	Spirochaetota	Spirochaetia	Spirochaetales	Spirochaetaceae	GWE2-31-10	-0.845	0.034	0.502	
Bacteria	Synergistota	Synergistia	Synergistales	Synergistaceae	Thermovirga	-0.841	0.036	0.502	

Positively Correlated Genera with Cable Bacteria at Depth; p < 0.05									
Kingdom	**Phylum**	**Class**	**Order**	**Family**	**Genus**	**Spearman's rho**	**p-value**	**fdr**	**follow criteria?**
Archaea	Crenarchaeota	Nitrososphaeria	Nitrosopumilales	Nitrosopumilaceae	Candidatus_Nitrosopumilus	0.463	0.035	0.557	
Bacteria	Bacteroidota	Bacteroidia	Bacteroidales	Prolixibacteraceae	WCHB1-32	0.575	0.006	0.275	
Bacteria	Desulfobacterota	Desulfobacteria	Desulfobacterales	Desulfobacteraceae	Desulfobacter	0.477	0.029	0.557	
Bacteria	Proteobacteria	Gammaproteobacteria	Ectothiorhodospirales	Ectothiorhodospiraceae	Thiogranum	0.477	0.029	0.557	yes
Bacteria	Proteobacteria	Gammaproteobacteria	Oceanospirillales	Pseudohongiellaceae	Pseudohongiella	0.481	0.027	0.557	

Negatively Correlated Genera with Cable Bacteria at Depth; p < 0.05									
Kingdom	**Phylum**	**Class**	**Order**	**Family**	**Genus**	**Spearman's rho**	**p-value**	**fdr**	**follow criteria?**
Archaea	Nanoarchaeota	Nanoarchaeia	Woesearchaeales	GW2011	AR15	-0.437	0.047	0.562	
Bacteria	Acidobacteriota	Thermoanaerobaculia	Thermoanaerobaculales	Thermoanaerobaculaceae	Subgroup_10	-0.459	0.036	0.557	
Bacteria	Calditrichota	Calditrichia	Calditrichales	Calditrichaceae	Calorithrix	-0.547	0.010	0.368	
Bacteria	Desulfobacterota	Desulfobacteria	Desulfobacterales	Desulfobacteraceae	Desulfoconvexum	-0.469	0.032	0.557	
Bacteria	Desulfobacterota	Desulfobacteria	Desulfobacterales	Desulfosarcinaceae	Incertae_Sedis	-0.508	0.019	0.503	yes
Bacteria	Desulfobacterota	Desulfobulbia	Desulfobulbales	Desulfocapsaceae	Desulfocapsa	-0.779	3.15E-05	0.007	yes
Bacteria	Myxococcota	Polyangia	Polyangiales	Sandaracinaceae	Sandaracinus	-0.585	0.005	0.275	
Bacteria	Proteobacteria	Alphaproteobacteria	Caulobacterales	Hyphomonadaceae	Hyphomonas	-0.689	0.001	0.060	yes
Bacteria	Proteobacteria	Alphaproteobacteria	Rhodobacterales	Rhodobacteraceae	Tateyamaria	-0.511	0.018	0.503	
Bacteria	Proteobacteria	Gammaproteobacteria	Thiomicrospirales	Thiomicrospiraceae	endosymbionts	-0.597	0.004	0.275	

References

Achtnich, C., Bak, F. and Conrad, R., 1995. Competition for electron donors among nitrate reducers, ferric iron reducers, sulfate reducers, and methanogens in anoxic paddy soil. *Biology and fertility of soils*, 19(1), pp.65-72.

Aller, R.C., Aller, J.Y., Zhu, Q., Heilbrun, C., Klingensmith, I. and Kaushik, A., 2019. Worm tubes as conduits for the electrogenic microbial grid in marine sediments. *Science advances*, 5(7), p.eaaw3651.

Arndt, S., Jørgensen, B.B., LaRowe, D.E., Middelburg, J.J., Pancost, R.D. and Regnier, P., 2013. Quantifying the degradation of organic matter in marine sediments: a review and synthesis. *Earth-science reviews*, 123, pp.53-86.

Banerjee, S., Schlaeppi, K. and van der Heijden, M.G., 2018. Keystone taxa as drivers of microbiome structure and functioning. *Nature Reviews Microbiology*, 16(9), pp.567-576.

Barlow, J.T., Bogatyrev, S.R. and Ismagilov, R.F., 2020. A quantitative sequencing framework for absolute abundance measurements of mucosal and lumenal microbial communities. *Nature communications*, *11*(1), pp.1-13.

Bazylinski, D.A. and Frankel, R.B., 2004. Magnetosome formation in prokaryotes. *Nature Reviews Microbiology*, 2(3), pp.217-230.

Bazylinski, D.A., Williams, T.J., Lefèvre, C.T., Trubitsyn, D., Fang, J., Beveridge, T.J., Moskowitz, B.M., Ward, B., Schübbe, S., Dubbels, B.L. and Simpson, B., 2013. *Magnetovibrio blakemorei* gen. nov., sp. nov., a magnetotactic bacterium (Alphaproteobacteria: Rhodospirillaceae) isolated from a salt marsh. *International journal of systematic and evolutionary microbiology*, 63(5), pp.1824-1833.

Berryman, A.A., 1992. The orgins and evolution of predator-prey theory. *Ecology*, 73(5), pp.1530-1535.

Bjerg, J.T., Boschker, H.T., Larsen, S., Berry, D., Schmid, M., Millo, D., Tataru, P., Meysman, F.J., Wagner, M., Nielsen, L.P. and Schramm, A., 2018. Long-distance electron transport in individual, living cable bacteria. *Proceedings of the National Academy of Sciences*, 115(22), pp.5786-5791.

Bodelier, P.L., Meima-Franke, M., Hordijk, C.A., Steenbergh, A.K., Hefting, M.M., Bodrossy, L., Von Bergen, M. and Seifert, J., 2013. Microbial minorities modulate methane consumption through niche partitioning. *The ISME journal*, 7(11), pp.2214-2228.

Boetius, A., Ravenschlag, K., Schubert, C.J., Rickert, D., Widdel, F., Gieseke, A., Amann, R., Jørgensen, B.B., Witte, U. and Pfannkuche, O., 2000. A marine microbial

consortium apparently mediating anaerobic oxidation of methane. *Nature*, 407(6804), pp.623-626.

Bond, D.R., Holmes, D.E., Tender, L.M. and Lovley, D.R., 2002. Electrode-reducing microorganisms that harvest energy from marine sediments. *Science*, 295(5554), pp.483-485.

Bryant, M.P., Wolin, E.A., Wolin, M.J. and Wolfe, R.S., 1967. *Methanobacillus omelianskii*, a symbiotic association of two species of bacteria. *Archiv für Mikrobiologie*, 59(1-3), pp.20-31.

Burdige, D.J., 2006. Geochemistry of marine sediments. Princeton University Press.

Burdorf, L.D., Hidalgo-Martinez, S., Cook, P.L. and Meysman, F.J., 2016. Long-distance electron transport by cable bacteria in mangrove sediments. *Marine Ecology Progress Series*, 545, pp.1-8.

Burdorf, L.D., Tramper, A., Seitaj, D., Meire, L., Hidalgo-Martinez, S., Zetsche, E.M., Boschker, H.T. and Meysman, F.J., 2017. Long-distance electron transport occurs globally in marine sediments. *Biogeosciences*, 14(3), p.683.

Canfield, D.E., 1993. Organic matter oxidation in marine sediments. *In Interactions of C, N, P and S biogeochemical Cycles and Global Change* (pp. 333-363). Springer, Berlin, Heidelberg.

Canfield, D., Kristensen, E. and Thamdrup, B., 2005. Aquatic geomicrobiology. Elsevier.

Chauhan, A., Cherrier, J. and Williams, H.N., 2009. Impact of sideways and bottom-up control factors on bacterial community succession over a tidal cycle. *Proceedings of the National Academy of Sciences*, 106(11), pp.4301-4306.

Chen, H., Athar, R., Zheng, G. and Williams, H.N., 2011. Prey bacteria shape the community structure of their predators. *The ISME journal*, 5(8), pp.1314-1322.

Cornelissen, R., Bøggild, A., Thiruvallur Eachambadi, R., Koning, R.I., Kremer, A., Hidalgo-Martinez, S., Zetsche, E.M., Damgaard, L.R., Bonné, R., Drijkoningen, J. and Geelhoed, J.S., 2018. The cell envelope structure of cable bacteria. *Frontiers in microbiology*, 9, p.3044.

Cottee-Jones, H.E.W. and Whittaker, R.J., 2012. Perspective: the keystone species concept: a critical appraisal. *Frontiers of Biogeography*, 4(3).

Dyksma, S., Bischof, K., Fuchs, B.M., Hoffmann, K., Meier, D., Meyerdierks, A., Pjevac, P., Probandt, D., Richter, M., Stepanauskas, R. and Mußmann, M., 2016. Ubiquitous Gammaproteobacteria dominate dark carbon fixation in coastal sediments. *The ISME journal*, 10(8), pp.1939-1953.

Einsiedl, F., Pilloni, G., Ruth-Anneser, B., Lueders, T. and Griebler, C., 2015. Spatial distributions of sulphur species and sulphate-reducing bacteria provide insights into sulphur redox cycling and biodegradation hot-spots in a hydrocarbon-contaminated aquifer. *Geochimica et Cosmochimica Acta*, 156, pp.207-221.

Finster, K.W., Kjeldsen, K.U., Kube, M., Reinhardt, R., Mussmann, M., Amann, R. and Schreiber, L., 2013. Complete genome sequence of *Desulfocapsa sulfexigens*, a marine deltaproteobacterium specialized in disproportionating inorganic sulfur compounds. *Standards in genomic sciences*, 8(1), pp.58-68.

Flood, B.E., Jones, D.S. and Bailey, J.V., 2015a. Complete genome sequence of Sedimenticola thiotaurini strain SIP-G1, a polyphosphate-and polyhydroxyalkanoate-accumulating sulfur-oxidizing gammaproteobacterium isolated from salt marsh sediments. *Genome announcements*, 3(3).

Flood, B.E., Jones, D.S. and Bailey, J.V., 2015b. *Sedimenticola thiotaurini* sp. nov., a sulfur-oxidizing bacterium isolated from salt marsh sediments, and emended descriptions of the genus *Sedimenticola* and *Sedimenticola selenatireducens*. *International journal of systematic and evolutionary microbiology*, 65(8), pp.2522-2530.

Fudou, R., Jojima, Y., Iizuka, T. and Yamanaka, S., 2002. *Haliangium ochraceum* gen. nov., sp. nov. and *Haliangium tepidum* sp. nov.: novel moderately halophilic myxobacteria isolated from coastal saline environments. *The Journal of general and applied microbiology*, *48*(2), pp.109-115.

Geerlings, N.M., Karman, C., Trashin, S., As, K.S., Kienhuis, M.V., Hidalgo-Martinez, S., Vasquez-Cardenas, D., Boschker, H.T., De Wael, K., Middelburg, J.J. and Polerecky, L., 2020. Division of labor and growth during electrical cooperation in multicellular cable bacteria. *Proceedings of the National Academy of Sciences*, 117(10), pp.5478-5485.

Gerbersdorf, S.U., Bittner, R., Lubarsky, H., Manz, W. and Paterson, D.M., 2009. Microbial assemblages as ecosystem engineers of sediment stability. *Journal of Soils and Sediments*, 9(6), pp.640-652.

Gokul, J.K., Hodson, A.J., Saetnan, E.R., Irvine-Fynn, T.D., Westall, P.J., Detheridge, A.P., Takeuchi, N., Bussell, J., Mur, L.A. and Edwards, A., 2016. Taxon interactions control the distributions of cryoconite bacteria colonizing a High Arctic ice cap. Molecular ecology, 25(15), pp.3752-3767.

Gorby, Y.A., Yanina, S., McLean, J.S., Rosso, K.M., Moyles, D., Dohnalkova, A., Beveridge, T.J., Chang, I.S., Kim, B.H., Kim, K.S. and Culley, D.E., 2006. Electrically conductive bacterial nanowires produced by *Shewanella oneidensis* strain MR-1 and other microorganisms. *Proceedings of the National Academy of Sciences*, 103(30), pp.11358-11363.

Gregory, K.B., Bond, D.R. and Lovley, D.R., 2004. Graphite electrodes as electron donors for anaerobic respiration. *Environmental microbiology*, 6(6), pp.596-604.

Hermans, M., Risgaard-Petersen, N., Meysman, F.J. and Slomp, C.P., 2020. Biogeochemical impact of cable bacteria on coastal Black Sea sediment. *Biogeosciences*, 17(23), pp.5919-5938.

Hibbing, M.E., Fuqua, C., Parsek, M.R. and Peterson, S.B., 2010. Bacterial competition: surviving and thriving in the microbial jungle. *Nature reviews microbiology*, 8(1), pp.15-25.

Hoehler, T.M., Alperin, M.J., Albert, D.B. and Martens, C.S., 1994. Field and laboratory studies of methane oxidation in an anoxic marine sediment: Evidence for a methanogen-sulfate reducer consortium. *Global biogeochemical cycles*, 8(4), pp.451-463.

Janssen, P.H., Schuhmann, A., Bak, F. and Liesack, W., 1996. Disproportionation of inorganic sulfur compounds by the sulfate-reducing bacterium *Desulfocapsa thiozymogenes* gen. nov., sp. nov. *Archives of Microbiology*, 166(3), pp.184-192.

Jones, C.G., Lawton, J.H. and Shachak, M., 1994. Organisms as ecosystem engineers. *In Ecosystem management* (pp. 130-147). Springer, New York, NY.

Jones, C.G., Lawton, J.H. and Shachak, M., 1997. Positive and negative effects of organisms as physical ecosystem engineers. *Ecology*, 78(7), pp.1946-1957.

Jørgensen, B.B., 2006. Bacteria and marine biogeochemistry. *In Marine geochemistry* (pp. 173-207). Springer, Berlin, Heidelberg.

Jousset, A., Bienhold, C., Chatzinotas, A., Gallien, L., Gobet, A., Kurm, V., Küsel, K., Rillig, M.C., Rivett, D.W., Salles, J.F. and Van Der Heijden, M.G., 2017. Where less may be more: how the rare biosphere pulls ecosystems strings. *The ISME journal*, 11(4), pp.853-862.

Joye, S.B. and Hollibaugh, J.T., 1995. Influence of sulfide inhibition of nitrification on nitrogen regeneration in sediments. *Science*, 270(5236), pp.623-625.

Jurkevitch, E., 2007. Predatory behaviors in bacteria-diversity and transitions. *Microbe-American Society for Microbiology*, 2(2), p.67.

Kallmeyer, J., Smith, D.C., Spivack, A.J. and D'Hondt, S., 2008. New cell extraction procedure applied to deep subsurface sediments. *Limnology and Oceanography: Methods*, 6(6), pp.236-245.

Kato, S., Hashimoto, K. and Watanabe, K., 2012a. Methanogenesis facilitated by electric syntrophy via (semi) conductive iron-oxide minerals. *Environmental microbiology*, 14(7), pp.1646-1654.

Kato, S., Hashimoto, K. and Watanabe, K., 2012b. Microbial interspecies electron transfer via electric currents through conductive minerals. *Proceedings of the National Academy of Sciences*, 109(25), pp.10042-10046.

Kato, S. and Yamagishi, A., 2016. A novel large filamentous deltaproteobacterium on hydrothermally inactive sulfide chimneys of the Southern Mariana Trough. *Deep Sea Research Part I: Oceanographic Research Papers*, 110, pp.99-105.

Kessler, A.J., Wawryk, M., Marzocchi, U., Roberts, K.L., Wong, W.W., Risgaard-Petersen, N., Meysman, F.J., Glud, R.N. and Cook, P.L., 2019. Cable bacteria promote DNRA through iron sulfide dissolution. *Limnology and Oceanography*, 64(3), pp.1228-1238.

Kevorkian, R., Callahan, S., Winstead, R. and Lloyd, K.G., 2021. ANME-1 archaea drive methane accumulation and removal in estuarine sediments. *bioRxiv*.

Kjeldsen, K.U., Schreiber, L., Thorup, C.A., Boesen, T., Bjerg, J.T., Yang, T., Dueholm, M.S., Larsen, S., Risgaard-Petersen, N., Nierychlo, M. and Schmid, M., 2019. On the evolution and physiology of cable bacteria. *Proceedings of the National Academy of Sciences*, 116(38), pp.19116-19125.

Kouzuma, A., Kato, S. and Watanabe, K., 2015. Microbial interspecies interactions: recent findings in syntrophic consortia. *Frontiers in microbiology*, 6, p.477.

Kristensen, E., 2008. Mangrove crabs as ecosystem engineers; with emphasis on sediment processes. *Journal of sea Research*, 59(1-2), pp.30-43.

Kurtz, Z.D., Müller, C.L., Miraldi, E.R., Littman, D.R., Blaser, M.J. and Bonneau, R.A., 2015. Sparse and compositionally robust inference of microbial ecological networks. *PLoS Comput Biol*, 11(5), p.e1004226.

Laanbroek, H.J., Geerligs, H.J., Sijtsma, L. and Veldkamp, H., 1984. Competition for sulfate and ethanol among Desulfobacter, Desulfobulbus, and Desulfovibrio species isolated from intertidal sediments. *Applied and Environmental Microbiology*, 47(2), pp.329-334.

Larsen, S., Nielsen, L.P. and Schramm, A., 2015. Cable bacteria associated with long-distance electron transport in N ew E ngland salt marsh sediment. *Environmental Microbiology Reports*, 7(2), pp.175-179.

Leang, C., Coppi, M.V. and Lovley, D.R., 2003. OmcB, a c-type polyheme cytochrome, involved in Fe (III) reduction in *Geobacter sulfurreducens*. *Journal of Bacteriology*, 185(7), pp.2096-2103.

Lenk, S., Moraru, C., Hahnke, S., Arnds, J., Richter, M., Kube, M., Reinhardt, R., Brinkhoff, T., Harder, J., Amann, R. and Mußmann, M., 2012. *Roseobacter* clade bacteria are abundant in coastal sediments and encode a novel combination of sulfur oxidation genes. *The ISME journal*, 6(12), pp.2178-2187.

Lever, M.A., Torti, A., Eickenbusch, P., Michaud, A.B., Šantl-Temkiv, T. and Jørgensen, B.B., 2015. A modular method for the extraction of DNA and RNA, and the separation of DNA pools from diverse environmental sample types. *Frontiers in Microbiology*, 6, p.476.

Li, C., Reimers, C.E. and Alleau, Y., 2020. Inducing the attachment of cable bacteria on oxidizing electrodes. Biogeosciences, 17(3), pp.597-607.

Liesack, W. and Finster, K., 1994. Phylogenetic analysis of five strains of gram-negative, obligately anaerobic, sulfur-reducing bacteria and description of *Desulfuromusa* gen. nov., including *Desulfuromusa kysingii* sp. nov., *Desulfuromusa bakii* sp. nov., and *Desulfuromusa succinoxidans* sp. nov. *International Journal of Systematic and Evolutionary Microbiology*, *44*(4), pp.753-758.

Light, S.H., Su, L., Rivera-Lugo, R., Cornejo, J.A., Louie, A., Iavarone, A.T., Ajo-Franklin, C.M. and Portnoy, D.A., 2018. A flavin-based extracellular electron transfer mechanism in diverse Gram-positive bacteria. *Nature*, 562(7725), pp.140-144.

Liu, F., Rotaru, A.E., Shrestha, P.M., Malvankar, N.S., Nevin, K.P. and Lovley, D.R., 2012. Promoting direct interspecies electron transfer with activated carbon. *Energy & Environmental Science*, 5(10), pp.8982-8989.

Liu, F., Rotaru, A.E., Shrestha, P.M., Malvankar, N.S., Nevin, K.P. and Lovley, D.R., 2015. Magnetite compensates for the lack of a pilin-associated c-type cytochrome in extracellular electron exchange. *Environmental microbiology*, 17(3), pp.648-655.

Liu, J., Meng, Z., Liu, X. and Zhang, X.H., 2019. Microbial assembly, interaction, functioning, activity and diversification: a review derived from community compositional data. *Marine Life Science & Technology*, pp.1-17.

Livingstone, P.G., Morphew, R.M. and Whitworth, D.E., 2017. Myxobacteria are able to prey broadly upon clinically-relevant pathogens, exhibiting a prey range which cannot be explained by phylogeny. *Frontiers in microbiology*, 8, p.1593.

Lovley, D.R., Dwyer, D.F. and Klug, M.J., 1982. Kinetic analysis of competition between sulfate reducers and methanogens for hydrogen in sediments. *Applied and Environmental Microbiology*, 43(6), pp.1373-1379.

Lovley, D.R. and Phillips, E.J., 1987. Competitive mechanisms for inhibition of sulfate reduction and methane production in the zone of ferric iron reduction in sediments. *Applied and Environmental Microbiology*, 53(11), pp.2636-2641.

Lovley, D.R. and Goodwin, S., 1988. Hydrogen concentrations as an indicator of the predominant terminal electron-accepting reactions in aquatic sediments. *Geochim. Cosmochim. Acta*, 52(12), pp.2993-3003.

Lovley, D.R., 2017a. Syntrophy goes electric: direct interspecies electron transfer. *Annual review of microbiology*, 71, pp.643-664.

Lovley, D.R., 2017b. Happy together: microbial communities that hook up to swap electrons. *The ISME journal*, 11(2), pp.327-336.

Lunau, M., Lemke, A., Walther, K., Martens-Habbena, W. and Simon, M., 2005. An improved method for counting bacteria from sediments and turbid environments by epifluorescence microscopy. *Environmental Microbiology*, 7(7), pp.961-968.

Malkin, S.Y., Rao, A.M., Seitaj, D., Vasquez-Cardenas, D., Zetsche, E.M., Hidalgo-Martinez, S., Boschker, H.T. and Meysman, F.J., 2014. Natural occurrence of microbial sulphur oxidation by long-range electron transport in the seafloor. *The ISME journal*, *8*(9), p.1843.

Malkin, S.Y., Seitaj, D., Burdorf, L.D., Nieuwhof, S., Hidalgo-Martinez, S., Tramper, A., Geeraert, N., De Stigter, H. and Meysman, F.J., 2017. Electrogenic sulfur oxidation by cable bacteria in bivalve reef sediments. *Frontiers in Marine Science*, *4*, p.28.

Malkin, S.Y., Liau, P., Kim, C., Hantsoo, K., Gomes, M., Song, B. *In preparation*. Contrasting controls on seasonal and spatial distribution of marine cable bacteria (*Ca.* Electrothrix) and *Beggiatoaceae* in seasonally hypoxic Chesapeake Bay.

Manz, W., Amann, R., Ludwig, W., Wagner, M. and Schleifer, K.H., 1992. Phylogenetic oligodeoxynucleotide probes for the major subclasses of proteobacteria: problems and solutions. *Systematic and applied microbiology*, 15(4), pp.593-600.

Martin, B.C., Bougoure, J., Ryan, M.H., Bennett, W.W., Colmer, T.D., Joyce, N.K., Olsen, Y.S. and Kendrick, G.A., 2019. Oxygen loss from seagrass roots coincides with colonisation of sulphide-oxidising cable bacteria and reduces sulphide stress. *The ISME journal*, 13(3), pp.707-719.

Marzocchi, U., Trojan, D., Larsen, S., Meyer, R.L., Revsbech, N.P., Schramm, A., Nielsen, L.P. and Risgaard-Petersen, N., 2014. Electric coupling between distant nitrate reduction and sulfide oxidation in marine sediment. *The ISME journal*, 8(8), pp.1682-1690.

Marzocchi, U., Bonaglia, S., van de Velde, S., Hall, P.O., Schramm, A., Risgaard-Petersen, N. and Meysman, F.J., 2018. Transient bottom water oxygenation creates a niche for cable bacteria in long-term anoxic sediments of the Eastern Gotland Basin. *Environmental microbiology*, 20(8), pp.3031-3041.

Marzocchi, U., Palma, E., Rossetti, S., Aulenta, F. and Scoma, A., 2020. Parallel artificial and biological electric circuits power petroleum decontamination: The case of snorkel and cable bacteria. *Water Research*, 173, p.115520.

Matturro, B., Cruz Viggi, C., Aulenta, F. and Rossetti, S., 2017. Cable bacteria and the bioelectrochemical snorkel: the natural and engineered facets playing a role in hydrocarbons degradation in marine sediments. *Frontiers in Microbiology*, 8, p.952.

McGlynn, S.E., Chadwick, G.L., Kempes, C.P. and Orphan, V.J., 2015. Single cell activity reveals direct electron transfer in methanotrophic consortia. *Nature*, 526(7574), pp.531-535.

Meysman, F.J., Risgaard-Petersen, N., Malkin, S.Y. and Nielsen, L.P., 2015. The geochemical fingerprint of microbial long-distance electron transport in the seafloor. *Geochimica et Cosmochimica Acta*, 152, pp.122-142.

Meysman, F.J., 2018. Cable bacteria take a new breath using long-distance electricity. *Trends in microbiology*, 26(5), pp.411-422.

Middelburg, J.J. and Levin, L.A., 2009. Coastal hypoxia and sediment biogeochemistry. *Biogeosciences Discussions*, 6(2).

Milucka, J., Ferdelman, T.G., Polerecky, L., Franzke, D., Wegener, G., Schmid, M., Lieberwirth, I., Wagner, M., Widdel, F. and Kuypers, M.M., 2012. Zero-valent sulphur is a key intermediate in marine methane oxidation. *Nature*, 491(7425), pp.541-546.

Mori, K., Suzuki, K.I., Yamaguchi, K., Urabe, T. and Hanada, S., 2015. *Thiogranum longum* gen. nov., sp. nov., an obligately chemolithoautotrophic, sulfur-oxidizing bacterium of the family *Ectothiorhodospiraceae* isolated from a deep-sea hydrothermal field, and an emended description of the genus *Thiohalomonas*. *International journal of systematic and evolutionary microbiology*, 65(1), pp.235-241.

Morris, B.E., Henneberger, R., Huber, H. and Moissl-Eichinger, C., 2013. Microbial syntrophy: interaction for the common good. *FEMS microbiology reviews*, 37(3), pp.384-406.

Muñoz-Dorado, J., Marcos-Torres, F.J., García-Bravo, E., Moraleda-Muñoz, A. and Pérez, J., 2016. Myxobacteria: moving, killing, feeding, and surviving together. *Frontiers in microbiology*, 7, p.781.

Müller, H., Bosch, J., Griebler, C., Damgaard, L.R., Nielsen, L.P., Lueders, T. and Meckenstock, R.U., 2016. Long-distance electron transfer by cable bacteria in aquifer sediments. *The ISME journal*, 10(8), pp.2010-2019.

Müller, H., Marozava, S., Probst, A.J. and Meckenstock, R.U., 2020. Groundwater cable bacteria conserve energy by sulfur disproportionation. *The ISME journal*, 14(2), pp.623-634.

Mußmann, M., Pjevac, P., Krüger, K. and Dyksma, S., 2017. Genomic repertoire of the Woeseiaceae/JTB255, cosmopolitan and abundant core members of microbial communities in marine sediments. *The ISME journal*, 11(5), pp.1276-1281.

Narasingarao, P. and Häggblom, M.M., 2006. Sedimenticola selenatireducens, gen. nov., sp. nov., an anaerobic selenate-respiring bacterium isolated from estuarine sediment. *Systematic and applied microbiology*, 29(5), pp.382-388.

Nauhaus, K., Boetius, A., Krüger, M. and Widdel, F., 2002. In vitro demonstration of anaerobic oxidation of methane coupled to sulphate reduction in sediment from a marine gas hydrate area. *Environmental microbiology*, 4(5), pp.296-305.

Nielsen, L.P., Risgaard-Petersen, N., Fossing, H., Christensen, P.B. and Sayama, M., 2010. Electric currents couple spatially separated biogeochemical processes in marine sediment. *Nature*, *463*(7284), p.1071.

Nielsen, L.P., 2016. Ecology: electrical cable bacteria save marine life. *Current Biology*, *26*(1), pp.R32-R33.

Noble, R.T. and Fuhrman, J.A., 1998. Use of SYBR Green I for rapid epifluorescence counts of marine viruses and bacteria. *Aquatic Microbial Ecology*, 14(2), pp.113-118.

Otte, J.M., Harter, J., Laufer, K., Blackwell, N., Straub, D., Kappler, A. and Kleindienst, S., 2018. The distribution of active iron-cycling bacteria in marine and freshwater sediments is decoupled from geochemical gradients. *Environmental microbiology*, *20*(7), pp.2483-2499.

Paine, R.T., 1969. A note on trophic complexity and community stability. *The American Naturalist*, 103(929), pp.91-93.

Passarelli, C., Olivier, F., Paterson, D.M., Meziane, T. and Hubas, C., 2014. Organisms as cooperative ecosystem engineers in intertidal flats. *Journal of Sea Research*, 92, pp.92-101.

Pérez, J., Moraleda-Muñoz, A., Marcos-Torres, F.J. and Muñoz-Dorado, J., 2016. Bacterial predation: 75 years and counting! *Environmental microbiology*, 18(3), pp.766-779.

Pfeffer, C., Larsen, S., Song, J., Dong, M., Besenbacher, F., Meyer, R.L., Kjeldsen, K.U., Schreiber, L., Gorby, Y.A., El-Naggar, M.Y. and Leung, K.M., 2012. Filamentous bacteria transport electrons over centimetre distances. *Nature*, *491*(7423), p.218.

Poser, A., Lohmayer, R., Vogt, C., Knoeller, K., Planer-Friedrich, B., Sorokin, D., Richnow, H.H. and Finster, K., 2013. Disproportionation of elemental sulfur by haloalkaliphilic bacteria from soda lakes. *Extremophiles*, *17*(6), pp.1003-1012.

Power, M.E., Tilman, D., Estes, J.A., Menge, B.A., Bond, W.J., Mills, L.S., Daily, G., Castilla, J.C., Lubchenco, J. and Paine, R.T., 1996. Challenges in the quest for keystones: identifying keystone species is difficult—but essential to understanding how loss of species will affect ecosystems. *BioScience*, 46(8), pp.609-620.

Props, R., Kerckhof, F.M., Rubbens, P., De Vrieze, J., Sanabria, E.H., Waegeman, W., Monsieurs, P., Hammes, F. and Boon, N., 2017. Absolute quantification of microbial taxon abundances. *The ISME journal*, *11*(2), pp.584-587.

Rao, A.M., Malkin, S.Y., Hidalgo-Martinez, S. and Meysman, F.J., 2016a. The impact of electrogenic sulfide oxidation on elemental cycling and solute fluxes in coastal sediment. *Geochimica et Cosmochimica Acta*, 172, pp.265-286.

Rao, A., Risgaard-Petersen, N. and Neumeier, U., 2016b. Electrogenic sulfur oxidation in a northern saltmarsh (St. Lawrence Estuary, Canada). *Canadian journal of microbiology*, 62(6), pp.530-537.

Reguera, G., McCarthy, K.D., Mehta, T., Nicoll, J.S., Tuominen, M.T. and Lovley, D.R., 2005. Extracellular electron transfer via microbial nanowires. *Nature*, 435(7045), pp.1098-1101.

Reimers, C.E., Li, C., Graw, M.F., Schrader, P.S. and Wolf, M., 2017. The identification of cable bacteria attached to the anode of a benthic microbial fuel cell: Evidence of long distance extracellular electron transport to electrodes. *Frontiers in microbiology*, 8, p.2055.

Reis, M.A.M., Almeida, J.S., Lemos, P.C. and Carrondo, M.J.T., 1992. Effect of hydrogen sulfide on growth of sulfate reducing bacteria. *Biotechnology and bioengineering*, 40(5), pp.593-600.

Risgaard-Petersen, N., Revil, A., Meister, P. and Nielsen, L.P., 2012. Sulfur, iron-, and calcium cycling associated with natural electric currents running through marine sediment. *Geochimica et Cosmochimica Acta*, *92*, pp.1-13.

Risgaard-Petersen, N., Kristiansen, M., Frederiksen, R.B., Dittmer, A.L., Bjerg, J.T., Trojan, D., Schreiber, L., Damgaard, L.R., Schramm, A. and Nielsen, L.P., 2015. Cable bacteria in freshwater sediments. *Applied and environmental microbiology*, 81(17), pp.6003-6011.

Robertson, E.K., Roberts, K.L., Burdorf, L.D., Cook, P. and Thamdrup, B., 2016. Dissimilatory nitrate reduction to ammonium coupled to Fe (II) oxidation in sediments of a periodically hypoxic estuary. *Limnology and Oceanography*, 61(1), pp.365-381.

Roncoroni, M., Brandani, J., Battin, T.I. and Lane, S.N., 2019. Ecosystem engineers: Biofilms and the ontogeny of glacier floodplain ecosystems. *Wiley Interdisciplinary Reviews: Water*, *6*(6), p.e1390.

Rotaru, A.E., Shrestha, P.M., Liu, F., Markovaite, B., Chen, S., Nevin, K.P. and Lovley, D.R., 2014. Direct interspecies electron transfer between *Geobacter metallireducens* and *Methanosarcina barkeri*. *Applied and environmental microbiology*, 80(15), pp.4599-4605.

Sandfeld, T., Marzocchi, U., Petro, C., Schramm, A. and Risgaard-Petersen, N., 2020. Electrogenic sulfide oxidation mediated by cable bacteria stimulates sulfate reduction in freshwater sediments. *The ISME Journal*, 14(5), pp.1233-1246.

Sanford, R.A., Cole, J.R. and Tiedje, J.M., 2002. Characterization and description of *Anaeromyxobacter dehalogenans* gen. nov., sp. nov., an aryl-halorespiring facultative anaerobic myxobacterium. *Applied and environmental microbiology*, 68(2), pp.893-900.

Schauer, R., Risgaard-Petersen, N., Kjeldsen, K.U., Bjerg, J.J.T., Jørgensen, B.B., Schramm, A. and Nielsen, L.P., 2014. Succession of cable bacteria and electric currents in marine sediment. *The ISME journal*, *8*(6), p.1314.

Scheller, S., Yu, H., Chadwick, G.L., McGlynn, S.E. and Orphan, V.J., 2016. Artificial electron acceptors decouple archaeal methane oxidation from sulfate reduction. *Science*, 351(6274), pp.703-707.

Scholz, V.V., Müller, H., Koren, K., Nielsen, L.P. and Meckenstock, R.U., 2019. The rhizosphere of aquatic plants is a habitat for cable bacteria. *FEMS microbiology ecology*, 95(6), p.fiz062.

Scholz, V.V., Meckenstock, R.U., Nielsen, L.P. and Risgaard-Petersen, N., 2020. Cable bacteria reduce methane emissions from rice-vegetated soils. *Nature communications*, 11(1), pp.1-5.

Schönheit, P., Kristjansson, J.K. and Thauer, R.K., 1982. Kinetic mechanism for the ability of sulfate reducers to out-compete methanogens for acetate. *Archives of Microbiology*, 132(3), pp.285-288.

Scyphers, S.B., Powers, S.P., Heck Jr, K.L. and Byron, D., 2011. Oyster reefs as natural breakwaters mitigate shoreline loss and facilitate fisheries. *PloS one*, 6(8), p.e22396.

Seitaj, D., Schauer, R., Sulu-Gambari, F., Hidalgo-Martinez, S., Malkin, S.Y., Burdorf, L.D., Slomp, C.P. and Meysman, F.J., 2015. Cable bacteria generate a firewall against euxinia in seasonally hypoxic basins. *Proceedings of the National Academy of Sciences*, *112*(43), pp.13278-13283.

Shrestha, P.M. and Rotaru, A.E., 2014. Plugging in or going wireless: strategies for interspecies electron transfer. *Frontiers in microbiology*, 5, p.237.

Simmons, S.L. and Edwards, K.J., 2007. Unexpected diversity in populations of the many-celled magnetotactic prokaryote. *Environmental Microbiology*, *9*(1), pp.206-215.

Sockett, R.E., 2009. Predatory lifestyle of *Bdellovibrio bacteriovorus*. *Annual review of microbiology*, 63, pp.523-539.

Stams, A.J. and Plugge, C.M., 2009. Electron transfer in syntrophic communities of anaerobic bacteria and archaea. *Nature Reviews Microbiology*, 7(8), pp.568-577.

Stumm, W. and Morgan, J.J., 1996. Aquatic Chemistry: Chemical Equilibria and Rates in Natural Waters. Wiley. New York.

Sulu-Gambari, F., Seitaj, D., Meysman, F.J., Schauer, R., Polerecky, L. and Slomp, C.P., 2016a. Cable bacteria control iron–phosphorus dynamics in sediments of a coastal hypoxic basin. *Environmental science & technolo*i, 50(3), pp.1227-1233.

Sulu-Gambari, F., Seitaj, D., Behrends, T., Banerjee, D., Meysman, F.J. and Slomp, C.P., 2016b. Impact of cable bacteria on sedimentary iron and manganese dynamics in a seasonally-hypoxic marine basin. *Geochimica et Cosmochimica Acta*, 192, pp.49-69.

Summers, Z.M., Fogarty, H.E., Leang, C., Franks, A.E., Malvankar, N.S. and Lovley, D.R., 2010. Direct exchange of electrons within aggregates of an evolved syntrophic coculture of anaerobic bacteria. *Science*, 330(6009), pp.1413-1415.

Thamdrup, B.O., Finster, K., Hansen, J.W. and Bak, F., 1993. Bacterial disproportionation of elemental sulfur coupled to chemical reduction of iron or manganese. *Applied and environmental microbiology*, *59*(1), pp.101-108.

Thayer, C.W., 1979. Biological bulldozers and the evolution of marine benthic communities. *Science*, 203(4379), pp.458-461.

Thiruvallur Eachambadi, R., Bonné, R., Cornelissen, R., Hidalgo-Martinez, S., Vangronsveld, J., Meysman, F.J., Valcke, R., Cleuren, B. and Manca, J.V., 2020. An Ordered and Fail-Safe Electrical Network in Cable Bacteria. *Advanced Biosystems*, p.2000006.

Tkacz, A., Hortala, M. and Poole, P.S., 2018. Absolute quantitation of microbiota abundance in environmental samples. *Microbiome*, *6*(1), pp.1-13.

Trojan, D., Schreiber, L., Bjerg, J.T., Bøggild, A., Yang, T., Kjeldsen, K.U. and Schramm, A., 2016. A taxonomic framework for cable bacteria and proposal of the candidate genera Electrothrix and Electronema. *Systematic and applied microbiology*, 39(5), pp.297-306.

Tsai, A.Y., Gong, G.C., Sanders, R.W. and Huang, J.K., 2013. Contribution of viral lysis and nanoflagellate grazing to bacterial mortality in the inner and outer regions of the Changjiang River plume during summer. *Journal of plankton research*, 35(6), pp.1283-1293.

van de Velde, S., Lesven, L., Burdorf, L.D., Hidalgo-Martinez, S., Geelhoed, J.S., Van Rijswijk, P., Gao, Y. and Meysman, F.J., 2016. The impact of electrogenic sulfur oxidation on the biogeochemistry of coastal sediments: A field study. *Geochimica et Cosmochimica Acta*, 194, pp.211-232.

Vasquez-Cardenas, D., Van De Vossenberg, J., Polerecky, L., Malkin, S.Y., Schauer, R., Hidalgo-Martinez, S., Confurius, V., Middelburg, J.J., Meysman, F.J. and Boschker, H.T., 2015. Microbial carbon metabolism associated with electrogenic sulphur oxidation in coastal sediments. *The ISME journal*.

Visscher, P.T., van den Ende, F.P., Schaub, B.E. and van Gemerden, H., 1992. Competition between anoxygenic phototrophic bacteria and colorless sulfur bacteria in a microbial mat. *FEMS Microbiology Letters*, 101(1), pp.51-58.

Vu, H.D., Wie˛ ski, K. and Pennings, S.C., 2017. Ecosystem engineers drive creek formation in salt marshes. *Ecology*, 98(1), pp.162-174.

Wang, F., Gu, Y., O'Brien, J.P., Sophia, M.Y., Yalcin, S.E., Srikanth, V., Shen, C., Vu, D., Ing, N.L., Hochbaum, A.I. and Egelman, E.H., 2019. Structure of microbial nanowires reveals stacked hemes that transport electrons over micrometers. *Cell*, 177(2), pp.361-369.

Wang, W., Luo, X., Ye, X., Chen, Y., Wang, H., Wang, L., Wang, Y., Yang, Y., Li, Z., Cao, H. and Cui, Z., 2020. Predatory Myxococcales are widely distributed in and closely correlated with the bacterial community structure of agricultural land. *Applied Soil Ecology*, 146, p.103365.

Walles, B., De Paiva, J.S., van Prooijen, B.C., Ysebaert, T. and Smaal, A.C., 2015. The ecosystem engineer *Crassostrea gigas* affects tidal flat morphology beyond the boundary of their reef structures. *Estuaries and Coasts*, 38(3), pp.941-950.

Ward, B.A., Dutkiewicz, S., Barton, A.D. and Follows, M.J., 2011. Biophysical aspects of resource acquisition and competition in algal mixotrophs. *The American Naturalist*, 178(1), pp.98-112.

Weerman, E.J., Van Der GEEST, H.G., Van Der MEULEN, M.D., Manders, E.M., Van De KOPPEL, J.O.H.A.N., Herman, P.M. and Admiraal, W.I.M., 2011. Ciliates as engineers of phototrophic biofilms. *Freshwater Biology*, 56(7), pp.1358-1369.

Wegener, G., Krukenberg, V., Riedel, D., Tegetmeyer, H.E. and Boetius, A., 2015. Intercellular wiring enables electron transfer between methanotrophic archaea and bacteria. *Nature*, 526(7574), pp.587-590.

Weiss, S., Van Treuren, W., Lozupone, C., Faust, K., Friedman, J., Deng, Y., Xia, L.C., Xu, Z.Z., Ursell, L., Alm, E.J. and Birmingham, A., 2016. Correlation detection strategies in microbial data sets vary widely in sensitivity and precision. *The ISME journal*, 10(7), pp.1669-1681.

Wild, C., Hoegh-Guldberg, O., Naumann, M.S., Colombo-Pallotta, M.F., Ateweberhan, M., Fitt, W.K., Iglesias-Prieto, R., Palmer, C., Bythell, J.C., Ortiz, J.C. and Loya, Y., 2011. Climate change impedes scleractinian corals as primary reef ecosystem engineers. *Marine and Freshwater research*, 62(2), pp.205-215.

Wright, J.P., Jones, C.G. and Flecker, A.S., 2002. An ecosystem engineer, the beaver, increases species richness at the landscape scale. *Oecologia*, 132(1), pp.96-101.

Wright, J.P. and Jones, C.G., 2006. The concept of organisms as ecosystem engineers ten years on: progress, limitations, and challenges. *BioScience*, 56(3), pp.203-209.

Wrótniak-Drzewiecka, W., Brzezińska, A.J., Dahm, H., Ingle, A.P. and Rai, M., 2016. Current trends in myxobacteria research. *Annals of microbiology*, 66(1), pp.17-33.

Wu, Q., Sanford, R.A. and Löffler, F.E., 2006. Uranium (VI) reduction by *Anaeromyxobacter dehalogenans* strain 2CP-C. *Applied and Environmental Microbiology*, 72(5), pp.3608-3614.

Xu, S., Jangir, Y. and El-Naggar, M.Y., 2016. Disentangling the roles of free and cytochrome-bound flavins in extracellular electron transport from *Shewanella* oneidensis MR-1. *Electrochimica Acta*, 198, pp.49-55.

Yan, L., Zhang, S., Chen, P., Liu, H., Yin, H. and Li, H., 2012. Magnetotactic bacteria, magnetosomes and their application. *Microbiological research*, 167(9), pp.507-519.